

DEVELOPMENT OF A MASH TL-3 LOW-PROFILE CONCRETE BARRIER

A Thesis

by

SHENGYI SHI

Submitted to the Office of Graduate and Professional Studies of
Texas A&M University
in partial fulfillment of the requirements for the degree of

MASTER OF SCIENCE

Chair of Committee,	Stefan Hurlebaus
Committee Members,	Arash Noshadravan
	Jeffrey Falzarano

Head of Department,	Robin Autenrieth
---------------------	------------------

December 2018

Major Subject: Civil Engineering

Copyright 2018 Shengyi Shi

ABSTRACT

A sight-distance problem is associated with use of 32-inch tall concrete longitudinal barriers, specifically in certain work zone locations and at nighttime. These 32-inch tall barriers can obstruct drivers' eyesight, making it difficult for drivers to detect oncoming vehicles on the other side of these barriers and result in potential hazards. To address this sight-distance problem while protecting the errant vehicles, researchers developed a 20-inch tall low-profile portable concrete barrier (PCB) for use in low-speed work zones in the early 1990s, according to NCHRP Report 350 testing criteria. After that, several research projects were conducted to solve the high speed application of low-profile barriers, but most of them failed. In 2008, the new testing guideline Manual for Assessing Safety Hardware (MASH) was published as the updated criteria. Therefore, a low-profile barrier for high speed work zones needs to be developed and evaluated under MASH.

In this research project, a new low-profile PCB was successfully developed for high speed application. This low-profile PCB was designed with a T-shaped profile with a height of only 26 inches and was a free standing barrier. Sight-distance obstruction problem was evaluated and a simplified experiment was conducted on 24 and 26-inch tall barriers. Finite element simulation analysis was conducted to determine the shape of the new barrier. Two different cases were considered for each profile concept—with and without impact tire disengagement—to represent the extreme tire behaviors during the impact event. Detailed simulations were conducted to predict the crashworthiness of the T-shaped PCB. Two successful full-scale crash tests were implemented according to MASH Test Level 3. The barrier model was then modified and validated based on the test results.

ACKNOWLEDGEMENTS

I would like to thank my committee chair Dr. Stefan Hurlebaus, and my committee members, Dr. Arash Noshadravan and Dr. Jeffrey Falzarano, for their guidance and support throughout my work. Additionally, I would like to thank my supervisor Dr. Chiara Silvestri Dobrovolny for her constant support since the beginning of this project. I also would like to thank Mr. Wade Odell, Mr. Ken Mora, and Mr. Chris Lindsey, with the TxDOT Design Division, for their valuable assistance and input on this project. Finally, thanks to my colleagues at Texas A&M Transportation Institute at RELIS Campus for their help.

Portions of this research were conducted with high performance research computing resources provided by Texas A&M University (<https://hprc.tamu.edu>).

CONTRIBUTORS AND FUNDING SOURCES

Contributors

This work was supervised by a thesis committee consisting of Professor Dr. Stefan Hurlebaus and Dr. Arash Noshadravan of the Department of Civil Engineering and Professor Dr. Jeffrey Falzarano of the Department of Ocean Engineering.

The full-scale crash tests in Section 7 were implemented by TTI Proving Ground, and the detailed reinforcement concrete design in the same section was supported by Engineers in TTI-Roadside Safety Division.

All other work conducted for the thesis was completed by the student independently.

Funding Sources

This work was made possible in part by Texas Department of Transportation, Research and Technology Implementation Office.

Its contents are solely the responsibility of the authors and do not necessarily represent the official views of the Texas Department of Transportation.

NOMENCLATURE

PCB	Portable Concrete Barrier
FE	Finite Element
FEA	Finite Element Analysis
TL	Test Level
NCHRP	National Cooperative Highway Research Program
MASH	Manual for Assessing Safety Hardware
mi/h	Miles Per Hour
TTI	Texas A&M Transportation Institute
TxDOT	Texas Department of Transportation
PHD	Post-Impact Head Decelerations
THIV	Theoretical Head Impact Velocity
ASI	Acceleration Severity Index
OIV	Occupant Impact Velocity
ORA	Occupant Ridedown Acceleration
G	Gravitational Force
ft/s	Feet Per Second
pcf	Pounds Per Cubic Foot

TABLE OF CONTENTS

	Page
ABSTRACT.....	ii
ACKNOWLEDGEMENTS.....	iii
CONTRIBUTORS AND FUNDING SOURCES	iv
NOMENCLATURE	v
TABLE OF CONTENTS.....	vi
LIST OF FIGURES	viii
LIST OF TABLES	xiii
1. INTRODUCTION	1
2. PROBLEM STATEMENT	3
3. LITERATURE REVIEW	4
3.1 Introduction.....	4
3.2 Development of Crash Testing Criteria	4
3.3 Portable Concrete Barrier	6
3.4 Previous Research on Low Height Barriers.....	10
4. SELECTION OF BARRIER HEIGHTS AND PROFILE CONCEPTS.....	17
4.1 Introduction.....	17
4.2 Barrier Heights Selection.....	17
4.3 Barrier Profile Concepts Development.....	25
5. PRELIMINARY FINITE ELEMENT ANALYSIS OF DESIGN CONCEPTS	27
5.1 Introduction.....	27
5.2 Evaluation Criteria.....	27
5.3 FE Models for Preliminary FE Simulations	29
5.4 Preliminary Finite Element Analysis of 26-Inch Tall PCB Concepts	32
5.5 Preliminary Finite Element Analysis of 24-Inch Tall PCB Concepts	57
5.6 Summary and Comparison of 24 and 26-Inch Tall Barrier Simulations	82
5.7 Conclusion of Preliminary Simulations.....	88

6. DETAILED FINITE ELEMENT ANALYSIS OF SELECTED CONCEPTS	90
6.1 Introduction.....	90
6.2 Detailed Finite Element Analysis 26-Inch Tall T Shaped PCB.....	90
6.3 Detailed Finite Element Analysis 24-Inch Tall T Shaped PCB.....	111
6.4 Conclusion of Detailed Simulations	127
7. FULL-SCALE CRASH TEST.....	128
7.1 Introduction.....	128
7.2 MASH Test 3-11.....	128
7.3 MASH Test 3-10.....	137
8. FEA MODIFICATION AND VALIDATION	141
8.1 Introduction.....	141
8.2 Comparison between Original FEA and Full-Scale Crash Test	141
8.3 Modification and Validation.....	144
8.4 Conclusion of the Modified FEA.....	153
9. CONCLUSION AND FUTURE WORK	154
REFERENCES	156

LIST OF FIGURES

	Page
Figure 3.1 Development of Crash Test Criteria.....	5
Figure 3.2 New Jersey Shape Barrier	7
Figure 3.3 F-Shape Barrier	7
Figure 3.4 42-Inch Tall Single Slope Barrier.....	8
Figure 3.5 20-Inch Tall Low-Profile Barrier	8
Figure 3.6 Summary of Conventional PCBs.....	9
Figure 3.7 Roadside Application	11
Figure 3.8 Median Application	11
Figure 3.9 Texas Type T202 Bridge Rail	13
Figure 3.10 Tubular Steel-Backed Timber Bridge Rail.....	13
Figure 3.11 Florida 18-Inch Tall TL-2 Low-Profile PCB	14
Figure 4.1 Requirement of Vehicle Lens Mounting Height	18
Figure 4.2 Sight Obstruction of Median Barrier.....	20
Figure 4.3 Sight Obstruction of Roadside Barrier	20
Figure 4.4 Sight Obstruction of 24-Inch Tall Barrier	22
Figure 4.5 Sight Obstruction of 26-Inch Tall Barrier	22
Figure 5.1 Roll, Pitch and Yaw Crash Test Sign Convention	28
Figure 5.2 Available MASH 2270P Pickup Truck FE Model	29
Figure 5.3 Impact Tire Disengagement after a MASH 3-11 Crash Test	30
Figure 5.4 FE Model of Front Impact Tire and Suspension Assembly	31

	Page
Figure 5.5 Angular Displacements of the Vehicle in Preliminary Simulation of 26-Inch Tall PCB with 1:20 Slope (Case 1).....	33
Figure 5.6 Angular Displacements of the Vehicle in Preliminary Simulation of 26-Inch Tall PCB with 1:20 Slope (Case 2).....	33
Figure 5.7 Angular Displacements of the Vehicle in Preliminary Simulation of 26-Inch Tall PCB with 1:15 Slope (Case 1).....	37
Figure 5.8 Angular Displacements of the Vehicle in Preliminary Simulation of 26-Inch Tall PCB with 1:15 Slope (Case 2).....	38
Figure 5.9 Angular Displacements of the Vehicle in Preliminary Simulation of 26-Inch Tall T Shaped PCB (Case 1).....	41
Figure 5.10 Angular Displacements of the Vehicle in Preliminary Simulation of 26-Inch Tall T Shaped PCB (Case 2).....	42
Figure 5.11 Angular Displacements of the Vehicle in Preliminary Simulation of 26-Inch Tall T Shaped PCB with 1:20 slope (Case 1)	45
Figure 5.12 Angular Displacements of the Vehicle in Preliminary Simulation of 26-Inch Tall T Shaped PCB with 1:20 Slope (Case 2).....	46
Figure 5.13 Angular Displacements of the Vehicle in Preliminary Simulation of 26-Inch Tall I Shaped PCB (Case 1).....	49
Figure 5.14 Angular Displacements of the Vehicle in Preliminary Simulation of 26-Inch Tall I Shaped PCB (Case 2).....	50
Figure 5.15 Angular Displacements of the Vehicle in Preliminary Simulation of 26-Inch Tall I Shaped PCB with 1:20 slope (Case 1)	53
Figure 5.16 Angular Displacements of the Vehicle in Preliminary Simulation of 26-Inch Tall I Shaped PCB with 1:20 Slope (Case 2).....	54
Figure 5.17 Angular Displacements of the Vehicle in Preliminary Simulation of 24-Inch Tall PCB with 1:20 Slope (Case 1).....	58
Figure 5.18 Angular Displacements of the Vehicle in Preliminary Simulation of 24-Inch Tall PCB with 1:20 Slope (Case 2).....	58
Figure 5.19 Angular Displacements of the Vehicle in Preliminary Simulation of 24-Inch Tall PCB with 1:15 Slope (Case 1).....	62

	Page
Figure 5.20 Angular Displacements of the Vehicle in Preliminary Simulation of 24-Inch Tall PCB with 1:15 Slope (Case 2).....	63
Figure 5.21 Angular Displacements of the Vehicle in Preliminary Simulation of 24-Inch Tall T Shaped PCB (Case 1).....	66
Figure 5.22 Angular Displacements of the Vehicle in Preliminary Simulation of 24-Inch Tall T Shaped PCB (Case 2).....	67
Figure 5.23 Angular Displacements of the Vehicle in Preliminary Simulation of 24-Inch Tall T Shaped PCB with 1:20 slope (Case 1).....	70
Figure 5.24 Angular Displacements of the Vehicle in Preliminary Simulation of 24-Inch Tall T Shaped PCB with 1:20 Slope (Case 2).....	71
Figure 5.25 Angular Displacements of the Vehicle in Preliminary Simulation of 24-Inch Tall I Shaped PCB (Case 1).....	74
Figure 5.26 Angular Displacements of the Vehicle in Preliminary Simulation of 24-Inch Tall I Shaped PCB (Case 2).....	75
Figure 5.27 Angular Displacements of the Vehicle in Preliminary Simulation of 24-Inch Tall I Shaped PCB with 1:20 slope (Case 1).....	78
Figure 5.28 Angular Displacements of the Vehicle in Preliminary Simulation of 24-Inch Tall I Shaped PCB with 1:20 Slope (Case 2).....	79
Figure 5.29 Roll Angle Comparison of 26-Inch Tall Barrier Concepts with Impact Tire Disengagement.....	83
Figure 5.30 Roll Angle Comparison of 26-Inch Tall Barriers without Impact Tire Disengagement.....	83
Figure 5.31 Range of Maximum Roll Angles of 26-Inch Tall Barrier Concepts	84
Figure 5.32 Roll Angle Comparison of 24-Inch Tall Barrier Concepts with Impact Tire Disengagement.....	86
Figure 5.33 Roll Angle Comparison of 24-Inch Tall Barriers without Impact Tire Disengagement.....	86
Figure 5.34 Range of Maximum Roll Angles of 24-Inch Tall Barrier Concepts	87
Figure 6.1 Overall Details of the 26-Inch Tall T Shaped PCB.....	92
Figure 6.2 Detailed Geometry of the 26-Inch Tall T Shaped PCB.....	93

	Page
Figure 6.3 Front, Perspective and Side Views of a Segment of the 26-Inch Tall Model	95
Figure 6.4 Images of the 26-Inch Tall Barrier FE Model with Connection Details	95
Figure 6.5 Angular Displacements of the Vehicle in Case 1 of 26-Inch Tall PCB Simulation....	97
Figure 6.6 Initial and Deflected Shape of the 26-Inch Tall T Shaped PCB in Case 1	97
Figure 6.7 Energy Distribution History in Case 1 (26-Inch Tall T Shaped PCB Simulation)	99
Figure 6.8 Summary of Detailed Simulation Results of 26-inch Tall T Shaped PCB (With Impact Tire Disengagement).....	101
Figure 6.9 Angular Displacements of the Vehicle in Case 2 of 26-inch Tall PCB Simulation..	103
Figure 6.10 Initial and Deflected Shape of the 26-Inch Tall PCB in Case 2	103
Figure 6.11 Energy Distribution History in Case 2 (26-Inch Tall PCB Simulation).....	105
Figure 6.12 Summary of Detailed Simulation Results of 26-inch Tall Low-Profile PCB (Without Impact Tire Disengagement)	106
Figure 6.13 Front, Perspective and Side Views of a Segment of the 24-Inch Tall PCB Model.	112
Figure 6.14 Images of the 24-Inch tall barrier FE Model with Connection Details	112
Figure 6.15 Angular Displacements of the Vehicle in Case 1 (24-Inch Tall PCB Simulation) .	114
Figure 6.16 Initial and Deflected Shape of the 24-Inch Tall T Shaped PCB in Case 1	114
Figure 6.17 Energy Distribution History in Case 1 (24-Inch Tall PCB Simulation).....	116
Figure 6.18 Summary of Detailed Simulation Results of 24-inch Tall Low-Profile PCB (With Impact Tire Disengagement)	117
Figure 6.19 Angular Displacements of the Vehicle in Case 2 (24-Inch Tall PCB Simulation) .	119
Figure 6.20 Initial and Deflected Shape of the 24-Inch Tall T Shaped PCB in Case 2	119
Figure 6.21 Energy Distribution History in Case 2 (24-Inch Tall PCB Simulation).....	121
Figure 6.22 Summary of Simulation Results of 24-Inch Tall Low-Profile PCB (Without Impact Tire Disengagement).....	122
Figure 7.1 Images of the 26-Inch Tall T Shaped Low-Profile PCB Prior to MASH Test 3-11 .	129

	Page
Figure 7.2 Test Vehicle Prior to MASH Test 3-11	130
Figure 7.3 Test Vehicle at Targeted Impact Point Prior to MASH Test 3-11	130
Figure 7.4 Test Schematic.....	131
Figure 7.5 Images of 26-Inch Tall T Shaped Low-Profile PCB after MASH Test 3-11	133
Figure 7.6 Concrete Spalling at Joint 2-3	134
Figure 7.7 Thread Rods Deformation at Joint 2-3	134
Figure 7.8 Test Vehicle after MASH Test 3-11	134
Figure 7.9 Summary of Results for MASH Test 3-11 on the 26-Inch Tall T Shaped Low- Profile PCB	136
Figure 7.10 Test Vehicle Prior to MASH Test 3-10	137
Figure 7.11 Test Vehicle at the Targeted Impact Point Prior to MASH Test 3-10	138
Figure 7.12 Images of 26-Inch Tall T Shaped Low-Profile PCB after MASH Test 3-10	139
Figure 7.13 Test Vehicle after MASH Test 3-10.....	139
Figure 7.14 Summary of Results For MASH Test 3-10 on The 26-Inch Tall T Shaped Low-Profile Barrier.....	140
Figure 8.1 Front Impact Tire Disengagement.....	142
Figure 8.2 Roll, Yaw and Pitch Angles Comparison between Modified FEA and Crash Test ..	145

LIST OF TABLES

	Page
Table 3.1 Summary of Previous TTI Non-Proprietary Low-Profile Barrier Crash Tests	12
Table 3.2 Summary of Other Non-Proprietary Low Height Barriers	16
Table 4.1 Sight Obstruction Experiment of 24-Inch and 26-Inch Tall PCBs	23
Table 4.2 Headlight Mounting Height of 10 Best-Sold Passenger Cars in the U.S. in 2017	24
Table 4.3 Preliminary Profile Concepts for Low-Profile PCB	26
Table 5.1 Occupant Risk Values Comparison between Case 1 and Case 2 (26-Inch Tall PCB with 1:20 Slope)	34
Table 5.2 Sequential Images of Preliminary Simulations for 26-Inch Tall PCB with 1:20 Slope (Front View)	35
Table 5.3 Sequential Images of Preliminary Simulations for 26-Inch Tall PCB with a 1:20 Slope (Overhead View)	36
Table 5.4 Occupant Risk Values Comparison between Case 1 and Case 2 (26-Inch Tall PCB with 1:15 Slope)	38
Table 5.5 Sequential Images of Preliminary Simulations for 26-Inch Tall PCB with 1:15 Slope (Front View)	39
Table 5.6 Sequential Images of Preliminary Simulations for 26-Inch Tall PCB with 1:15 Slope (Overhead View)	40
Table 5.7 Occupant Risk Values Comparison between Case 1 and Case 2 (26-Inch Tall T Shaped PCB)	42
Table 5.8 Sequential Images of Preliminary Simulations for 26-Inch Tall T Shaped PCB (Front View)	43
Table 5.9 Sequential Images of Preliminary Simulations for 26-Inch Tall T Shaped PCB (Overhead View)	44
Table 5.10 Occupant Risk Values Comparison between Case 1 and Case 2 (26-Inch Tall T Shaped PCB with 1:20 Slope)	46

	Page
Table 5.11 Sequential Images of Preliminary Simulations for 26-Inch Tall T Shaped PCB with 1:20 Slope (Front View)	47
Table 5.12 Sequential Images of Preliminary Simulations for 26-Inch Tall T Shaped PCB with 1:20 Slope (Overhead View)	48
Table 5.13 Occupant Risk Values Comparison between Case 1 and Case 2 (26-Inch Tall I Shaped PCB).....	50
Table 5.14 Sequential Images of Preliminary Simulations for 26-Inch Tall I Shaped PCB (Front View).....	51
Table 5.15 Sequential Images of Preliminary Simulations for 26-Inch Tall I Shaped PCB (Overhead View).....	52
Table 5.16 Occupant Risk Values Comparison between Case 1 and Case 2 (26-Inch Tall I Shaped PCB with 1:20 Slope).....	54
Table 5.17 Sequential Images of Preliminary Simulations for 26-Inch Tall I Shaped PCB with 1:20 Slope (Front View)	55
Table 5.18 Sequential Images of Preliminary Simulations for 26-Inch Tall I Shaped PCB with 1:20 Slope (Overhead View)	56
Table 5.19 Occupant Risk Values Comparison between Case 1 and Case 2 (24-Inch Tall PCB with 1:20 Slope)	59
Table 5.20 Sequential Images of Preliminary Simulations for 24-Inch Tall PCB with 1:20 Slope (Front View)	60
Table 5.21 Sequential Images of Preliminary Simulations for 24-Inch Tall PCB with a 1:20 Slope (Overhead View)	61
Table 5.22 Occupant Risk Values Comparison between Case 1 and Case 2 (24-Inch Tall PCB with 1:15 Slope)	63
Table 5.23 Sequential Images of Preliminary Simulations for 24-Inch Tall PCB with 1:15 Slope (Front View)	64
Table 5.24 Sequential Images of Preliminary Simulations for 24-Inch Tall PCB with 1:15 Slope (Overhead View).....	65
Table 5.25 Occupant Risk Values Comparison between Case 1 and Case 2 (24-Inch Tall T Shaped PCB)	67

	Page
Table 5.26 Sequential Images of Preliminary Simulations for 24-Inch Tall T Shaped PCB (Front View).....	68
Table 5.27 Sequential Images of Preliminary Simulations for 24-Inch Tall T Shaped PCB (Overhead View).....	69
Table 5.28 Occupant Risk Values Comparison between Case 1 and Case 2 (24-Inch Tall T Shaped PCB with 1:20 Slope).....	71
Table 5.29 Sequential Images of Preliminary Simulations for 24-Inch Tall T Shaped PCB with 1:20 Slope (Front View)	72
Table 5.30 Sequential Images of Preliminary Simulations for 24-Inch Tall T Shaped PCB with 1:20 Slope (Overhead View)	73
Table 5.31 Occupant Risk Values Comparison between Case 1 and Case 2 (24-Inch Tall I Shaped PCB).....	75
Table 5.32 Sequential Images of Preliminary Simulations for 24-Inch Tall I Shaped PCB (Front View).....	76
Table 5.33 Sequential Images of Preliminary Simulations for 24-Inch Tall I Shaped PCB (Overhead View).....	77
Table 5.34 Occupant Risk Values Comparison between Case 1 and Case 2 (24-Inch Tall I Shaped PCB with 1:20 Slope).....	79
Table 5.35 Sequential Images of Preliminary Simulations for 24-Inch Tall I Shaped PCB with 1:20 Slope (Front View)	80
Table 5.36 Sequential Images of Preliminary Simulations for 24-Inch Tall I Shaped PCB with 1:20 Slope (Overhead View)	81
Table 5.37 Occupant Risk and Maximum Angular Displacements of Preliminary Simulations .	89
Table 6.1 Occupant Risk Values Comparison between Case 1 and Case 2 (26-Inch Height) ...	108
Table 6.2 Sequential Images of Case 1 and Case 2 of 26-Inch Tall PCB (Front View).....	109
Table 6.3 Sequential Images of Case 1 and Case 2 of 26-Inch Tall PCB (Overhead View).....	110
Table 6.4 Occupant Risk Values Comparison between Case 1 and Case 2 (24-Inch Height) ...	124
Table 6.5 Sequential Images of Case 1 and Case 2 of 24-Inch Tall PCB (Front View).....	125

	Page
Table 6.6 Sequential Images of Case 1 and Case 2 of 24-Inch Tall PCB (Overhead View).....	126
Table 8.1 Occupant Risk Factors Comparison between Original FEA and Crash Test	142
Table 8.2 Sequential Images of Full-Scale Crash Test and Original FEA	143
Table 8.3 Occupant Risk Factors Comparison between Modified FEA and Crash Test.....	145
Table 8.4 Sequential Comparison between Modified FEA and Crash Test (Front View)	146
Table 8.5 Sequential Comparison between Modified FEA and Crash Test (Overhead View) ..	148
Table 8.6 Roadside Safety Validation Metrics Rating Table (Single-Channel Option).....	151
Table 8.7 Roadside Safety Validation Metrics Rating Table for Validation (Multi-Channel Option Using Area II Method)	152

1. INTRODUCTION

Portable Concrete Barrier (PCB) system was developed to be used in work zones. The purpose of the PCB system was to prevent vehicles from crossing over medians into opposing traffic, or to prevent errant vehicles from traveling into work zones. However, the use of conventional 32-inch tall PCBs could cause a sight distance problem in certain work zone locations. These 32-inch tall barriers could obstruct a driver's line of sight, making it difficult for a driver to detect oncoming vehicles approaching on the other side of the barrier. Cross-traffic had to pull out into mainstream traffic before making eye contact with mainstream vehicles. This was especially a problem at night because the barrier could be taller than the height of some vehicle's headlight. To solve the problem, low-profile PCB system was initially developed in the early 1990s to enhance the visibility of drivers in low speed areas. Various shapes of low-profile PCB systems have been developed and crash tested by different research institutes in the last three decades. Most of them were developed under National Cooperative Highway Research Program (NCHRP) Report 350 Test Level 2 (TL-2, impact speed: 45mi/h) criteria [1]. In 2008, the crash test criteria was updated from NCHRP Report 350 to Manual for Assessing Safety Hardware (MASH) [2]. To enhance the roadside safety in high speed work zones, a new low-profile PCB system needs to be developed for high speed applications and under the requirement of MASH Test Level 3 (TL-3 impact speed: 62mi/h).

The first objective of this research was to develop a new low-profile PCB system which had a lower height compared with conventional 32-inch tall longitudinal barriers. Parametric study was conducted to select the appropriate barrier heights and profile shapes. To provide enough visibility for drivers, two barrier heights, 24 and 26 inches were chosen for further

investigation in this study. The development and evaluation of the preliminary barrier profile concepts were completed with engineering judgment and finite element analysis (FEA).

The second objective of the research project was to test and evaluate the new low-profile PCB in accordance with MASH testing criteria. Two full-scale crash tests were implemented. In the first crash test, MASH requires a 2270-kg pickup truck to be used to impact the barrier at a speed of 62 mi/h and an angle of 25.0 degrees. This test designation was used to test the strength of the barrier system. In the second crash test, barrier's ability to contain and redirect small passenger vehicles during the collision event was investigated. An 1100-kg passenger car impacted the barrier at a speed of 62mi/h and an angle of 25.0 degrees.

2. PROBLEM STATEMENT

In the past, it was felt that the sight distance problem would have to be tolerated if longitudinal barriers were to maintain a high degree of redirective capability. However, based upon the development of a low-profile PCB for use in low speed work zones by researchers in 1992 [3] , it has become clear that it is possible to significantly reduce the height of concrete barriers while continuing to maintain a significant amount of redirective capability. This advance was accomplished by designing a barrier contact face that prevents errant vehicles from rising during impact. This concept was demonstrated in the development of a 20-inch low-profile barrier for low speed work zones, in accordance with NCHRP Report 350 TL-2. After the crash test criteria was updated to MASH, there are few portable concrete barrier systems available for MASH TL-3 applications, but they all have a height of 32 inches.

Therefore, a new MASH TL-3 low-profile PCB needs to be developed and evaluated.

The design constraints of this new low-profile barrier are the following:

- The barrier's height should be short enough to provide sufficient visibility for drivers;
- The barrier should be capable of redirecting errant vehicles over an appropriate range of vehicle weights, speeds and impact angles;
- The barrier should be easy to transport, construct and remove ;
- The barrier should be able to use as a free standing barrier, no anchorage to ground;
- The barrier should have an appropriate small deflection after high speed impact.

3. LITERATURE REVIEW

3.1 Introduction

The section herein presents an overall review of what has been accomplished in the area of low height barriers. The literature review is divided into three different parts. The first part (Section 3.2) introduces the development of crash testing criteria. The second part (Section 3.3) includes a review of concrete portable barriers. The third part (Section 3.4) summarizes low height barriers developed and evaluated by TTI and other research institutes.

3.2 Development of Crash Testing Criteria

In 1974, NCHRP Report 153 “Recommended Procedures for Vehicle Crash Testing of Highway Appurtenances” was published [4]. This document provided the first complete test matrix for evaluating safety features. Data collection methods, evaluation criteria, and limited guidance on reporting formats were included. These procedures gained wide acceptance following their publication, but it was recognized at that time that periodic updating would be needed.

Published in 1978, Transportation Research Circular 191 “Recommended Procedures for Vehicle Crash Testing of Highway Appurtenances” [5] provided limited interim changes to NCHRP 153 to address minor changes requiring modified treatment of particular problem areas. An extensive revision and update to these procedures was made in 1981 with the publication of the NCHRP Report 230 “Recommended Procedures for the Safety Performance Evaluation of Highway Appurtenances [6].” In 1993, NCHRP Report 350 “Recommended Procedures for the Safety Performance Evaluation of Highway Features” was published. This document, which was prepared by TTI researchers under NCHRP Project 22-7, represented a comprehensive update to

crash test and evaluation procedures. It incorporated significant changes and additions to procedures for safety-performance evaluation, and updates reflecting the changing character of the highway network and the vehicles using it.

An update to NCHRP Report 350 was developed under NCHRP Project 22-14(02), “Improvement of Procedures for the Safety-Performance Evaluation of Roadside Features.” This document, “Manual for Assessing Safety Hardware (MASH)” published by AASHTO, contains revised criteria for safety-performance evaluation of virtually all roadside safety features. For example, MASH recommends testing with heavier light truck vehicles to better represent the current fleet of vehicles in the pickup/van/sport-utility vehicle class. Further, MASH increases the impact angle for most of the small car crash tests to the same angle as the light truck test conditions. These changes place greater safety-performance demands on many of the current roadside safety features. In late 2016, AASHTO published an updated edition of the MASH document (referred to as “MASH 2016”) [7].

Figure 3.1 shows the development of crash test criteria.

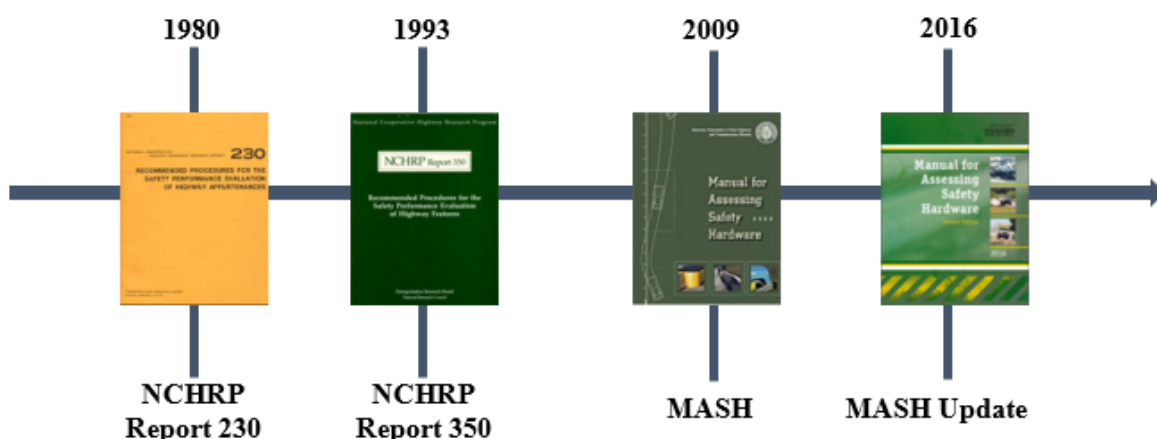


Figure 3.1 Development of Crash Test Criteria

3.3 Portable Concrete Barrier

PCBs are the most widely used type of work zone barrier to keep errant vehicles from traveling off the road or into opposing traffic, and provide an excellent form of safety for construction workers without investing too much time installing protection. Per FHWA definition, a portable barrier is “a barrier that is intended to be moved to a new location at a future time.”

The impact performance of PCBs is influenced by a number of variables including: barrier shape/profile, barrier height, segment length, barrier-roadway friction, etc. Among these factors, profile and height of the barrier affect vehicle stability most during an impact event. Different profiles of PCBs have been successfully developed and accepted for application by FHWA. The most common types of PCBs are New Jersey shape barrier, F-shape barrier, single-slope barrier and low-profile barrier.

The New Jersey shape barrier was developed by the New Jersey State Highway Department in the 1950s [8]. The state highway department observed the accident results of its barrier installations, and evolved the shape of the barrier [9]. As Figure 3.2 shows, this barrier design is intended to minimize sheet metal damage by allowing the vehicle tires to ride up on the lower sloped face in the shallow-angle impacts.

During the 1970s, FHWA set out to design a new concrete safety barrier shape that would perform the same functions as the New Jersey Barrier, but would have a lower incidence of vehicle rollovers. A parametric study was performed through computer simulations of barrier profiles labeled “A” through “F” [10]. From full-scale crash tests, the “F” was found to have the lowest potential for small cars to rollover upon impact. These results showed that “F” performed

distinctly better than the New Jersey-shape. Thus, configuration “F” became known as the F-shape, Figure 3.3 shows the illustration of F-shape barrier.

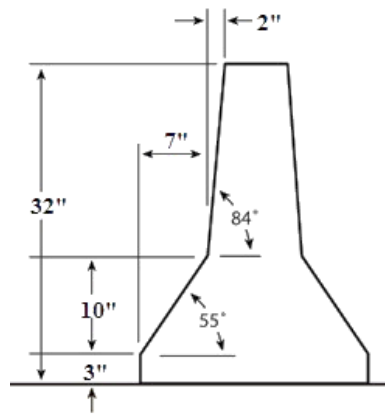


Figure 3.2 New Jersey Shape Barrier

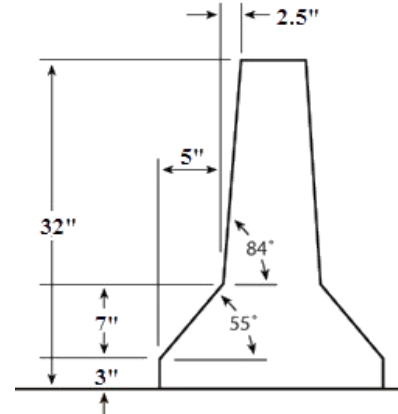


Figure 3.3 F-Shape Barrier

Though the New Jersey and F-Shape barrier shapes gained widespread acceptance, there were practical disadvantages with their use, such as the fact that they do not accommodate any road re-surfacing without substantially changing the height and shape of the barriers, which would make both barriers performance unsatisfactory as the pavement overlay increases. Thus, TTI and Texas State Department of Highways and Public Transportation (SDHPT) developed a new profile of concrete barrier with a single slope face [11], as Figure 3.4 shows. Full-scale crash tests demonstrated that the single-slope concrete barrier performed acceptably according to NCHRP Report 230 criteria.

Since the 32-inch concrete longitudinal barriers were widely used, there have been a sight-distance problem associated with these barriers, especially in certain combination of work zone locations with horizontal and vertical curvature. The barriers can obstruct drivers' eyesight. This was particularly a problem in work zones at night because the barrier can be taller than the headlights. To solve the sight-distance problem while protecting the errant vehicles, researchers

at TTI originally developed a 20-inch tall low-profile portable concrete barrier (Figure 3.5) for the application in low-speed work zones in the early 1990s [3].

A summary of the portable concrete barriers is reported in Figure 3.6.

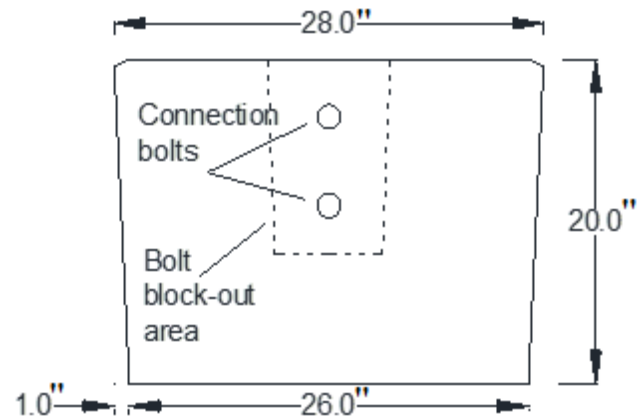
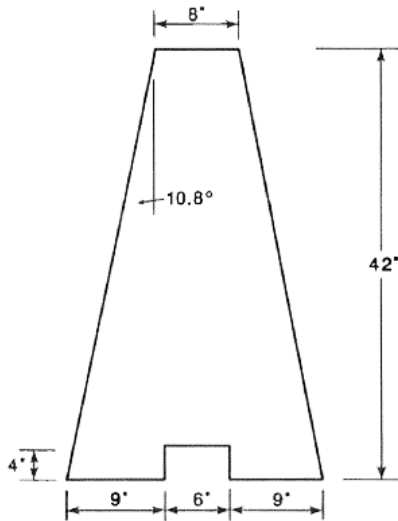


Figure 3.4 42-Inch Tall Single Slope Barrier Figure 3.5 20-Inch Tall Low-Profile Barrier



New Jersey Shape Barrier

The New Jersey shape was initially developed to minimize vehicle sheet metal damage during shallow angle impacts by allowing the vehicle tires to ride up onto the lower sloped toe of the barrier. However, the flatter lower slope can cause significant instability to vehicles impacting at high speed and angles.



F-Shape Barrier

The F-shape profile has the same basic geometry as the New Jersey barrier. The primary difference between two profiles is the height of the lower sloped toe. It is widely believed that F-shape provides better overall impact performance than the New Jersey shape profile.



Single Slope Barrier

The 10.8 degree single-slope barrier performs comparably to the New Jersey barrier. The primary advantage of the single-slope barrier is that the pavement adjacent to the barrier can be overlaid several times without changing the performance of the barrier.



Low-Profile Barrier

The 20-inch tall portable concrete barrier with a reverse slope can be used for low speed work zones and intersections. However, there is a need to develop a concrete only low-profile barrier for high speed applications.

Figure 3.6 Summary of Conventional PCBs

3.4 Previous Research on Low Height Barriers

3.4.1 Low-Profile Concrete Barriers Development in TTI

Low-profile portable concrete barrier was initially developed by researchers at TTI. The 20-inch tall low-profile barrier was designed with a negative 1:20 vertical slope, which could reduce the vertical displacement of the vehicle on the impact side. The 20-ft long segments and the segment connection tolerance were designed to allow the system to accommodate application at a wide variety of vertical and horizontal roadway curvatures. Full-scale crash tests demonstrated that the 20-inch tall low-profile barrier was capable of redirecting a reasonable range of vehicles impacting with speeds of 45 mi/h. Testing was conducted according to the NCHRP Report 230 evaluation criteria. Based on a comprehensive review of the original testing conducted with the low-profile PCB system, it was determined that the original test results were sufficient to be deemed compliant with the new NCHRP Report 350 evaluation criteria [12]. The 20-inch tall low-profile PCB was accepted for NCHRP Report 350 TL-2 applications.

After the successful development of the 20-inch tall low-profile PCB, TTI researchers conducted several studies and full-scale crash tests to develop and evaluate low-profile barriers for high speed applications. Table 3.1 summarizes the crash tests completed at TTI from 1991 to 2007. These barriers were tested in compliance with NCHRP Report 230 or NCHRP Report 350. It should be noted that there are not any MASH tests implemented.

As Table 3.1 shows, in 1993, TTI implemented a successful low-profile PCB crash test with a 1981 Cadillac Coupe Deville. The objective of the test was to evaluate the application of the 20-inch tall low-profile PCB in high speed condition. The 4500lb large sedan (2043 kg)

impacted the barrier at a speed of 61.1 mi/h and with an angle of 24.9 degrees. The barrier received moderate damage at the impact connection and had a 7.0-inch lateral displacement.

In 1995, a pickup truck (Chevrolet 2500) was used to impact with the 20-inch tall low-profile PCB. The impact speed was 63.1 mi/h and the impact angle was 25.0 degrees. However, the result turned to be unacceptable due to the vehicle roll over. Based on the failure of the previous test, TTI researchers reviewed and analyzed the results. Two additional high speed pickup truck crash tests were performed in 1996. Researchers increased the heights of the low-profile PCB to 22.6 inch and 25.4 inch respectively, while kept the negative slope for the PCB. The two PCBs were crash tested in compliance with NCHRP Report 350 TL-3, but the pickup trucks rolled over in both tests.

To address the problem for high speed application, TTI researchers applied modifications to the 20-inch tall low-profile PCB [13]. Researchers used the existing 20-inch tall low-profile PCB as the base and designed two steel rail retrofit attachments on the top for roadside and median applications. Both retrofit systems performed acceptably and met the evaluation criteria for NCHRP Report 350 TL-3. Figure 3.7 and Figure 3.8 show the two designs, respectively.











Figure 3.7 Roadside Application



Figure 3.8 Median Application

Table 3.1 Summary of Previous TTI Non-Proprietary Low-Profile Barrier Crash Tests

Test Year	Test Criteria	Barrier Height (inch)	Test Vehicle	Impact Condition		Picture	Result
				Speed (mi/h)	Angle (degree)		
1991	NCHRP Report 230	20	2000P GMC Sierra 2500	44.4	26.1		Pass
1991	NCHRP Report 230	20	820C Honda Civic	45.7	23.1		Pass
1993	NCHRP Report 230	20	4500S large sedan	61.1	24.9		Pass
1995	NCHRP Report 230	20	2000P Chevrolet 2500	63.1	25.0		Fail
1996	NCHRP Report 350	22.6	2000P Chevrolet 2500	61.8	26.4		Fail
1996	NCHRP Report 350	25.4	2000P Chevrolet Cheyenne	62.0	26.7		Fail
2006	NCHRP Report 350	39 (includes 19-inch tall attachment)	2000P Chevrolet C2500	62.8	25.5		Pass
2007	NCHRP Report 350	39 (includes 19-inch tall attachment)	2000P Chevrolet C2500	62.0	26.1		Pass

3.4.2 NCHRP Report 350 TL-3 Rigid Barriers with Low Heights

In 1998, a successful NCHRP Report 350 TL-3 cash test was implemented on the Texas type T202 bridge rail [14]. The bridge rail was 27-inch tall and tested by a 2000-kg 1993 Chevrolet pickup truck with a 62.14 mi/h speed and a 25-degree angle. The picture of the T202 bridge rail is shown in Figure 3.9.

In 2003, TTI conducted a crash test to evaluate the performance of the tubular steel-backed timber bridge rail [15] in accordance with the guidelines presented in NCHRP Report 350 test 3-11. The bridge rail was a tubular steel-backed timber beam and post railing system constructed to provide a more rustic appearance than a conventional steel or concrete barrier. Figure 3.10 shows the installation of this bridge rail. The 27-inch tall bridge rail was impacted by a 1998 Chevrolet Cheyenne 2500 pickup truck with a 61.9 mi/h speed and a 25.5-degree angle. The test results met the required specifications of NCHRP Report 350 TL-3.

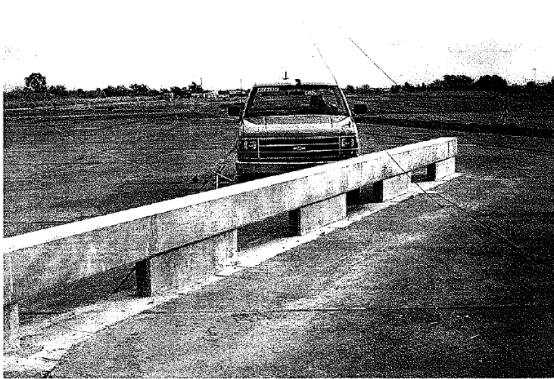


Figure 3.9 Texas Type T202 Bridge Rail



Figure 3.10 Tubular Steel-Backed Timber Bridge Rail

3.4.3 Other Low Height Barriers

Besides the low-profile barriers developed in TTI, there is a number of low-profile barrier options from other institutes. These institutes include Caltrans, Florida DOT, Midwest Roadside Safety Facility, etc. These barriers have been successfully developed and evaluated through crash tests at TL-2 or TL-3.

University of Florida developed a low-profile PCB for use in roadside work zone environments in 2003 [16]. The barrier was only 18 inches in height with segment lengths of 12 ft. The barrier was crash tested and met the NCHRP Report 350 TL-2 requirements. Figure 3.11 demonstrates the cross-section of the low-profile PCB. The connection bolts were embedded in the concrete near the back face of the barrier. This connection design was able to carry the tensile loads in the bolts and transfer shear from one segment to the adjacent one during impact, with the attempt to limit vehicle snagging during impact event. Rather than relying on mechanical anchoring between the barrier and the roadway surface, the barriers could be formed as curved barrier system.

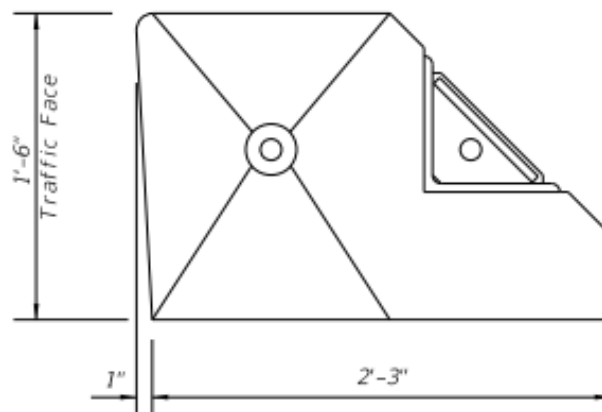


Figure 3.11 Florida 18-Inch Tall TL-2 Low-Profile PCB







The California Department of Transportation (Caltrans) developed a low-maintenance low-profile barrier for low speed applications [17] . This barrier consisted in metal post and beam railing attached to a 6-inch curb and it was designed to provide better visibility while increasing aesthetics. Posts are spaced 10-ft apart, and the system includes a 12-inch deep footing below ground. Full-scale crash tests proved that the barrier met NCHRP Report 350 TL-2 requirements.

There are a few low height barrier systems designed for rigid applications by the Midwest Roadside Safety Facility (MwRSF). The MwRSF developed and crash tested a 75-ft long, 20-inch tall, low-profile reinforced concrete bridge railing system [18]. This system was successfully evaluated according to the NCHRP Report 350 TL-2 criteria. The MwRSF also developed two rough stone masonry guardwalls, 22-inch and 20-inch tall, respectively [19]. Crash tests performed according to NCHRP Report 350 TL-2 criteria showed acceptable results for both heights.

TTI developed and completed a safety performance evaluation of a 27 inches tall, double-faced, rough stone masonry guardwall system according to the NCHRP Report 350 TL-3 criteria [20].

Table 3.2 summarizes the developed non-proprietary low height barrier systems, for both temporary and rigid applications.

Table 3.2 Summary of Other Non-Proprietary Low Height Barriers

Barrier	Test Criteria	Test Level	Barrier Height (Inch)	Connection with Ground	Impact Condition		Figure
					Speed (mi/h)	Angle (degree)	
Caltrans Low-Profile Barrier	NCHRP Report 350	TL-2	18	Embedded in the ground	43.6	25.3	
Midwest Low Profile Concrete Bridge Rail	NCHRP Report 350	TL-2	20	Pinned to the ground	43.5	27.1	
Florida DOT Low-Profile Barrier	NCHRP Report 350	TL-2	18	No mechanical anchoring	41.9	25	
TL-2 Rough Stone Masonry Guardrail I	NCHRP Report 350	TL-2	22	Rigid	44.4	24.2	
TL-2 Rough Stone Masonry Guardrail II	NCHRP Report 350	TL-2	20	Rigid	43.6	24.4	
TL-3 Stone Masonry Guardwall	NCHRP Report 350	TL-3	27	Rigid	58.4	24.5	

4. SELECTION OF BARRIER HEIGHTS AND PROFILE CONCEPTS

4.1 Introduction

The ability of a PCB to adequately contain and redirect an impacting vehicle is affected by various factors, including its height and profile. In order to offer proper vehicle containment and redirection, the barrier needs to be designed with an appropriate height. In fact, an impact against a barrier which is not designed to provide adequate minimum height, can cause the impacting vehicle either vault or roll over after it impacts the barrier system. Even when designed to a minimum required height, a barrier needs to have a crashworthy profile, meaning that its impacted face geometry needs to be adequately designed to provide proper tire (and vehicle) interaction to maintain vehicle stability throughout the impact event. The need for a low-profile barrier is dictated by the necessity for drivers to have clear visibility of upcoming vehicles on the other side of such barrier. In other words, a low-profile system needs to be adequately designed to allow needed driver's visibility, while maintaining required height, strength, and crashworthy profile.

4.2 Barrier Heights Selection

4.2.1 General Considerations

An unobstructed line-of-sight between the cross-traffic drivers' eye and the center of the headlight of the oncoming vehicle provides the boundary for acceptable barrier performance. To study the sight-distance problem, it is necessary to define the eye height of the driver, headlight heights and other related geometric constraints.

According to "A Policy on Geometric Design of Highways and Streets, 2011" [21]. Sight distance is the distance along a roadway throughout which an object of specified height is

continuously visible to the driver. This distance is dependent on the height of the driver's eye above the road surface, the specified object height above the road surface, and the height and lateral position of sight obstructions within the driver's line of sight. For all sight distance calculations for passenger vehicles, the height of the driver's eye is considered 42 inches (3.50 ft) inches above the road surface. This value is based on a study that found average vehicle heights have decreased to 51 inches (4.25 ft) with a comparable decrease in average eye heights to 42 inches (3.50 ft).

Federal Motor Vehicle Safety Standard 108 (FMVSS 108) [22] requires the center of the device lens must be mounted no less than 24 inches above the road surface. Figure 4.1 illustrates the requirement of headlight mounting height.

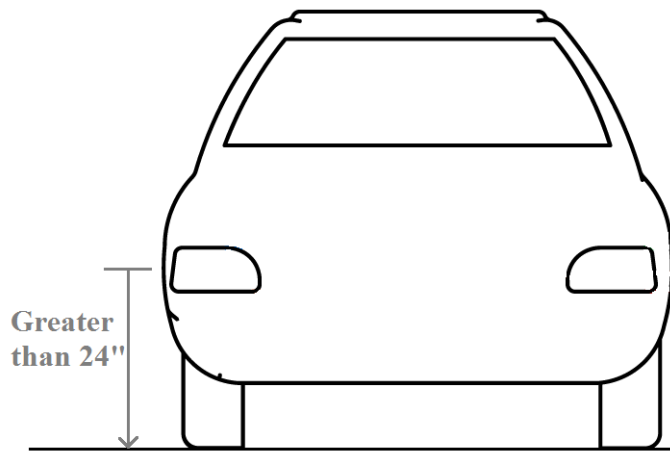


Figure 4.1 Requirement of Vehicle Lens Mounting Height

In 1991, researchers [3] conducted a random survey of one hundred vehicles to establish the range of typical headlight heights and found most of the cars at that time had headlight mounting heights between 24 and 28 inches. Simplified geometric analyses were conducted to study the sight-distance problem. It was found that the cross-traffic driver's sight-distance is unlimited as long as the barrier height is less than 24 inches (minimum headlight mounting height) for constant slope and sag vertical curves. In the case of crest vertical curves, it was found that the cross-traffic driver's sight-distance is significantly increased by the use of barrier heights less than 24 inches.

To date, no minimum portable concrete barrier height for MASH TL-3 applications has been investigated or determined. Barriers with height lower than 24 inches may not be able to contain and redirect an errant vehicle impacting at MASH TL-3 conditions. Therefore, heights of 24 and 26 inches were chosen as candidate barrier heights to be further investigated within this study.

4.2.2 Sight Obstruction

Barriers installed near intersections can cause issues for sight-distance obstruction. Each quadrant of an intersection should contain a triangular area free of obstructions that might block an approaching driver's view of potentially conflicting vehicles. Figure 4.2 and Figure 4.3 illustrate the geometry of sight obstruction problem of median and roadside barriers in intersections.

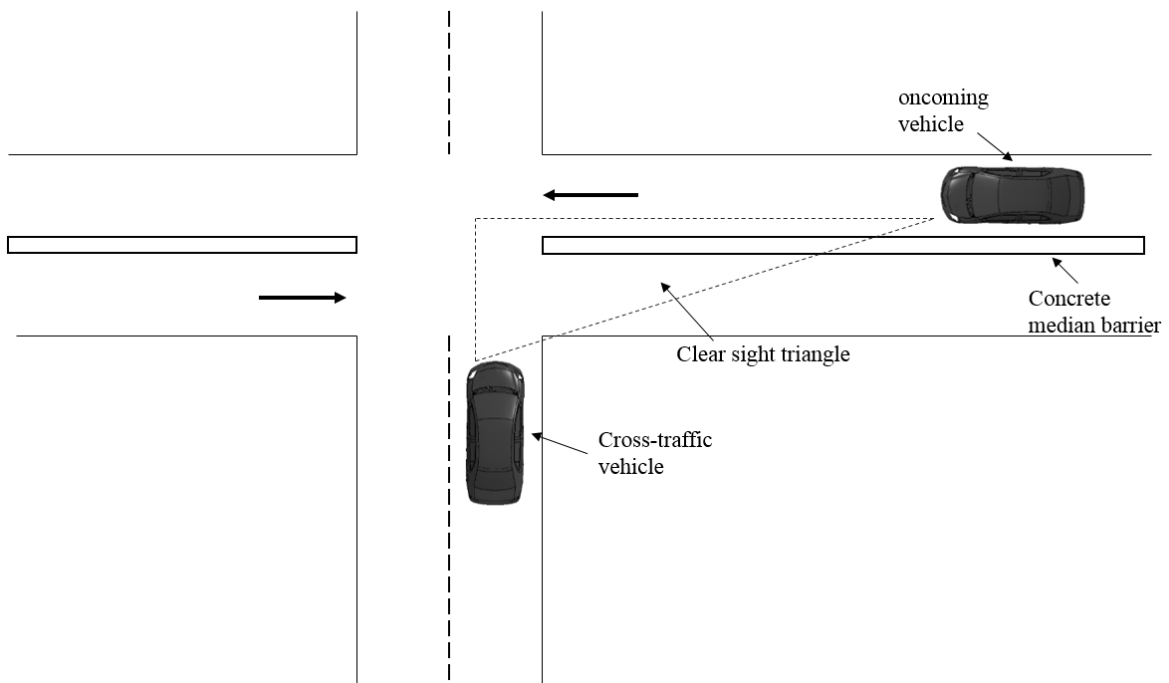


Figure 4.2 Sight Obstruction Of Median Barrier

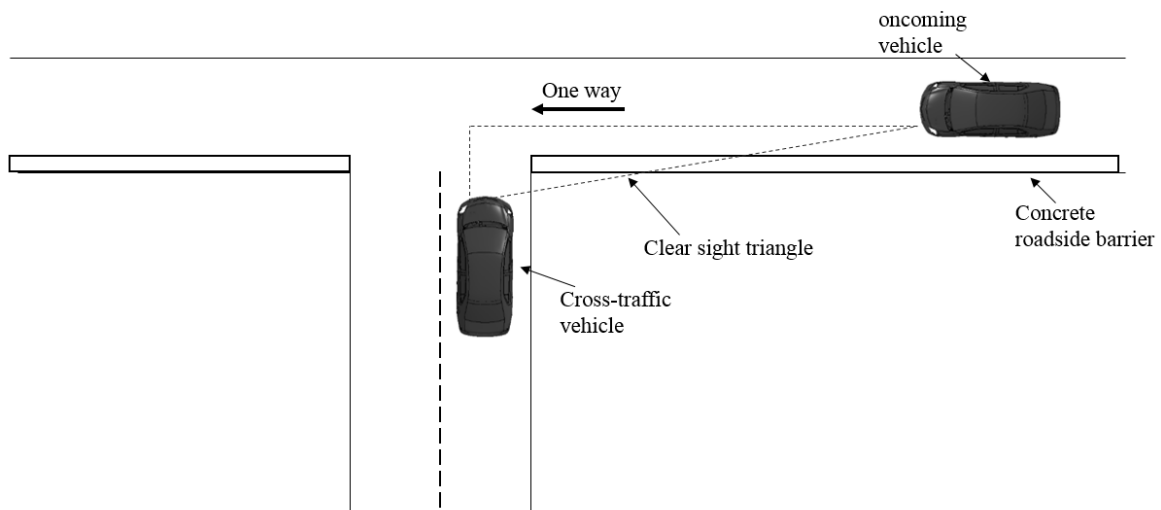


Figure 4.3 Sight Obstruction Of Roadside Barrier

A simplified experiment was conducted to check the sight distance obstruction problem of 24-inch and 26-inch tall barriers. The vehicle used in this experiment was a 2011 Kia Rio. A camera was placed at a distance of 600 ft from the vehicle. Based on the driver's eye height concept, the camera was set to be 42 inches above the ground surface. Two different lateral distances from the barrier to the camera were considered to replicate roadside and median barrier applications. The relative vehicle headlight mounting height was adjusted to be 24 inches. The relative headlight mounting height was adjusted to be 24 inches. Figure 4.4 and Figure 4.5 illustrate the geometric analyses for sight obstruction of 24-inch and 26-inch tall barriers. Table 4.1 shows the zoomed-in views of the experiments. Results from this analysis showed that the 24-inch tall barrier allowed sufficient vision of both headlights of an upcoming passenger car. While the upcoming vehicle's right headlight resulted basically unobstructed by the barrier, the left headlight was just minimally obstructed. With the barrier height increased to 26 inches, a higher percentage of both headlights was obstructed. There was, however, still sufficient visibility of both headlights to allow seeing the upcoming vehicle at night.

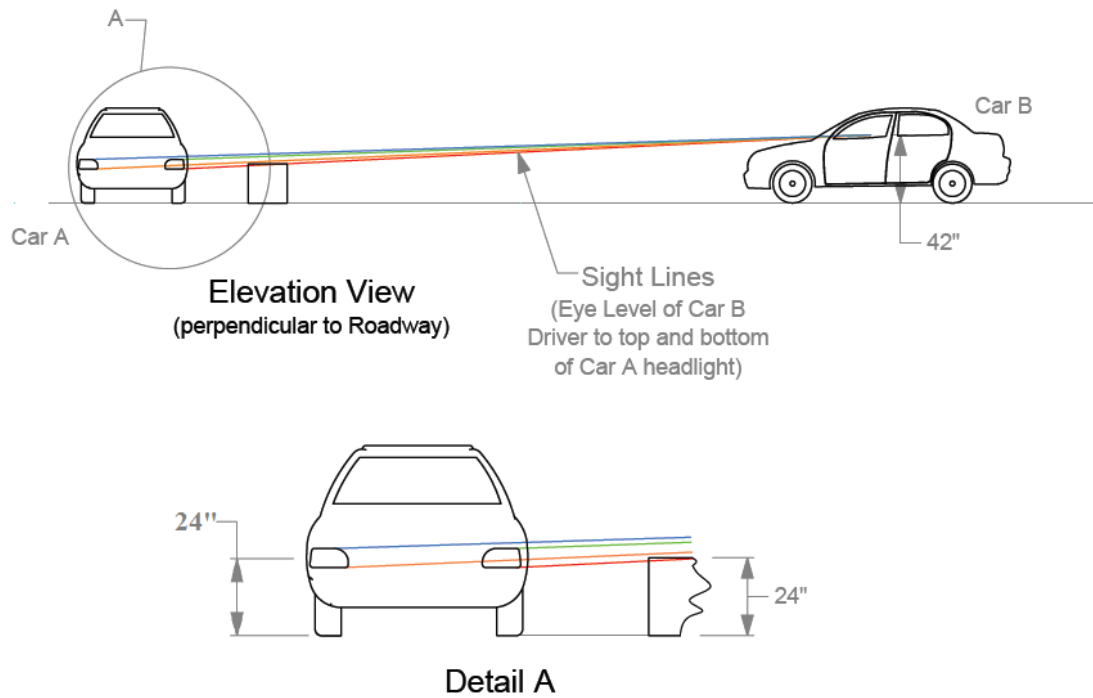


Figure 4.4 Sight Obstruction of 24-Inch Tall Barrier

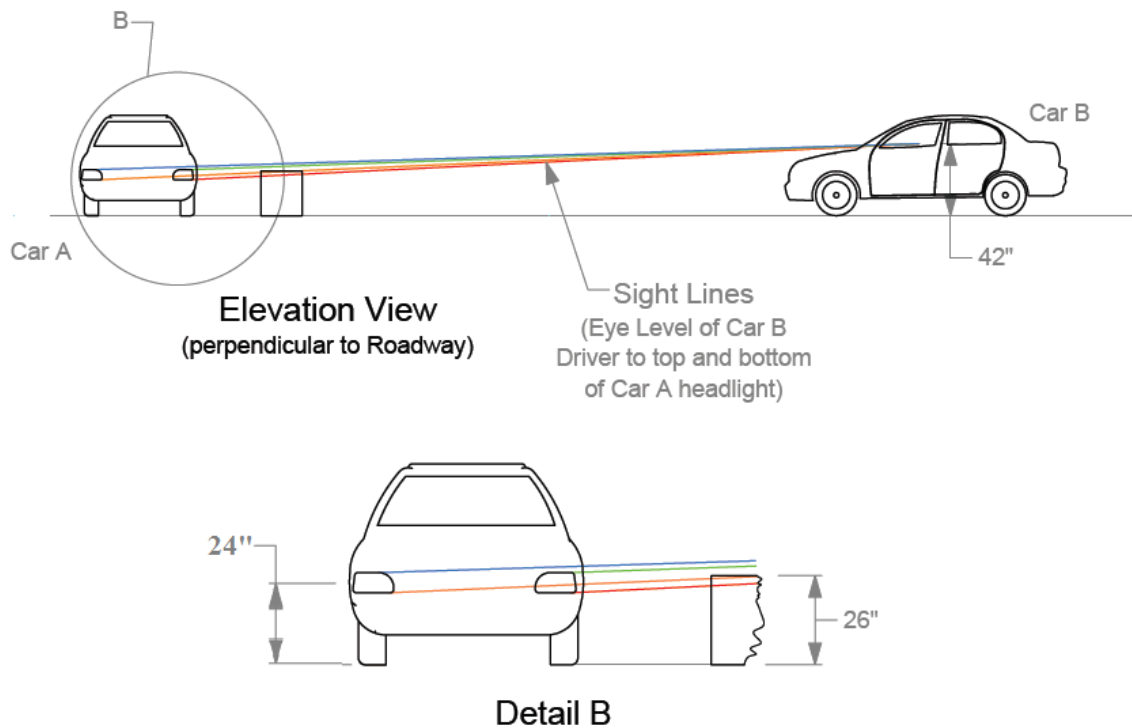






Figure 4.5 Sight Obstruction of 26-Inch Tall Barrier

Table 4.1 Sight Obstruction Experiment of 24-Inch and 26-Inch Tall PCBs

Barrier Height (Inch)	Lateral Distance from Vehicle (Feet)	
	18	30
24		
26		

It has been 25 years since the 20-inch tall TL-2 low-profile PCB was developed. With the auto industry continuing to innovate and adapt, a search was conducted on the best-sold passenger cars in the U.S in 2017 as listed in Table 4.2 [23]. The search concluded that all best-sold passenger cars have headlight mounting height greater than or equal to 26 inches. Among them, only the Ford Fusion has the minimum headlight mounting height of 26 inches among all of them. These cars represent most popular passenger cars on road and give evidence that a 26-inch tall concrete barrier is still available to provide sufficient visibility for drivers.

Table 4.2 Headlight Mounting Height of 10 Best-Sold Passenger Cars in the U.S. in 2017

Type of vehicle	Headlight mounting height (inch)
Toyota Camry (L4) 4 door sedan	29
Honda Civic 4 door sedan	27
Toyota Corolla 4 door sedan	27
Honda Accord (L4) 4 door sedan	27
Nissan Altima (L4) 4 door sedan	27
Nissan Sentra 4 door sedan	28
Ford Fusion 4 door sedan	26
Hyundai Elantra 4 door sedan	27
Chevrolet Malibu 4 door sedan	28
Chevrolet Cruze 4 door sedan	27

4.3 Barrier Profile Concepts Development


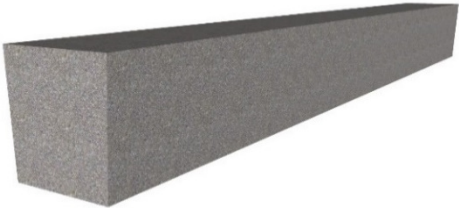



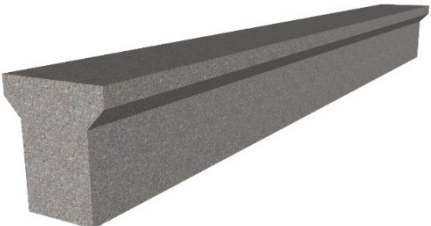

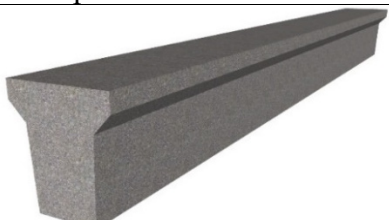

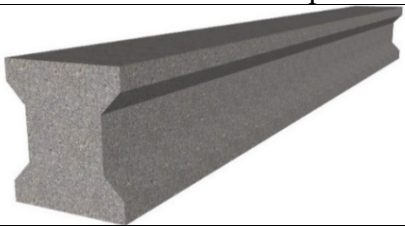

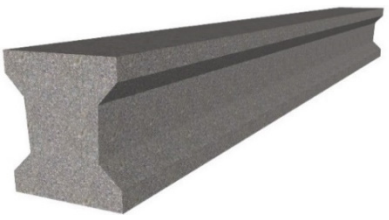
Several profile shape concepts were developed for the new MASH TL-3 barrier. Particular attention was given towards developing a barrier profile that would limit vehicle climbing. Specifically, the new barrier profile concepts focused on keeping the impacting vehicle tires closer to ground level, thus limiting vehicle instability during the impact event.

Table 4.3a shows a concept of a low-profile barrier with a negative angle slope. Based on the 20-inch tall low-profile barrier, this concept increases the barrier height while keeping the 1:20 negative slope, since this negative slope was determined to be able to restrict the tendency for the impact side of the vehicle to rise. Table 4.3b shows a low-profile barrier with a 1:15 slope, this concept can be considered as a variation of the original low-profile barrier concept.

Table 4.3c shows a concept of a T shaped low-profile barrier. This concept can be considered as a vertical wall with a protruding step at the top of the barrier. It is believed that the probability of the tire climbing the barrier's face could be reduced if the barrier face extended further out at the top than at the lower regions. To further reduce the rise of the vehicle, a 1:20 negative slope is applied to the T shaped low-profile barrier as Table 4.3d shows.

Table 4.3e and Table 4.3f show the concepts of I shaped low-profile barrier and I shaped low-profile barrier with a 1:20 negative slope, respectively. The I shaped concept can be considered as a variation of the T shaped concept.

Table 4.3 Preliminary Profile Concepts for Low-Profile PCB

	
(a) Low-profile PCB with 1:20 slope	
	
(b) Low-profile PCB with 1:15 slope	
	
(c) T shaped low-profile PCB	
	
(d) T shaped low-profile PCB with 1:20 slope	
	
(e) I shaped low-profile PCB	
	
(f) I shaped low-profile PCB with 1:20 slope	

5. PRELIMINARY FINITE ELEMENT ANALYSIS OF DESIGN CONCEPTS

5.1 Introduction

Implementing multiple full-scale crash tests to evaluate the performance of the concepts developed in Section 4 would be costly and not feasible in the research period. Instead of implementing full-scale crash tests, preliminary finite element computer simulations were performed with the objective to evaluate and compare the crashworthiness of the proposed low-profile PCB concepts using the finite element model of a pickup truck, under MASH Test 3-11 conditions. It was opted not to evaluate a small car impact in finite element simulations since the pickup truck has more significant impact severity and instability. For each of the preliminary barrier concepts, two barrier heights were evaluated: 24 and 26 inches. Under these preliminary computer simulations, the various barrier systems were modeled as free-standing 120-ft long concrete blocks, without simulating barrier segment lengths or connections.

A commercially available finite element software package LS-DYNA [24] was used to simulate vehicular impacts with low-profile concrete barriers. LS-DYNA is a general purpose, explicit finite element code. It is widely used to solve nonlinear, dynamic response of three-dimensional problems and is capable of capturing complex interactions and dynamic load-time history responses that occur when a vehicle impacts a barrier system.

5.2 Evaluation Criteria

Each of the proposed barrier concepts and heights were evaluated under two different cases:

- Case 1. Vehicle's front impact tire was modeled with the ability of disengage from the suspension assembly, to represent failure of the tire system;

- Case 2. Vehicle's front impact tire was not given the ability to disengage from the suspension system.

Vehicle stability, occupant risk, and structural adequacy were mainly evaluated in the preliminary finite element simulations. Vehicle angular velocities, also known as yaw, pitch and roll angles, were used to evaluate the vehicle stability. As Figure 5.1 shows, yaw, pitch and roll describe the vehicle rotation about the x-axis, y-axis and z-axis, respectively. MASH specifies that the maximum roll and pitch angles are not to exceed 75 degrees. Occupant risk describes the risk of hazard to occupants. It is evaluated from the data collected by the accelerometer located at the center of gravity in the vehicle. Two factors were mainly analyzed in preliminary simulations through the acceleration data: Occupant Impact Velocity (OIV), Occupant Ridedown Acceleration (ORA). OIV and ORA are the change in velocity the hypothetical occupant feels at impact and the acceleration from the collision just after impact. MASH requires the OIV to be lower than 40 ft/s and ORA to be smaller than 20.49 G in longitudinal and lateral directions. The structural adequacy of the system is determined by the barrier's ability to redirect and contain the vehicle.

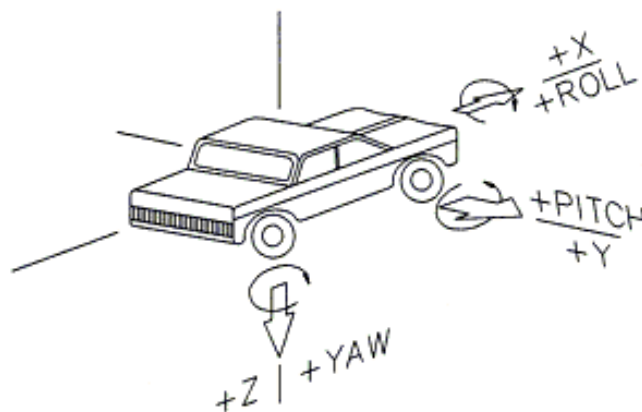


Figure 5.1 Roll, Pitch and Yaw Crash Test Sign Convention

5.3 FE Models for Preliminary FE Simulations

5.3.1 Vehicle FE Model and Modifications

Testing conditions of MASH Test 3-11 were replicated with the use of an available pickup truck model representing MASH vehicle 2270P (Figure 5.2), impacting the PCB system at MASH TL-3 nominal conditions with a speed of 62 mi/h and an angle of 25 degrees [25].

Several modifications were made to the existing vehicle model. Under MASH TL-3 pickup truck impacts, crash tests experience shows that it is not uncommon for the pickup truck front impact tire to disengage from the suspension assembly. Figure 5.3 shows the disengagement of the impact tire after a MASH 3-11 test. Disengagement of the front tire can increase vehicle roll and decrease vehicle climb on the barrier. Additionally, disengagement of the front impact tire tends to produce instabilities in some impact configurations due to the interaction of the disengaged tire with the barrier and ground.

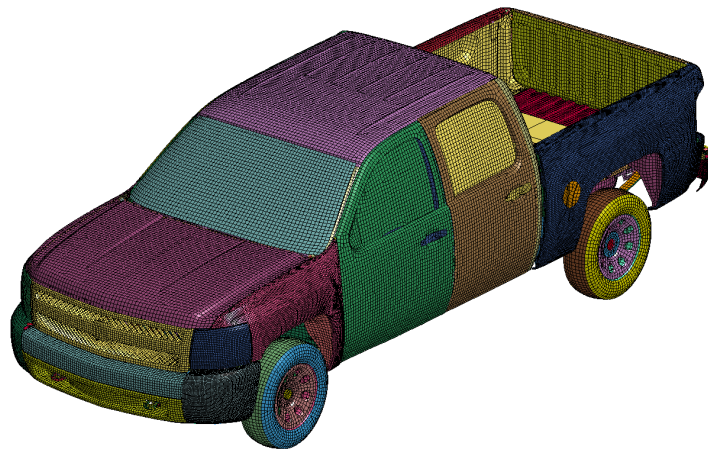


Figure 5.2 Available MASH 2270P Pickup Truck FE Model



Figure 5.3 Impact Tire Disengagement after a MASH 3-11 Crash Test

Figure 5.4a shows the impact tire and suspension assembly of the MASH 2270P pickup truck model. The suspension assembly is composed of upper and lower rotating control arms. Spherical joints connect the control arms to the knuckle of the tire assembly and revolute joints connect the wheel to the chassis rail so that the tire can rotate about the axes of the revolute joint. Figure 5.4b shows the location of those joints.

To achieve the disengagement, force-based failure options were applied in the joint card in LS-DYNA. During the impact event, when forces in the joints exceeded the failure limits, front impact tire would be disengaged from the suspension system and chassis rail.

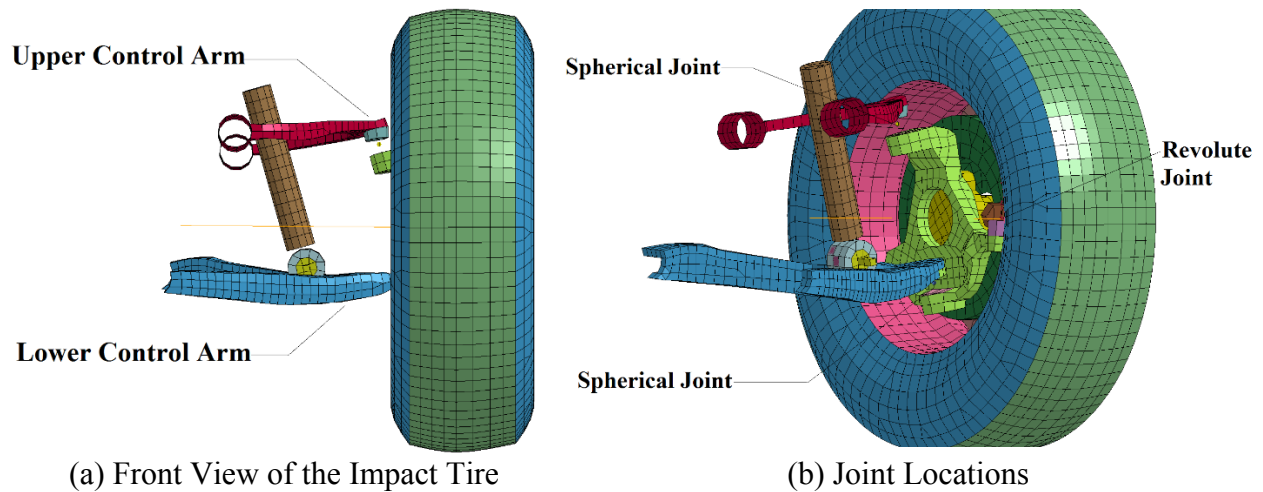


Figure 5.4 FE Model of Front Impact Tire and Suspension Assembly

5.3.2 Portable Concrete Barrier FE Models

Since the preliminary simulations were used to determine the best profile concept, to be cost-efficient and to save computational resources, it was decided to build the barrier models as 120-ft long free-standing rigid concrete blocks. There were no connections or segments. Eight-node solid brick elements with rigid material were used to construct the concrete barrier model, and four-node shell elements were used to build the ground. The static frictional coefficient between the ground and barriers was 0.63 while the dynamic frictional coefficient was 0.26. These values were selected based on testing conducted by NCAC in which they drag PCBs on concrete to determine frictional coefficients [26]. It should be noted that the failure of the concrete was not included in the preliminary FE simulations.

5.4 Preliminary Finite Element Analysis of 26-Inch Tall PCB Concepts

5.4.1 Introduction

In the preliminary FE simulations, all of the 26-inch tall, 180-feet long, free-standing concrete block with different profile shapes were impacted by the 2270P pickup truck with a speed of 62 mi/h and an angle of 25 degrees. Based on MASH requirements, the vehicle impacted the barrier at about one-third of the system length. Two cases were considered in the simulation: Case 1, with impact tire disengagement; Case 2, without impact tire disengagement.

5.4.2 26-Inch Tall PCB with 1:20 Slope

In both cases, the pickup truck remained upright during and after the collision events. Figure 5.5 and Figure 5.6 show vehicle roll, pitch and yaw angles throughout the impact events against the 26-inch tall PCB with 1:20 slope in both cases, respectively. Maximum roll angle resulted to be -35.3 degrees in case 1 and -29.6 degrees in case 2. Table 5.1 compares the occupant risk values, all of them met the requirement of MASH. Table 5.2 and Table 5.3 include the sequential images of the two cases in front view and overhead view, respectively.

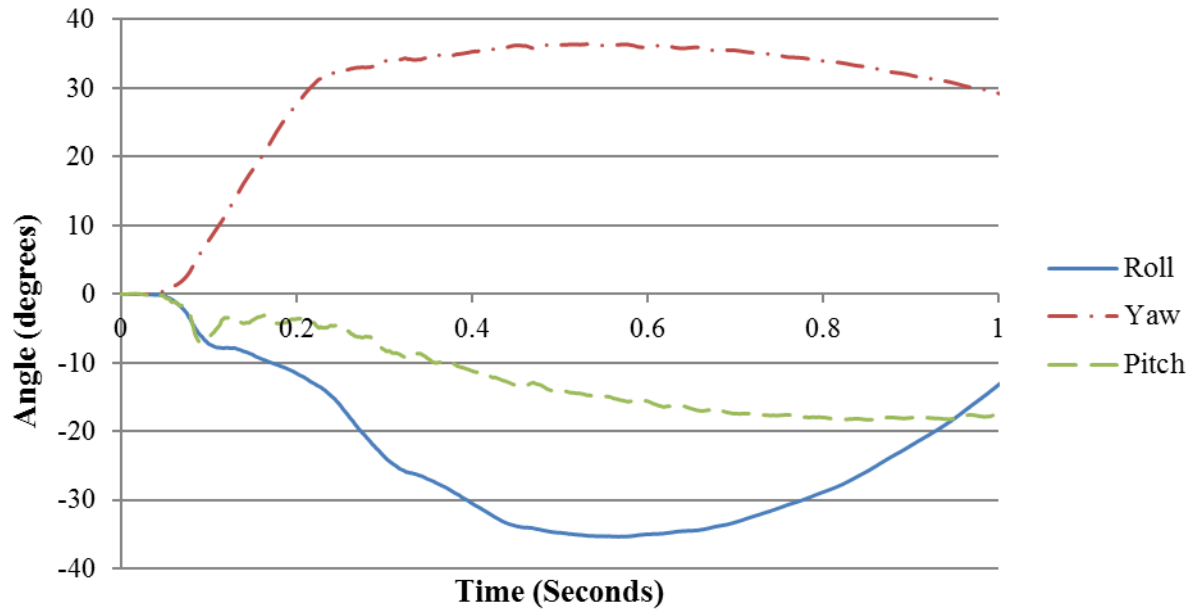


Figure 5.5 Angular Displacements of the Vehicle in Preliminary Simulation of 26-Inch Tall PCB with 1:20 Slope (Case 1)

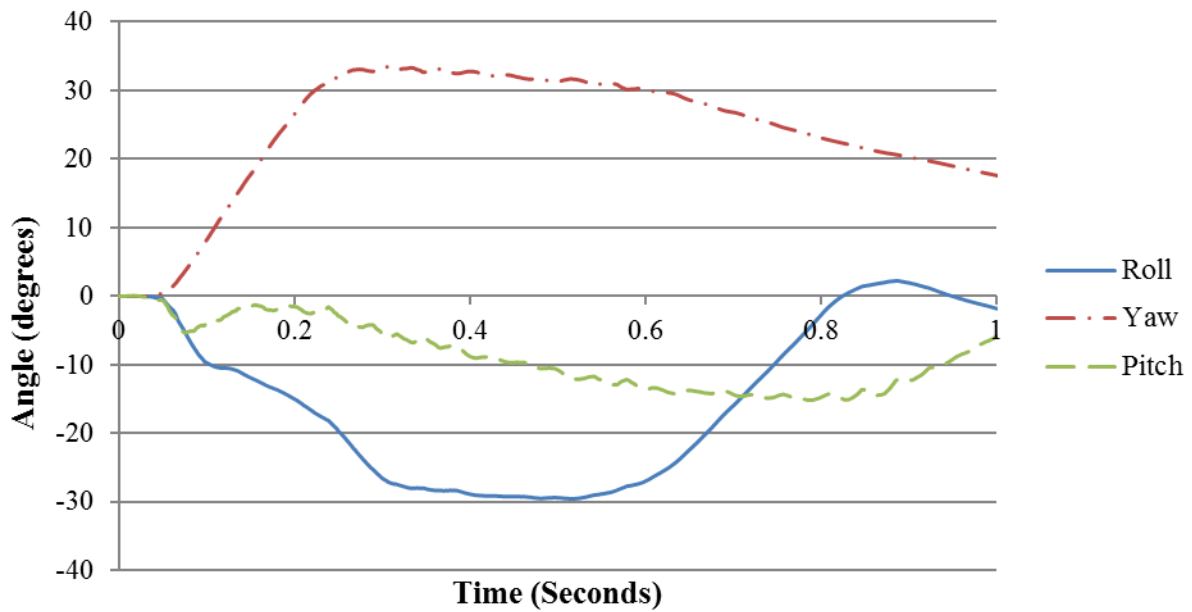


Figure 5.6 Angular Displacements of the Vehicle in Preliminary Simulation of 26-Inch Tall PCB with 1:20 Slope (Case 2)

Table 5.1 Occupant Risk Values Comparison between Case 1 and Case 2 (26-Inch Tall PCB with 1:20 Slope)

Occupant Risk Factors and Maximum Angular Displacement		Case 1 - With Impact Tire Disengagement	Case 2 - Without Impact Tire Disengagement
Impact Velocity (ft/s)	x-direction	20.0	18.7
	y-direction	-27.2	-24.3
Ridedown Acceleration (G)	x-direction	-10.2	-8.2
	y-direction	11.2	12.1
Maximum Angular Displacement (Degrees)	Roll	-35.3	-29.6
	Pitch	-18.3	-15.2
	Yaw	36.4	33.5

Table 5.2 Sequential Images of Preliminary Simulations for 26-Inch Tall PCB with 1:20 Slope (Front View)


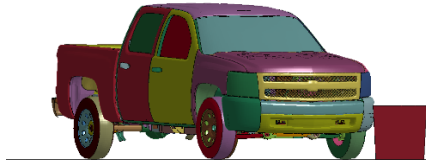
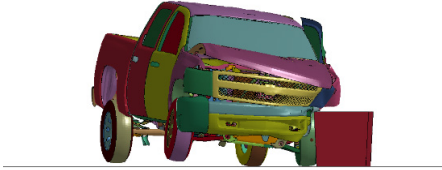
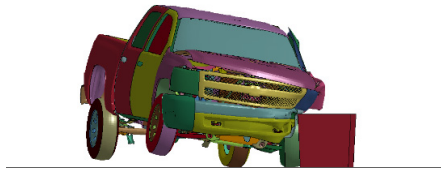

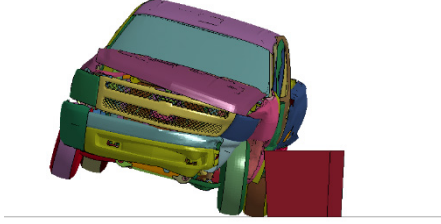
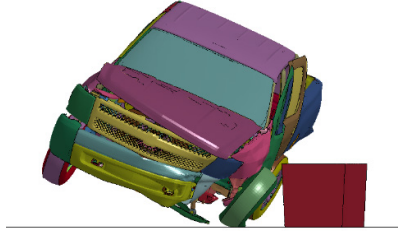
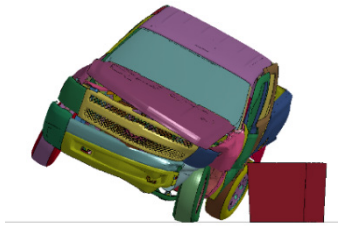
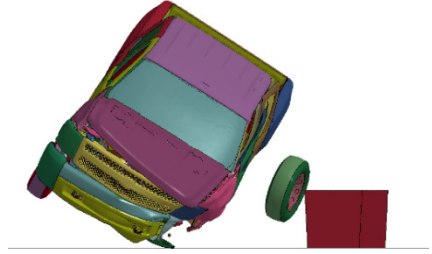
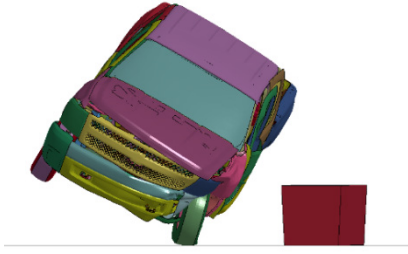
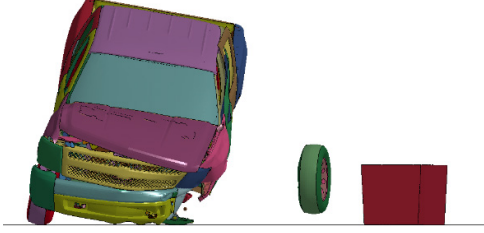
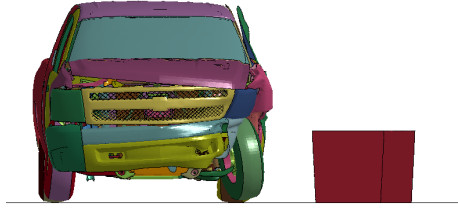


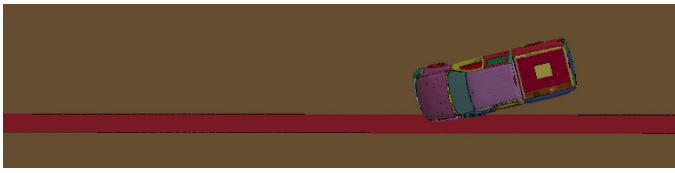

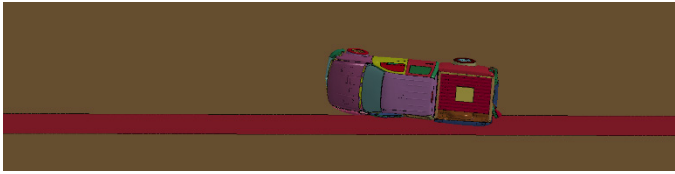
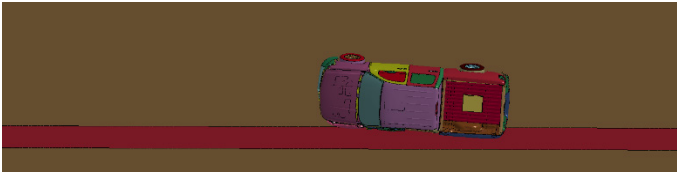
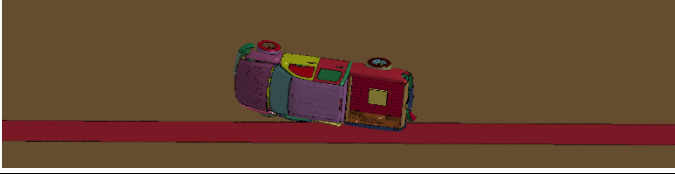





Time (seconds)	With Impact Tire Disengagement	Without Impact Tire Disengagement
0.0		
0.1		
0.2		
0.3		
0.6		
1.0		

Table 5.3 Sequential Images of Preliminary Simulations for 26-Inch Tall PCB with a 1:20 Slope (Overhead View)

Time (seconds)	With Impact Tire Disengagement	Without Impact Tire Disengagement
0.0		
0.1		
0.2		
0.3		
0.6		
1.0		

5.4.3 26-Inch Tall PCB with 1:15 Slope

In both cases, the pickup truck remained upright during and after the collision events. Figure 5.7 and Figure 5.8 show vehicle roll, pitch and yaw angles throughout the impact events against the 26-inch tall PCB with 1:15 slope in both cases, respectively. Maximum roll angle resulted to be -40.5 degrees in case 1 and -33.6 degrees in case 2. Table 5.4 compares the occupant risk values, which all remained in the limitation required by MASH criteria. Table 5.5 and Table 5.6 include the sequential images of the two cases in front view and overhead view, respectively.

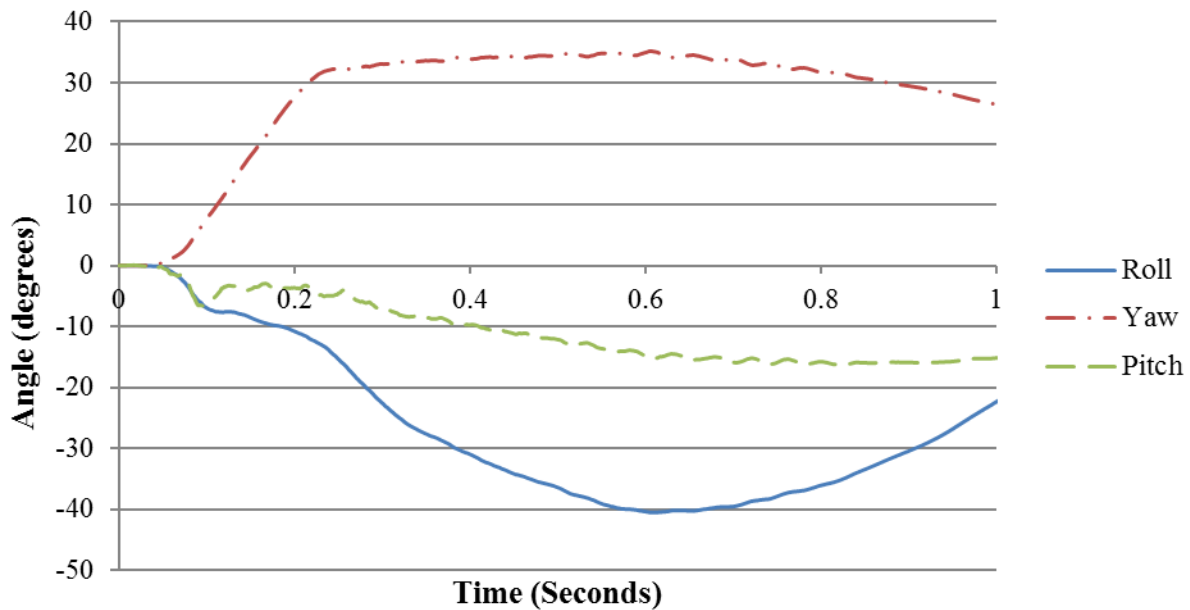


Figure 5.7 Angular Displacements of the Vehicle in Preliminary Simulation of 26-Inch Tall PCB with 1:15 Slope (Case 1)

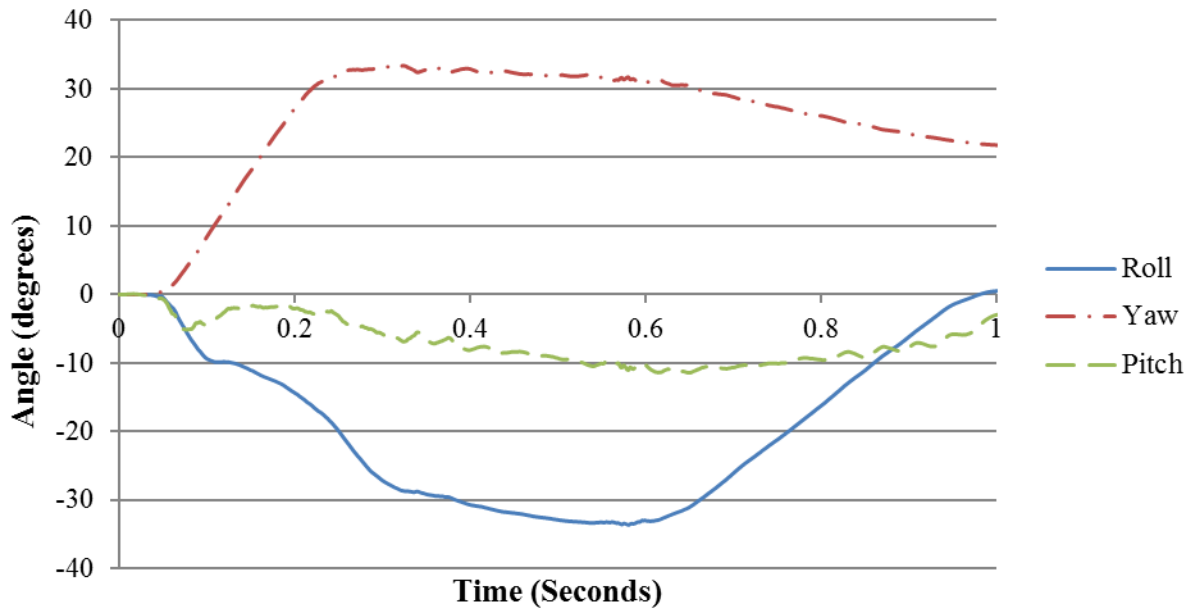


Figure 5.8 Angular Displacements of the Vehicle in Preliminary Simulation of 26-Inch Tall PCB with 1:15 Slope (Case 2)

Table 5.4 Occupant Risk Values Comparison between Case 1 and Case 2 (26-Inch Tall PCB with 1:15 Slope)

Occupant Risk Factors and Maximum Angular Displacement		Case 1 - With Impact Tire Disengagement	Case 2 - Without Impact Tire Disengagement
Impact Velocity (ft/s)	x-direction	20.7	16.7
	y-direction	-20.3	-24.3
Ridedown Acceleration (G)	x-direction	-11.2	-7.7
	y-direction	11.5	12.0
Maximum Angular Displacement (Degrees)	Roll	-40.5	-33.6
	Pitch	-16.3	-11.4
	Yaw	35.2	33.4

Table 5.5 Sequential Images of Preliminary Simulations for 26-Inch Tall PCB with 1:15 Slope (Front View)




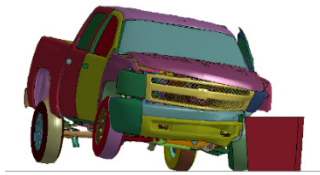

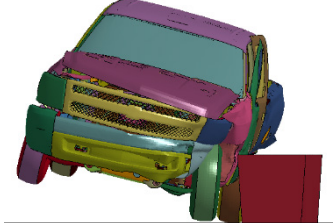
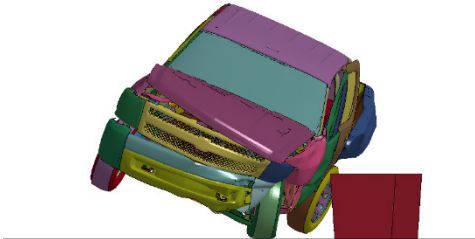
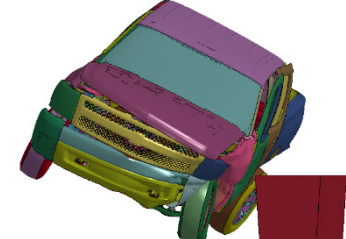
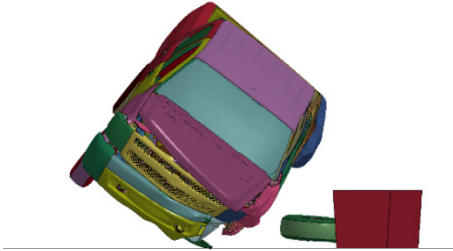
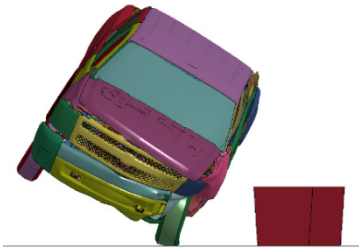
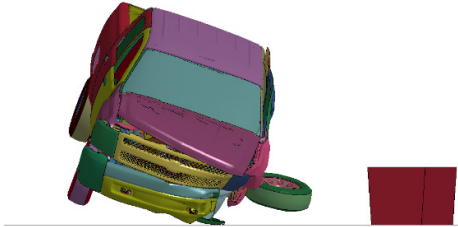
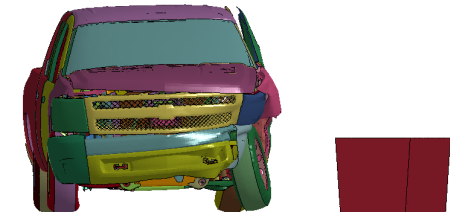


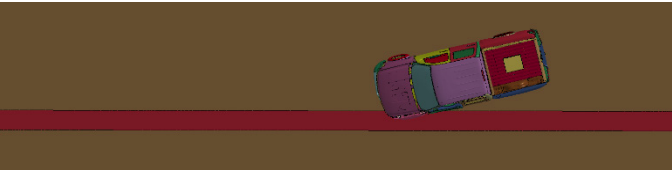

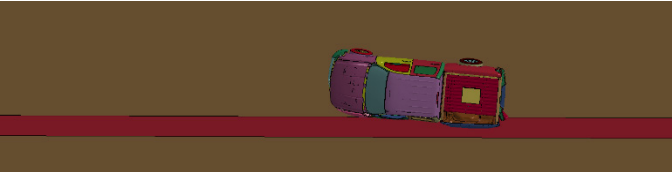
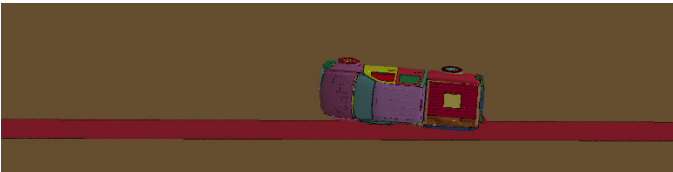
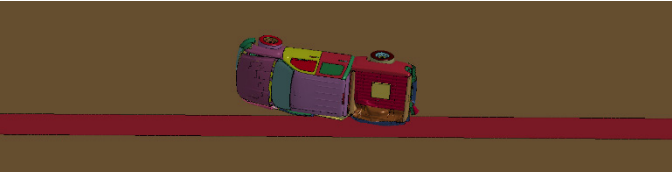
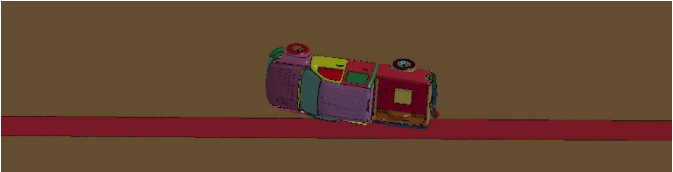


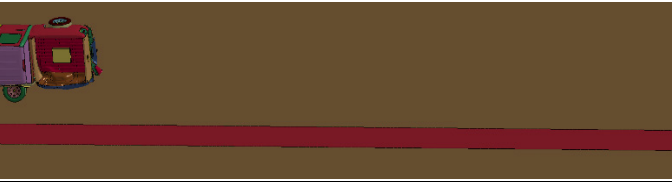
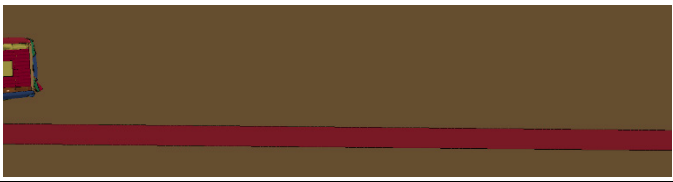
Time (seconds)	With Impact Tire Disengagement	Without Impact Tire Disengagement
0.0		
0.1		
0.2		
0.3		
0.6		
1.0		

Table 5.6 Sequential Images of Preliminary Simulations for 26-Inch Tall PCB with 1:15 Slope (Overhead View)

Time (seconds)	With Impact Tire Disengagement	Without Impact Tire Disengagement
0.0		
0.1		
0.2		
0.3		
0.6		
1.0		

5.4.4 26-Inch Tall T Shaped PCB

The pickup truck remained upright during and after the collision events in both cases. Figure 5.9 and Figure 5.10 show vehicle roll, pitch and yaw angles throughout the impact events against the 26-inch tall T shaped PCB in both cases, respectively. Maximum roll angle resulted to be -30.1 degrees in case 1 and -31.2 degrees in case 2. Table 5.7 compares the occupant risk values, which all remained in the limitation required by MASH criteria. Table 5.8 and Table 5.9 include the sequential images of the two cases in front view and overhead view, respectively.

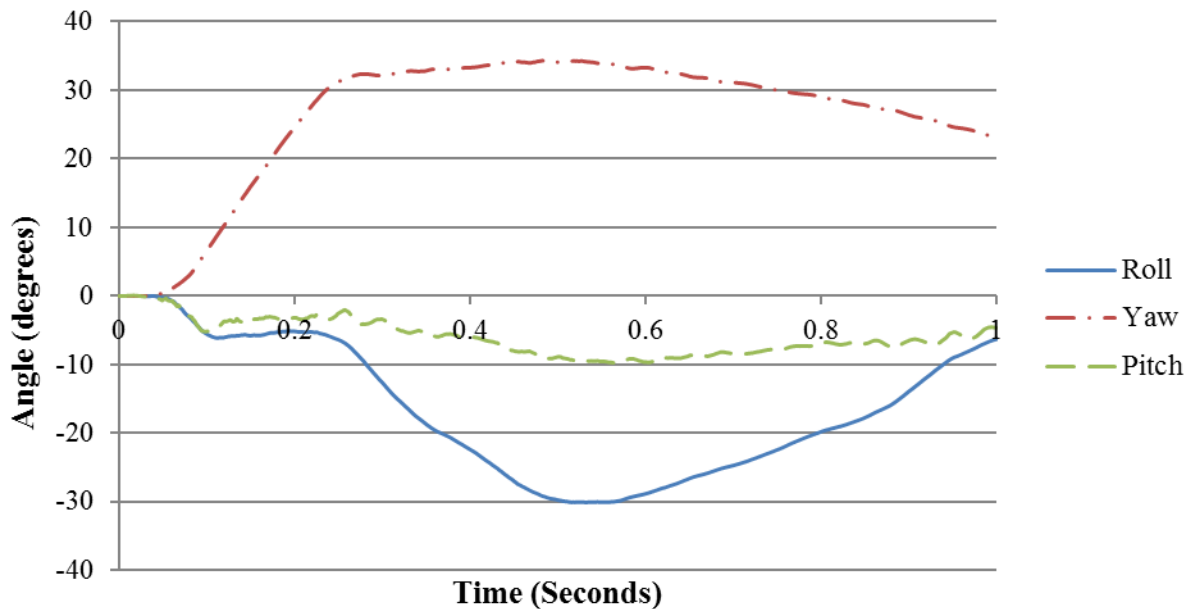


Figure 5.9 Angular Displacements of the Vehicle in Preliminary Simulation of 26-Inch Tall T Shaped PCB (Case 1)

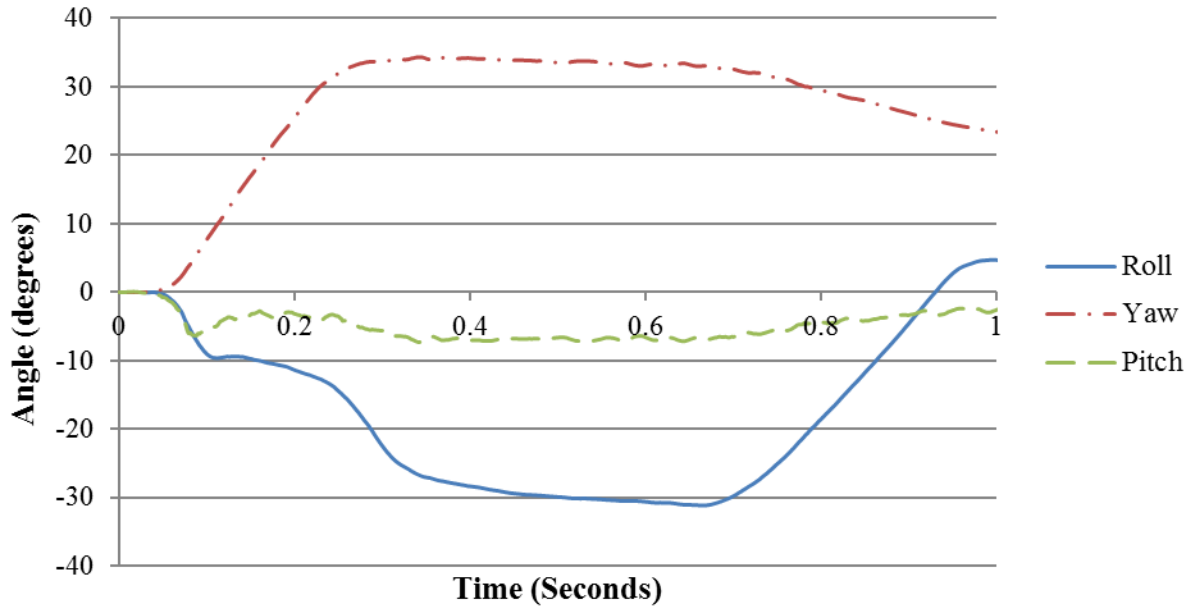


Figure 5.10 Angular Displacements of the Vehicle in Preliminary Simulation of 26-Inch Tall T Shaped PCB (Case 2)

Table 5.7 Occupant Risk Values Comparison between Case 1 and Case 2 (26-Inch Tall T Shaped PCB)

Occupant Risk Factors and Maximum Angular Displacement		Case 1 - With Impact Tire Disengagement	Case 2 - Without Impact Tire Disengagement
Impact Velocity (ft/s)	x-direction	19.3	19.0
	y-direction	23.0	-23.9
Ridedown Acceleration (G)	x-direction	-7.6	-13.4
	y-direction	8.9	14.0
Maximum Angular Displacement (Degrees)	Roll	-30.1	-31.2
	Pitch	-9.8	-7.3
	Yaw	34.3	34.3

Table 5.8 Sequential Images of Preliminary Simulations for 26-Inch Tall T Shaped PCB (Front View)


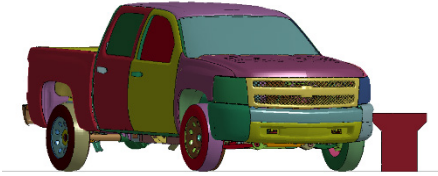

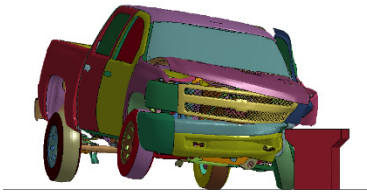
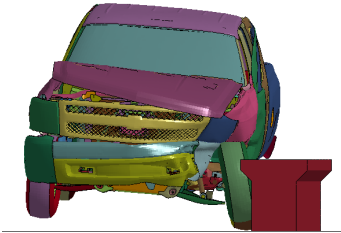

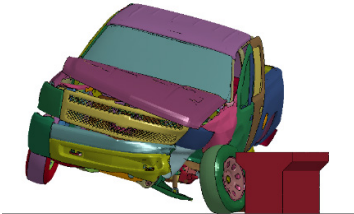
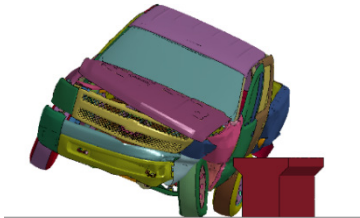
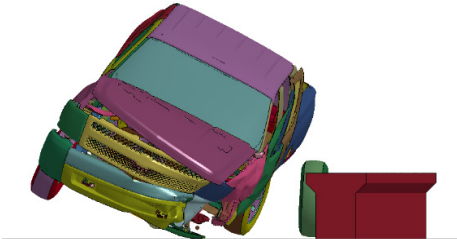
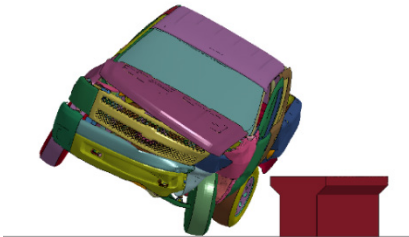
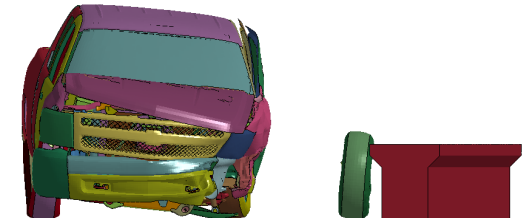

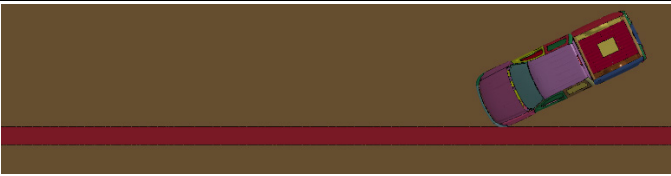

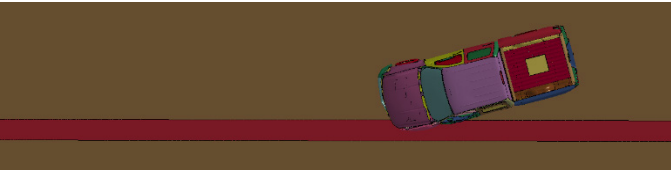
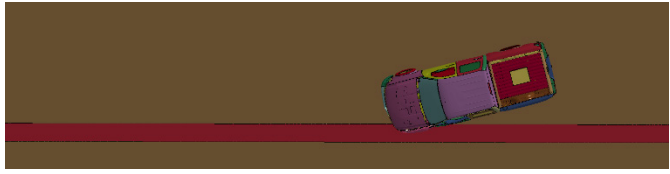
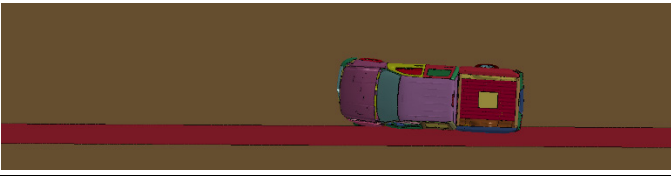
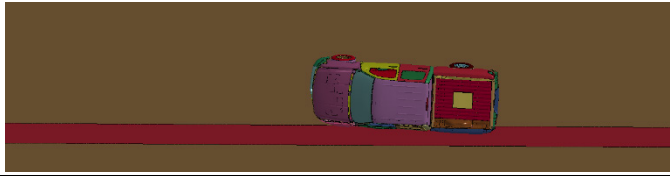
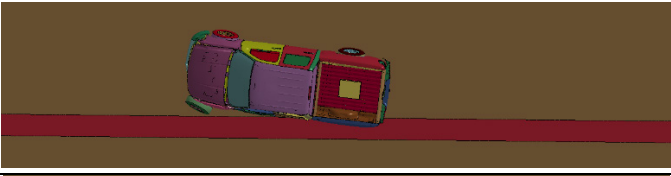
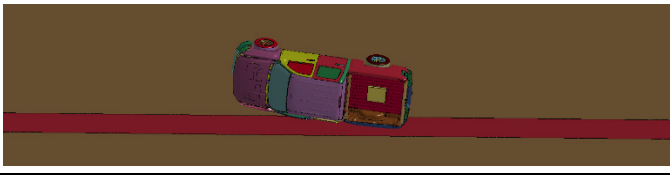




Time (seconds)	With Impact Tire Disengagement	Without Impact Tire Disengagement
0.0		
0.1		
0.2		
0.3		
0.6		
1.0		

Table 5.9 Sequential Images of Preliminary Simulations for 26-Inch Tall T Shaped PCB (Overhead View)

Time (seconds)	With Impact Tire Disengagement	Without Impact Tire Disengagement
0.0		
0.1		
0.2		
0.3		
0.6		
1.0		

5.4.5 26-Inch Tall T Shaped PCB with 1:20 Slope

In both cases, the pickup truck remained upright during and after the collision events. Figure 5.11 and Figure 5.12 show vehicle roll, pitch and yaw angles throughout the impact events against the 26-inch tall T shaped PCB with 1:20 slope in both cases, respectively. Maximum roll angle resulted to be -27.3 degrees in case 1 and -30.1 degrees in case 2. Table 5.10 compares the occupant risk values, which all remained in the limitation of MASH criteria. Table 5.11 and Table 5.12 show the sequential images of the two cases in front view and overhead view, respectively.

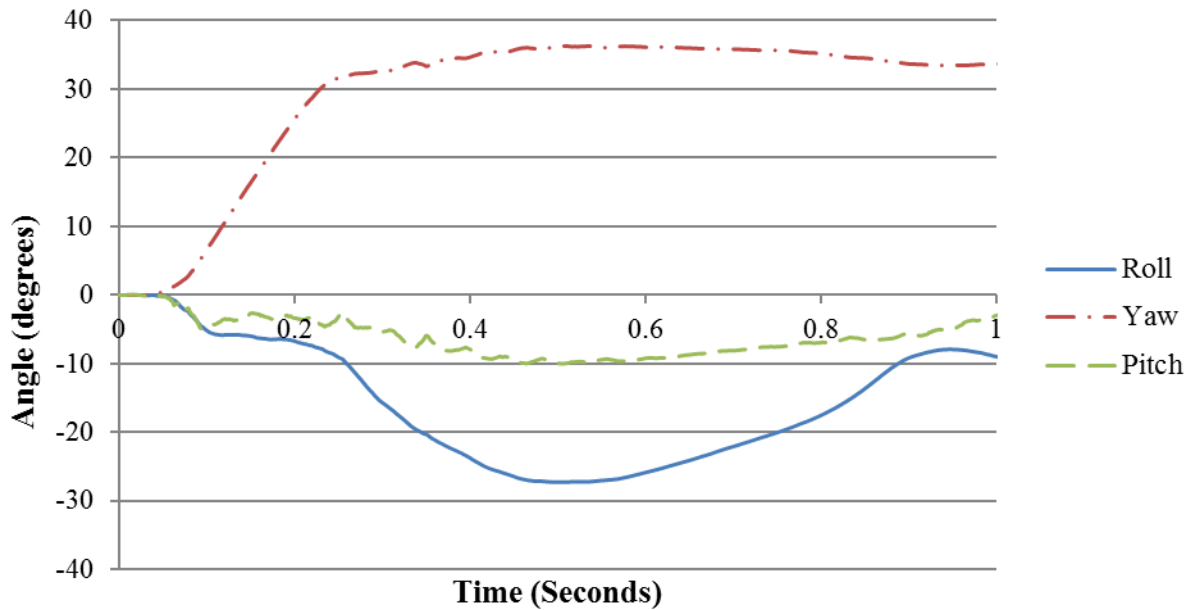


Figure 5.11 Angular Displacements of the Vehicle in Preliminary Simulation of 26-Inch Tall T Shaped PCB with 1:20 slope (Case 1)

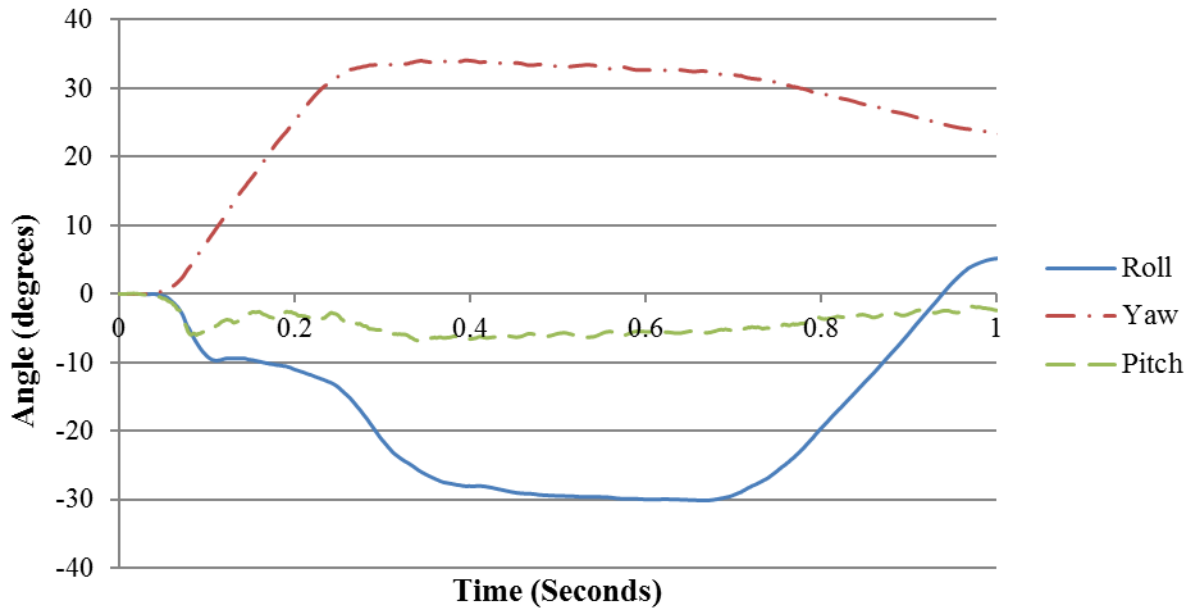


Figure 5.12 Angular Displacements of the Vehicle in Preliminary Simulation of 26-Inch Tall T Shaped PCB with 1:20 Slope (Case 2)

Table 5.10 Occupant Risk Values Comparison between Case 1 and Case 2 (26-Inch Tall T Shaped PCB with 1:20 Slope)

Occupant Risk Factors and Maximum Angular Displacement		Case 1 - With Impact Tire Disengagement	Case 2 - Without Impact Tire Disengagement
Impact Velocity (ft/s)	x-direction	14.1	20.7
	y-direction	-25.3	-25.3
Ridedown Acceleration (G)	x-direction	-8.0	-7.0
	y-direction	9.9	15.7
Maximum Angular Displacement (Degrees)	Roll	-27.3	-30.1
	Pitch	-10.0	-6.9
	Yaw	36.3	34.1

Table 5.11 Sequential Images of Preliminary Simulations for 26-Inch Tall T Shaped PCB with 1:20 Slope (Front View)


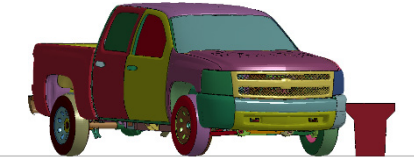
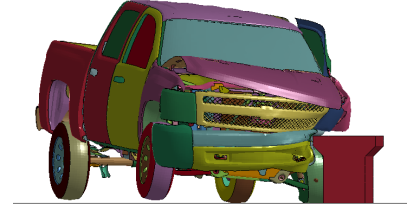
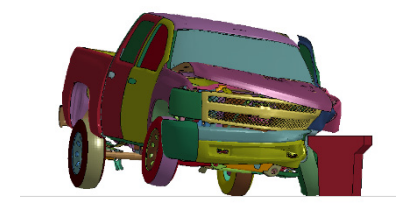
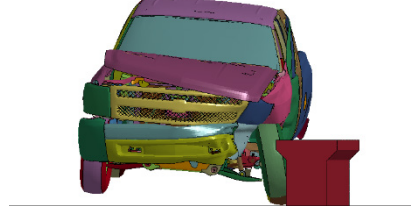
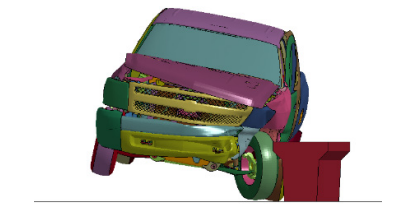
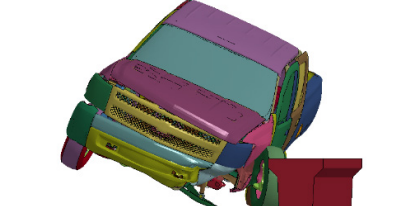
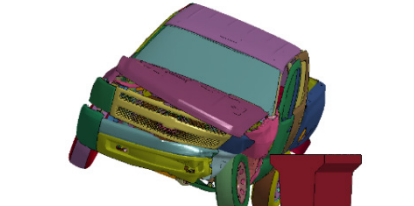
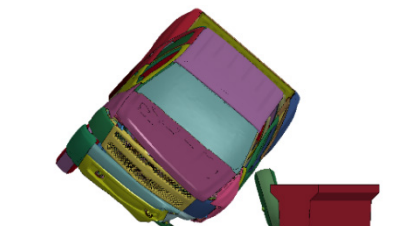
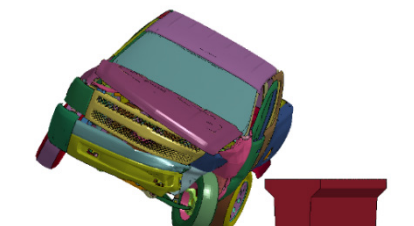
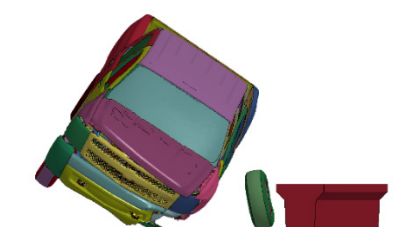
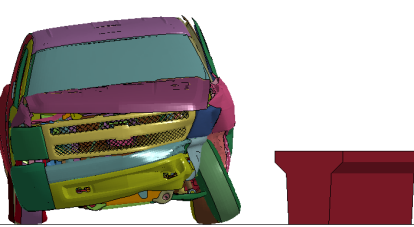



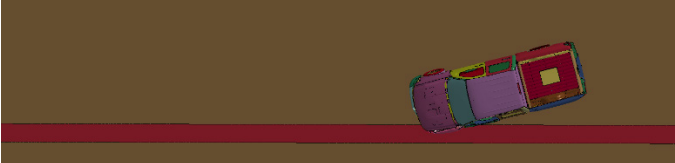
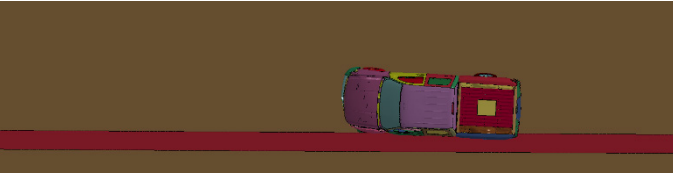
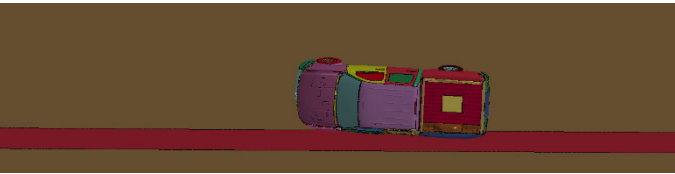
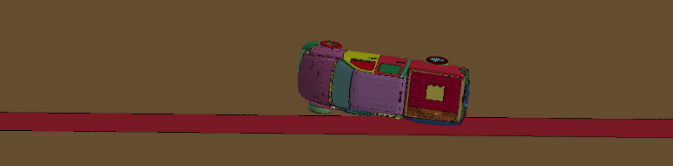
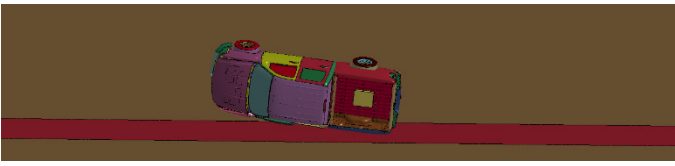

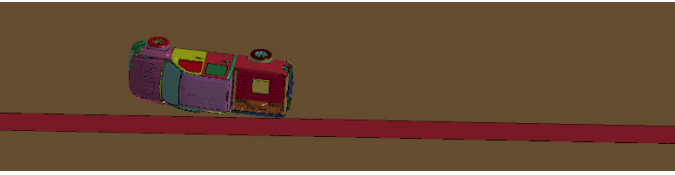


Time (seconds)	With Impact Tire Disengagement	Without Impact Tire Disengagement
0.0		
0.1		
0.2		
0.3		
0.6		
1.0		

Table 5.12 Sequential Images of Preliminary Simulations for 26-Inch Tall T Shaped PCB with 1:20 Slope (Overhead View)

Time (seconds)	With Impact Tire Disengagement	Without Impact Tire Disengagement
0.0		
0.1		
0.2		
0.3		
0.6		
1.0		

5.4.6 26-Inch Tall I Shaped PCB

In both cases, the pickup truck remained upright during and after the collision events. Figure 5.13 and Figure 5.14 show vehicle roll, pitch and yaw angles throughout the impact events against the 26-inch tall I shaped PCB in both cases, respectively. Maximum roll angle resulted to be -25.2 degrees in case 1 and -34.1 degrees in case 2. Table 5.13 compares the occupant risk values, which all remained in the limitation required by MASH criteria. Table 5.14 and Table 5.15 include the sequential images of the two cases in front and overhead view, respectively.

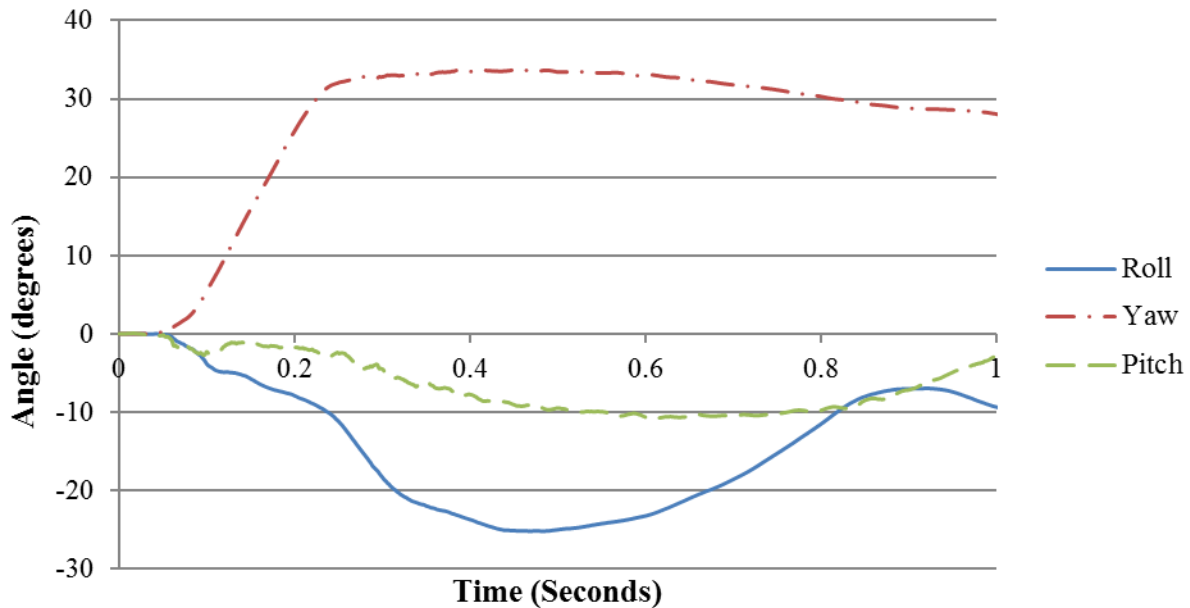


Figure 5.13 Angular Displacements of the Vehicle in Preliminary Simulation of 26-Inch Tall I Shaped PCB (Case 1)

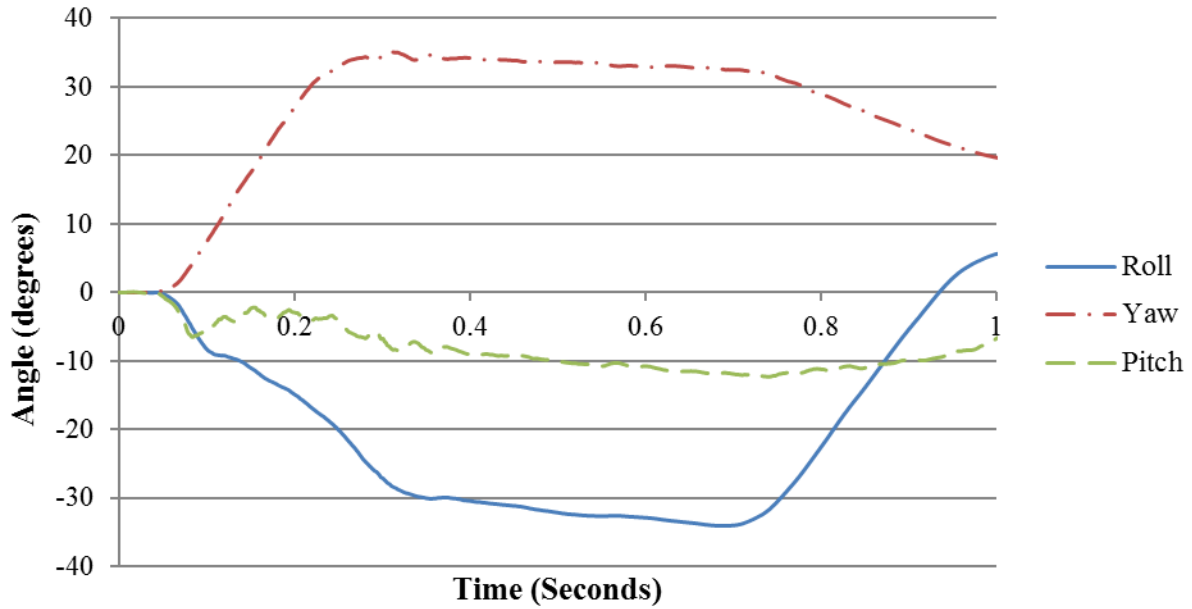


Figure 5.14 Angular Displacements of the Vehicle in Preliminary Simulation of 26-Inch Tall I Shaped PCB (Case 2)

Table 5.13 Occupant Risk Values Comparison between Case 1 and Case 2 (26-Inch Tall I Shaped PCB)

Occupant Risk Factors and Maximum Angular Displacement		Case 1 - With Impact Tire Disengagement	Case 2 - Without Impact Tire Disengagement
Impact Velocity (ft/s)	x-direction	13.4	16.7
	y-direction	-26.9	-26.9
Ridedown Acceleration (G)	x-direction	-5.8	-14.4
	y-direction	12.5	14.7
Maximum Angular Displacement (Degrees)	Roll	-25.2	-34.1
	Pitch	-10.9	-12.3
	Yaw	33.8	35.1

**Table 5.14 Sequential Images of Preliminary Simulations for 26-Inch Tall I Shaped PCB
(Front View)**




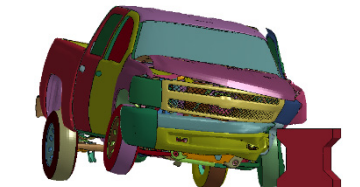
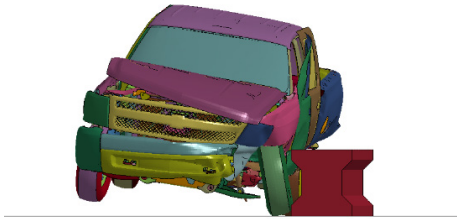
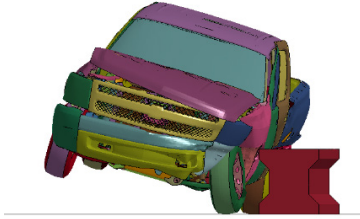
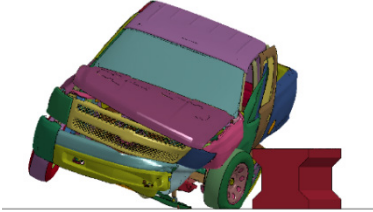
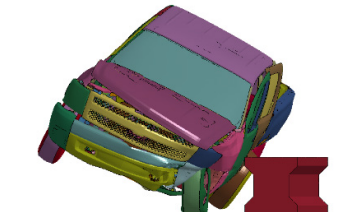
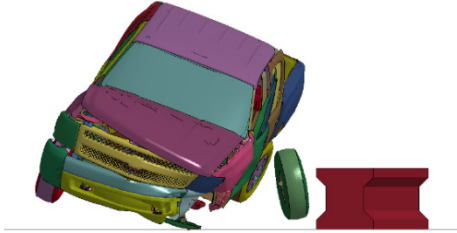
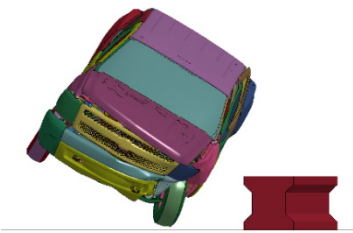
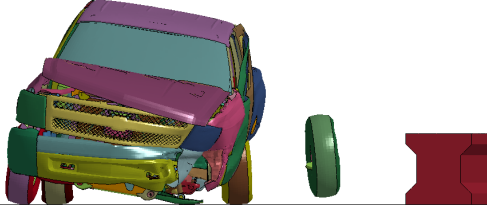
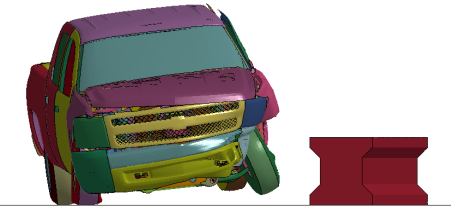
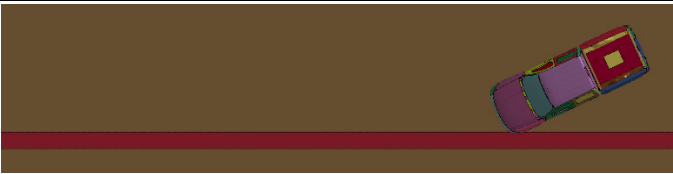

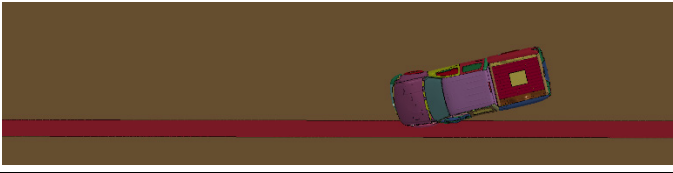
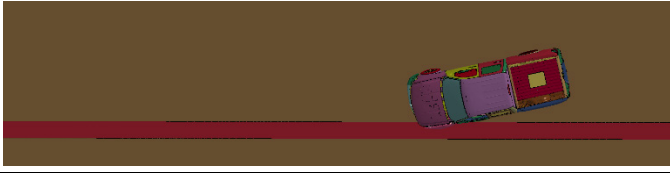
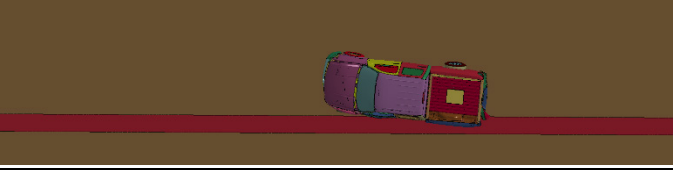
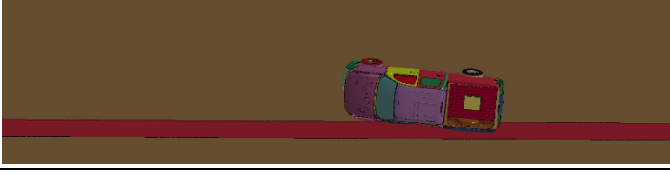
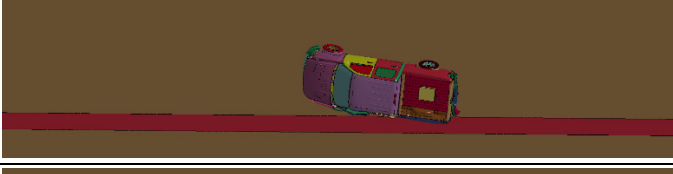

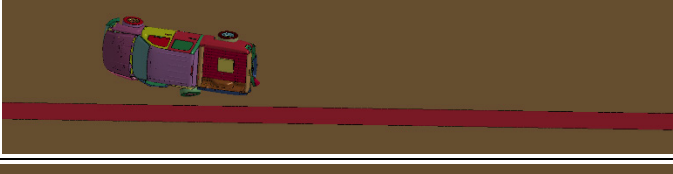
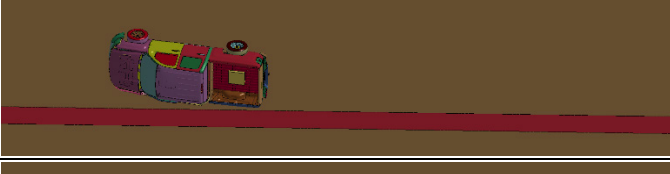


Time (seconds)	With Impact Tire Disengagement	Without Impact Tire Disengagement
0.0		
0.1		
0.2		
0.3		
0.6		
1.0		

Table 5.15 Sequential Images of Preliminary Simulations for 26-Inch Tall I Shaped PCB (Overhead View)

Time (seconds)	With Impact Tire Disengagement	Without Impact Tire Disengagement
0.0		
0.1		
0.2		
0.3		
0.6		
1.0		

5.4.7 26-Inch Tall I Shaped PCB with 1:20 Slope

The pickup truck was redirected and remained upright during and after the collision events in both cases. Figure 5.15 and Figure 5.16 show vehicle roll, pitch and yaw angles throughout the impact events against the 26-inch tall I PCB with 1:20 slope in both cases, respectively. Maximum roll angle resulted to be -24.3 degrees in case 1 and -29.5 degrees in case 2. Table 5.16 compares the occupant risk values, which all remained in the limitation required by MASH criteria. Table 5.17 and Table 5.18 include the sequential images of the two cases in front view and overhead view, respectively.

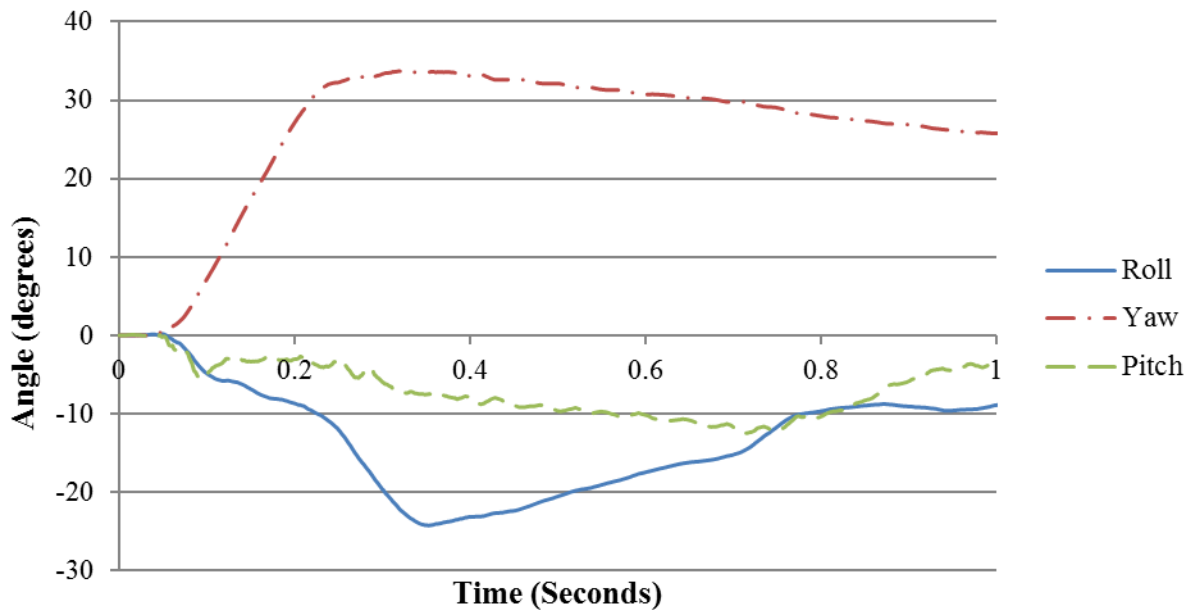


Figure 5.15 Angular Displacements of the Vehicle in Preliminary Simulation of 26-Inch Tall I Shaped PCB with 1:20 slope (Case 1)

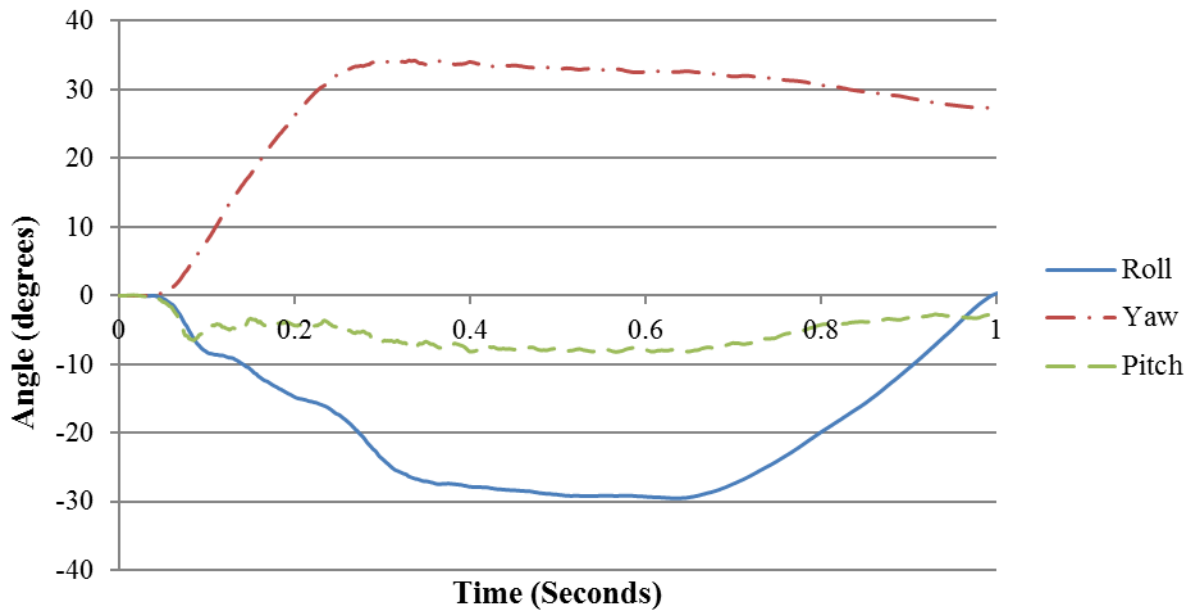


Figure 5.16 Angular Displacements of the Vehicle in Preliminary Simulation of 26-Inch Tall I Shaped PCB with 1:20 Slope (Case 2)

Table 5.16 Occupant Risk Values Comparison between Case 1 and Case 2 (26-Inch Tall I Shaped PCB with 1:20 Slope)

Occupant Risk Factors and Maximum Angular Displacement		Case 1 - With Impact Tire Disengagement	Case 2 - Without Impact Tire Disengagement
Impact Velocity (ft/s)	x-direction	17.4	14.8
	y-direction	-26.6	-22.6
Ridedown Acceleration (G)	x-direction	-8.8	-14.6
	y-direction	13.1	20.0
Maximum Angular Displacement (Degrees)	Roll	-24.3	-29.5
	Pitch	-12.5	-8.2
	Yaw	38.0	34.3

Table 5.17 Sequential Images of Preliminary Simulations for 26-Inch Tall I Shaped PCB with 1:20 Slope (Front View)


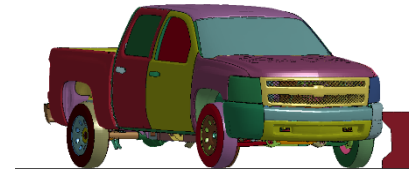
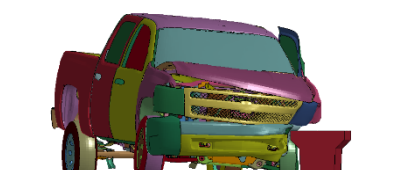
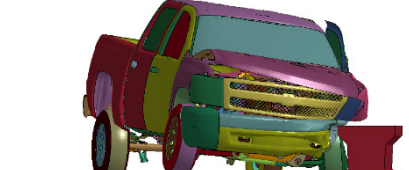
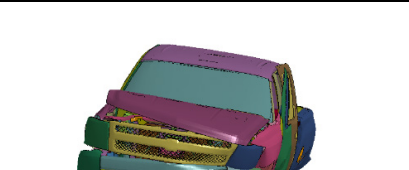

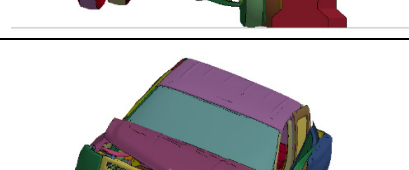

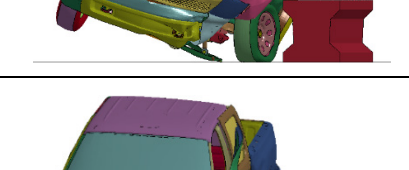
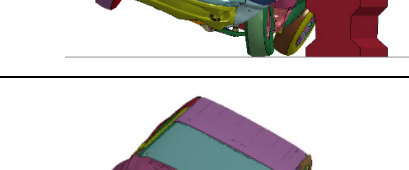

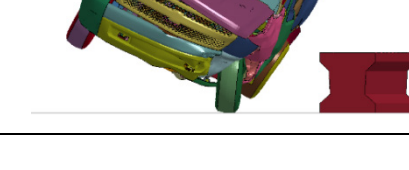




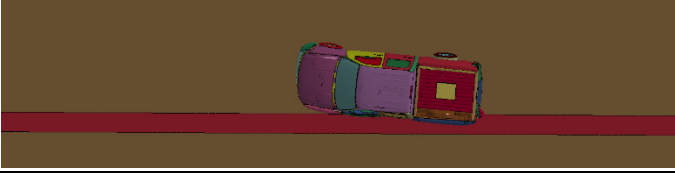

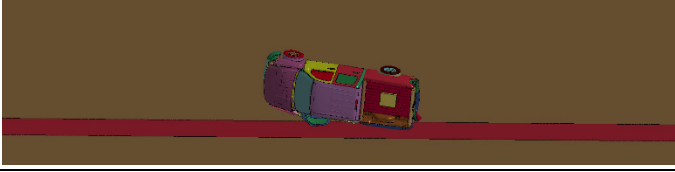
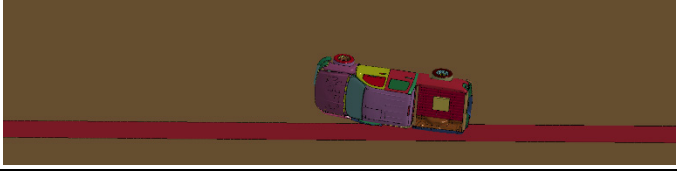
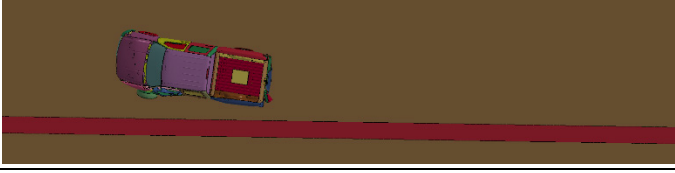
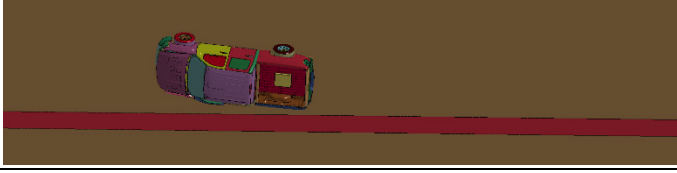


Time (seconds)	With Impact Tire Disengagement	Without Impact Tire Disengagement
0.0		
0.1		
0.2		
0.3		
0.6		
1.0		

Table 5.18 Sequential Images of Preliminary Simulations for 26-Inch Tall I Shaped PCB with 1:20 Slope (Overhead View)

Time (seconds)	With Impact Tire Disengagement	Without Impact Tire Disengagement
0.0		
0.1		
0.2		
0.3		
0.6		
1.0		

5.5 Preliminary Finite Element Analysis of 24-Inch Tall PCB Concepts

5.5.1 Introduction

Preliminary simulation conditions for 24-inch tall barrier concepts are identical to the 26-inch tall barriers. All of the 24-inch tall, 180-feet long, free-standing concrete block with different profile shapes were impacted by the 2270P pickup truck with a speed of 62 mi/h and an angle of 25 degrees. The impact location was at about one-third of the system length. Two cases were considered in the simulation: Case 1, with impact tire disengagement; Case 2, without impact tire disengagement.

5.5.2 24-Inch Tall PCB with 1:20 Slope

In the simulation of case 1, the pickup truck was contained and redirected but showed an unacceptable result. The roll angle of the vehicle exceeded the maximum value that MASH requires. In case 2, the pickup truck remained upright during and after the collision event. Figure 5.17 and Figure 5.18 show vehicle roll, pitch and yaw angles throughout the impact events against the 24-inch tall PCB with 1:20 slope in both cases, respectively. Maximum roll angle resulted to be -82 degrees in case 1 and -35.2 degrees in case 2. Table 5.19 compares the occupant risk values, all of them were under the limitation of MASH. Table 5.20 and Table 5.21 include the sequential images of the two cases in front view and overhead view, respectively.

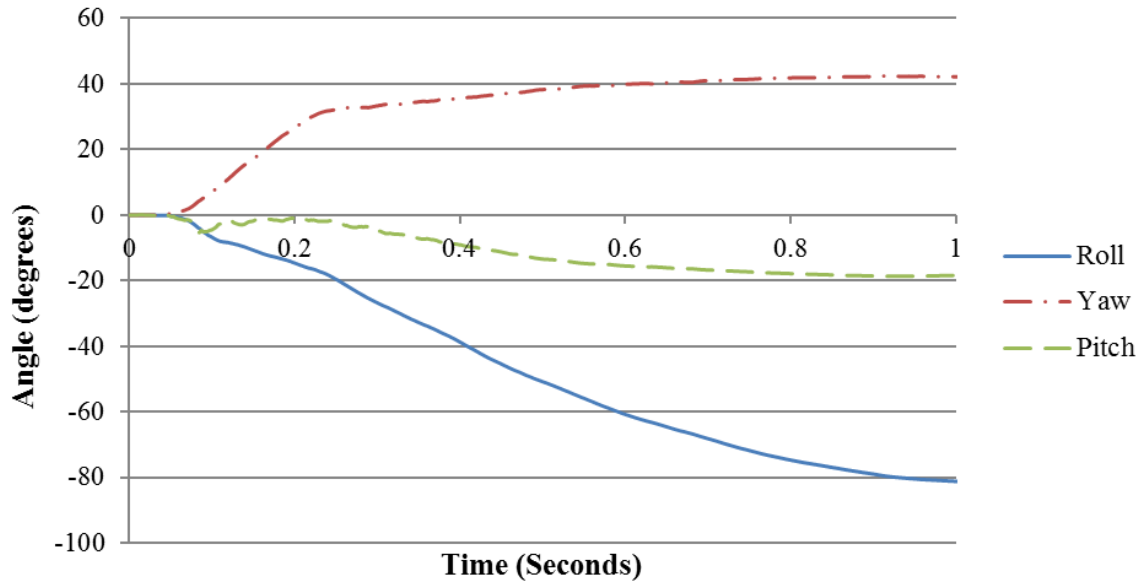


Figure 5.17 Angular Displacements of the Vehicle in Preliminary Simulation of 24-Inch Tall PCB with 1:20 Slope (Case 1)

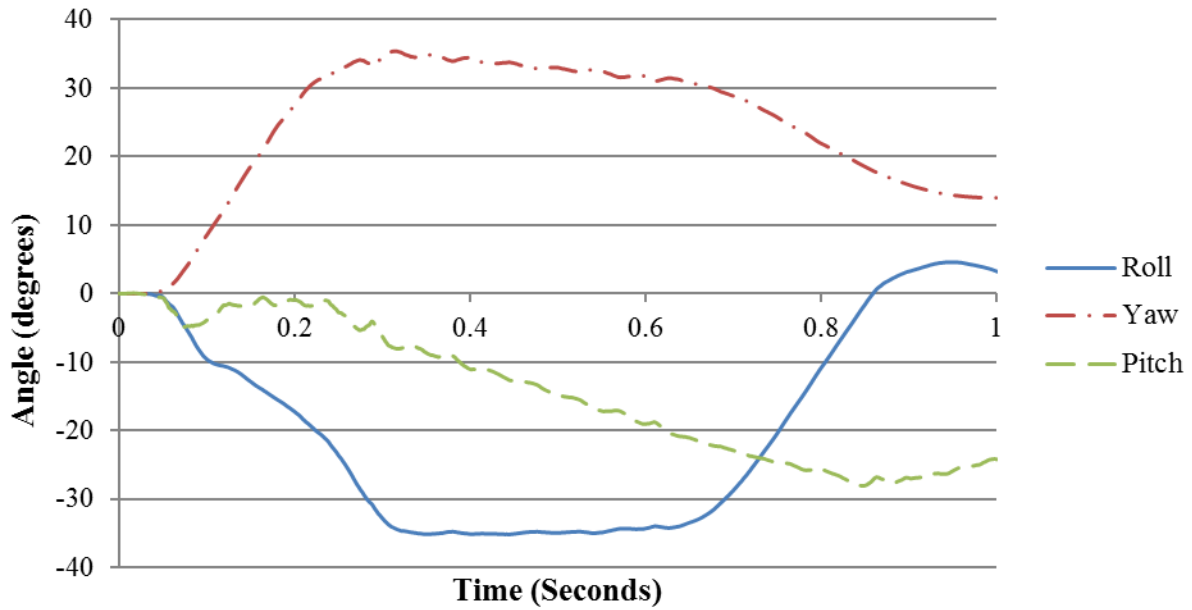


Figure 5.18 Angular Displacements of the Vehicle in Preliminary Simulation of 24-Inch Tall PCB with 1:20 Slope (Case 2)

Table 5.19 Occupant Risk Values Comparison between Case 1 and Case 2 (24-Inch Tall PCB with 1:20 Slope)

Occupant Risk Factors and Maximum Angular Displacement		Case 1 - With Impact Tire Disengagement	Case 2 - Without Impact Tire Disengagement
Impact Velocity (ft/s)	x-direction	13.8	16.7
	y-direction	-26.9	-25.3
Ridedown Acceleration (G)	x-direction	-5.7	-15.1
	y-direction	12.2	14.8
Maximum Angular Displacement (Degrees)	Roll	-82.0	-35.2
	Pitch	-18.6	-28.1
	Yaw	42.5	35.4

Table 5.20 Sequential Images of Preliminary Simulations for 24-Inch Tall PCB with 1:20 Slope (Front View)

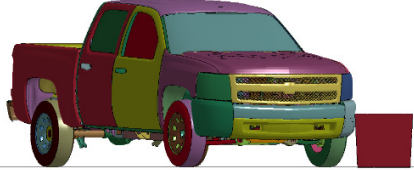
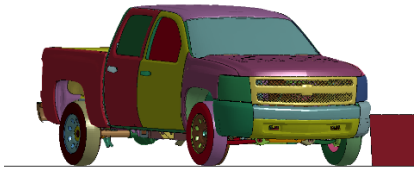
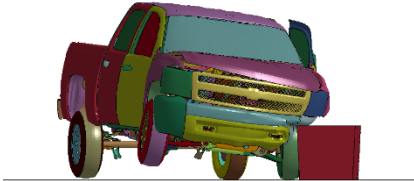
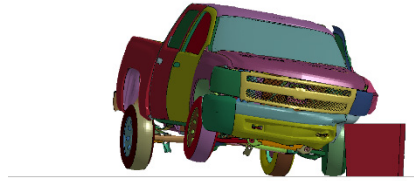
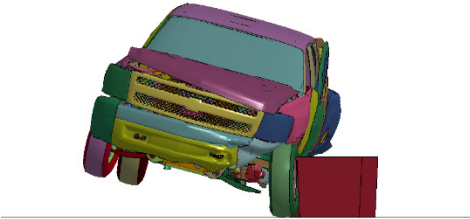

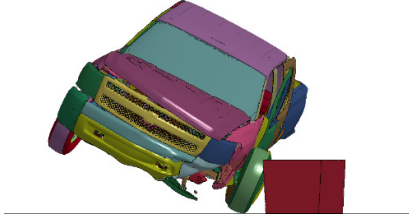
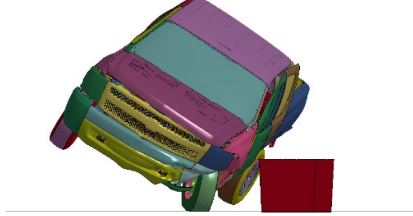
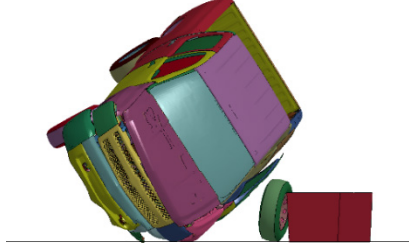
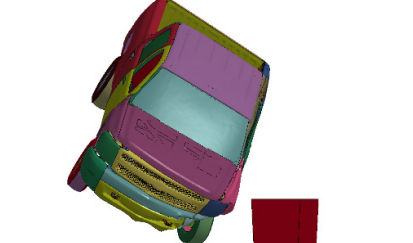
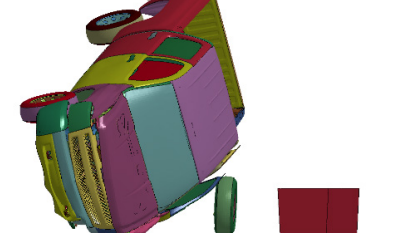
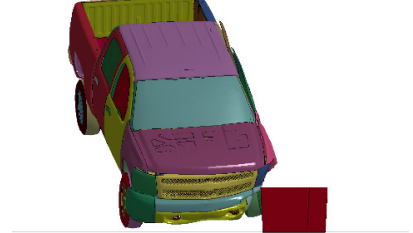


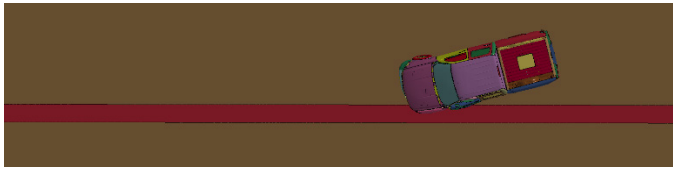

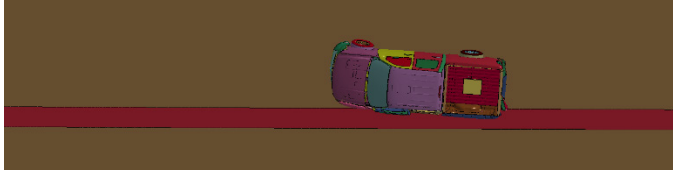
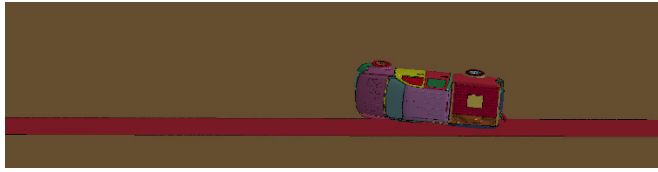
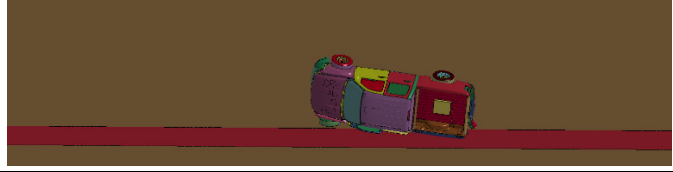





Time (seconds)	With Impact Tire Disengagement	Without Impact Tire Disengagement
0.0		
0.1		
0.2		
0.3		
0.6		
1.0		

Table 5.21 Sequential Images of Preliminary Simulations for 24-Inch Tall PCB with a 1:20 Slope (Overhead View)

Time (seconds)	With Impact Tire Disengagement	Without Impact Tire Disengagement
0.0		
0.1		
0.2		
0.3		
0.6		
1.0		

5.5.3 24-Inch Tall PCB with 1:15 Slope

In case 1, the pickup truck rolled over after impact with the barrier. In case 2, the pickup truck remained upright during and after the collision event. Figure 5.19 and Figure 5.20 show vehicle roll, pitch and yaw angles throughout the impact events against the 24-inch tall PCB with 1:15 slope in both cases, respectively. Maximum roll angle resulted to be -82.9 degrees in case 1 and -34.8 degrees in case 2. Table 5.22 compares the occupant risk values, all of them were under the limitation of MASH. Table 5.23 and Table 5.24 include the sequential images of the two cases in front view and overhead view, respectively.

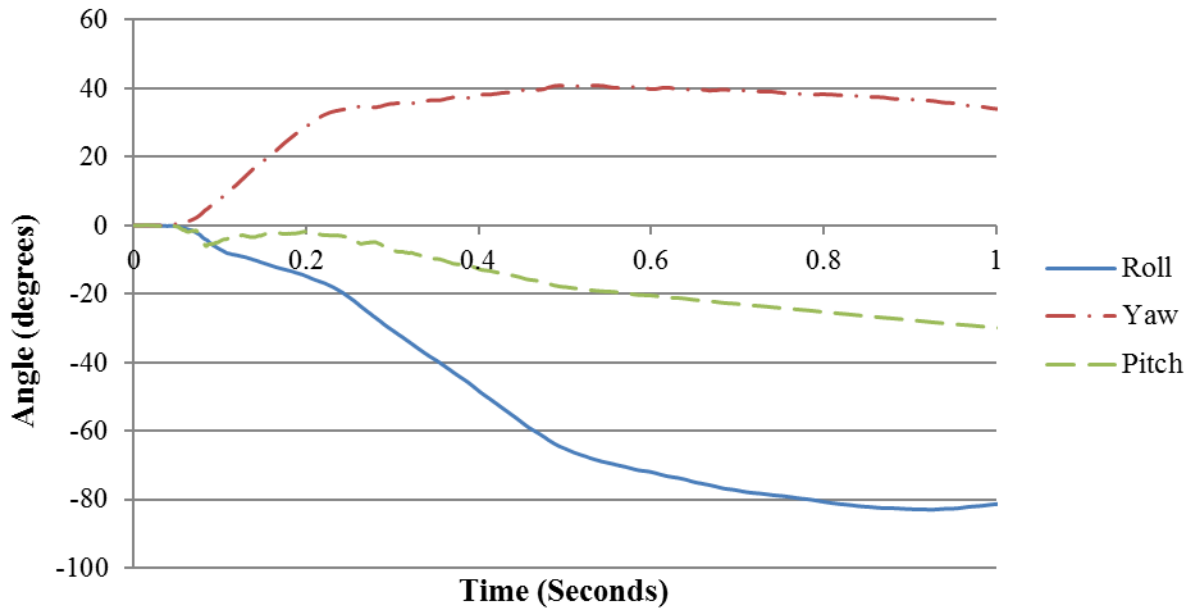


Figure 5.19 Angular Displacements of the Vehicle in Preliminary Simulation of 24-Inch Tall PCB with 1:15 Slope (Case 1)

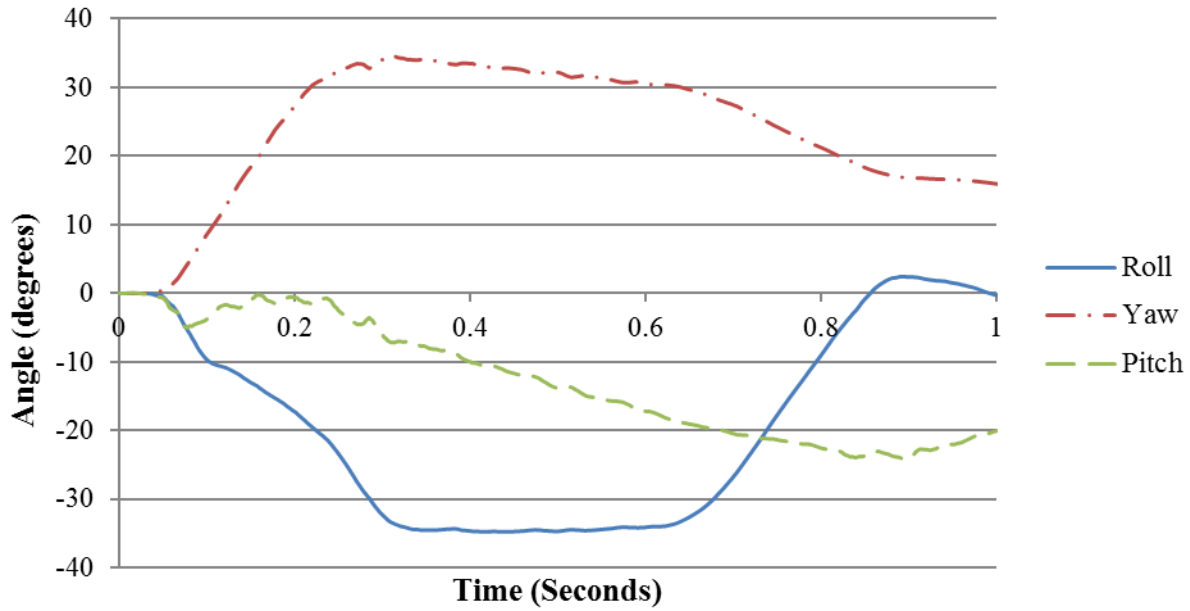


Figure 5.20 Angular Displacements of the Vehicle in Preliminary Simulation of 24-Inch Tall PCB with 1:15 Slope (Case 2)

Table 5.22 Occupant Risk Values Comparison between Case 1 and Case 2 (24-Inch Tall PCB with 1:15 Slope)

Occupant Risk Factors and Maximum Angular Displacement		Case 1 - With Impact Tire Disengagement	Case 2 - Without Impact Tire Disengagement
Impact Velocity (ft/s)	x-direction	14.1	14.1
	y-direction	-24.9	-20.0
Ridedown Acceleration (G)	x-direction	-5.9	-11.0
	y-direction	12.6	11.1
Maximum Angular Displacement (Degrees)	Roll	-82.9	-34.8
	Pitch	-35.0	-24.2
	Yaw	40.9	34.6

Table 5.23 Sequential Images of Preliminary Simulations for 24-Inch Tall PCB with 1:15 Slope (Front View)




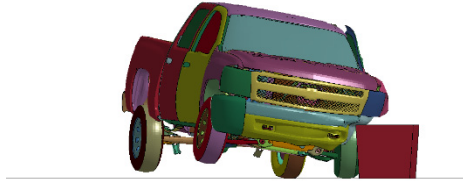
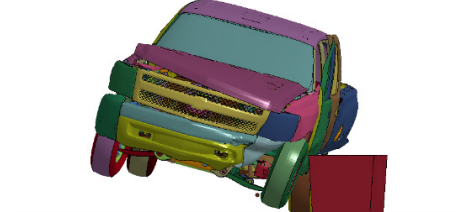
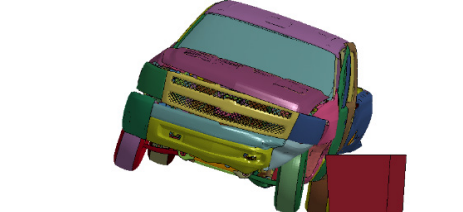
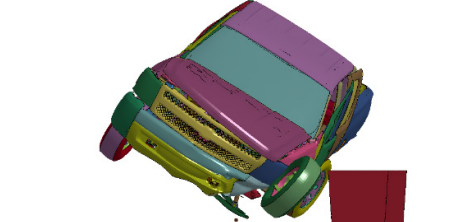
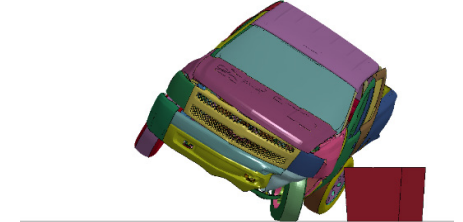
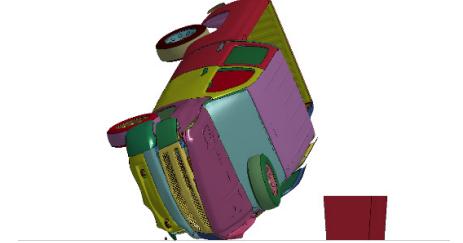
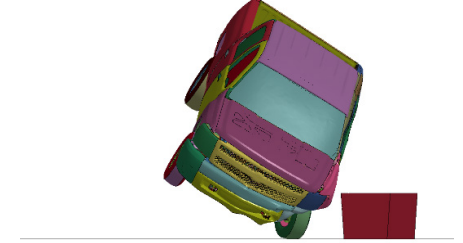
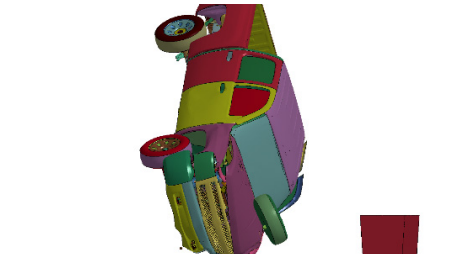
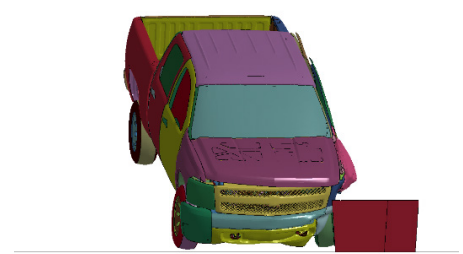
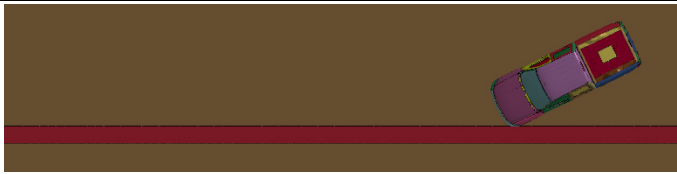

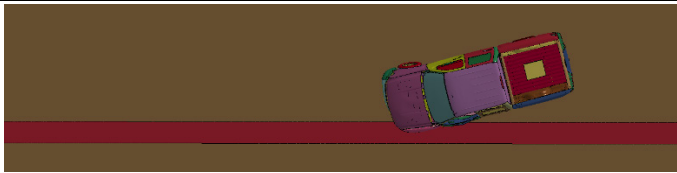
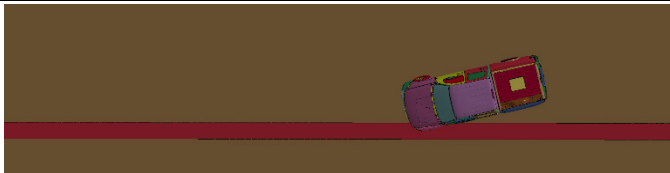

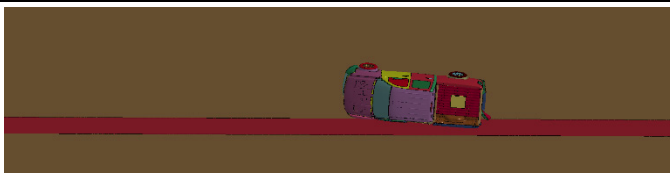
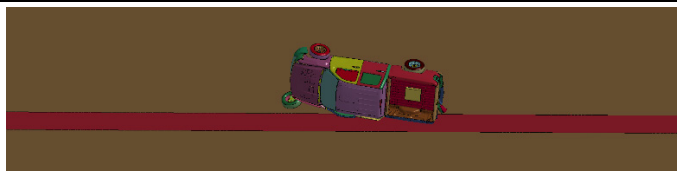


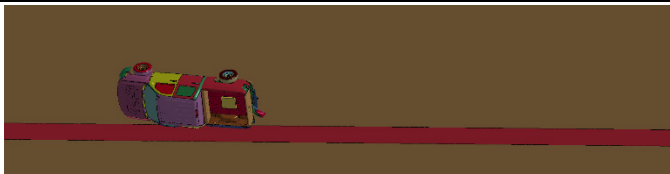
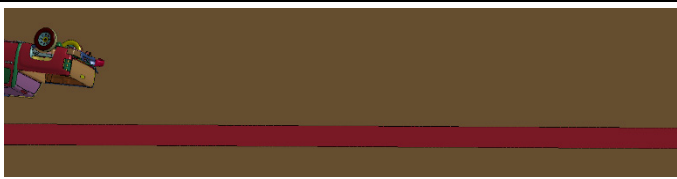

Time (seconds)	With Impact Tire Disengagement	Without Impact Tire Disengagement
0.0		
0.1		
0.2		
0.3		
0.6		
1.0		

Table 5.24 Sequential Images of Preliminary Simulations for 24-Inch Tall PCB with 1:15 Slope (Overhead View)

Time (seconds)	With Impact Tire Disengagement	Without Impact Tire Disengagement
0.0		
0.1		
0.2		
0.3		
0.6		
1.0		

5.5.4 24-Inch Tall T Shaped PCB

The pickup truck remained upright during and after the collision events in both cases. Figure 5.21 and Figure 5.22 show vehicle roll, pitch and yaw angles throughout the impact events against the 24-inch tall T shaped PCB in both cases, respectively. Maximum roll angle resulted to be -44.4 degrees in case 1 and -34.8 degrees in case 2. Table 5.25 compares the occupant risk values, which all remained in the limitation required by MASH criteria. Table 5.26 and Table 5.27 include the sequential images of the two cases in front view and overhead view, respectively.

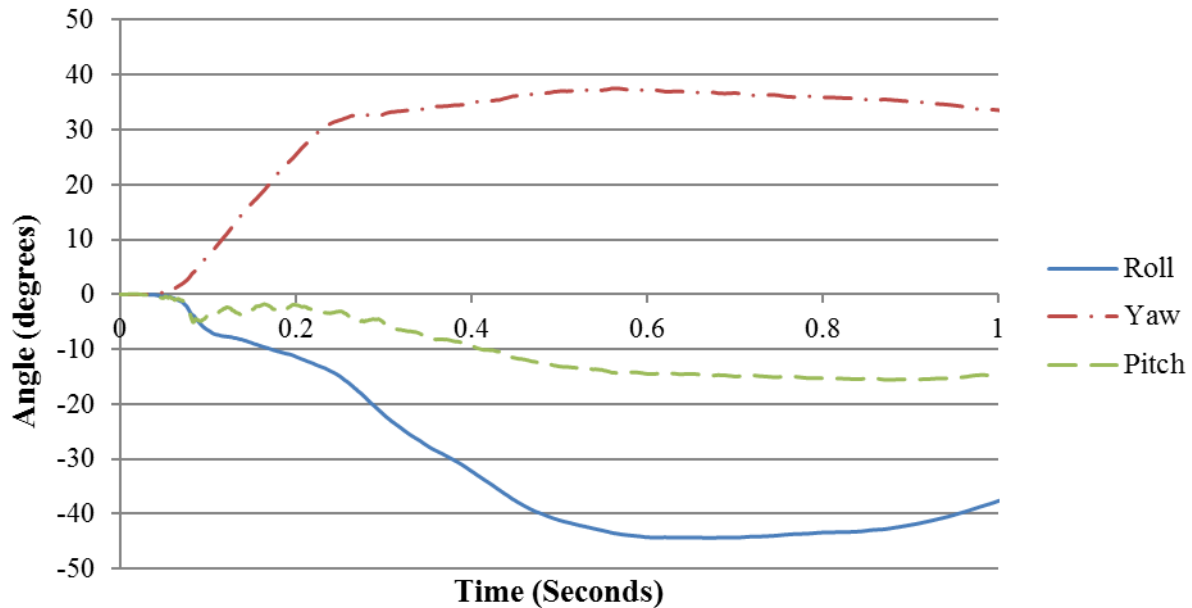


Figure 5.21 Angular Displacements of the Vehicle in Preliminary Simulation of 24-Inch Tall T Shaped PCB (Case 1)

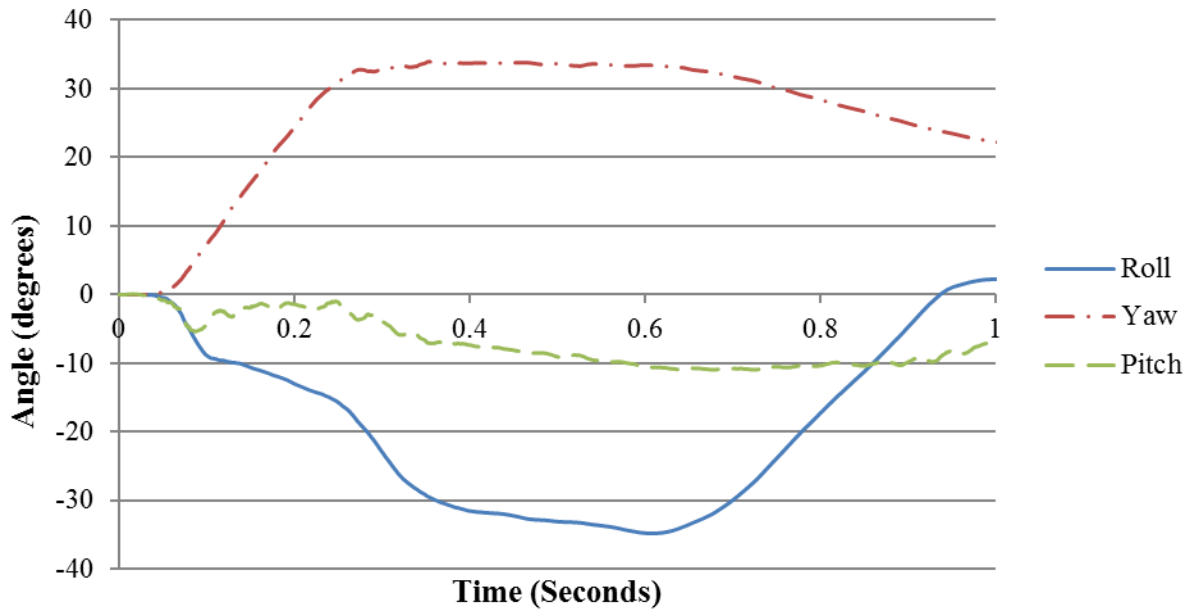


Figure 5.22 Angular Displacements of the Vehicle in Preliminary Simulation of 24-Inch Tall T Shaped PCB (Case 2)

Table 5.25 Occupant Risk Values Comparison between Case 1 and Case 2 (24-Inch Tall T Shaped PCB)

Occupant Risk Factors and Maximum Angular Displacement		Case 1 - With Impact Tire Disengagement	Case 2 - Without Impact Tire Disengagement
Impact Velocity (ft/s)	x-direction	19.0	20.3
	y-direction	22.6	-20.7
Ridedown Acceleration (G)	x-direction	-5.0	-7.8
	y-direction	11.5	11.0
Maximum Angular Displacement (Degrees)	Roll	-44.4	-34.8
	Pitch	-15.6	-11.0
	Yaw	37.5	33.9

Table 5.26 Sequential Images of Preliminary Simulations for 24-Inch Tall T Shaped PCB (Front View)



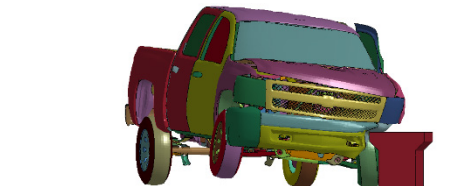
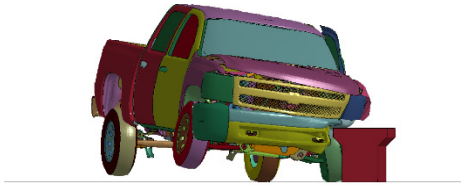
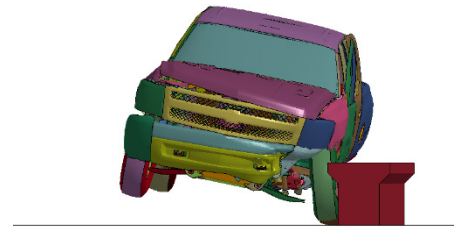
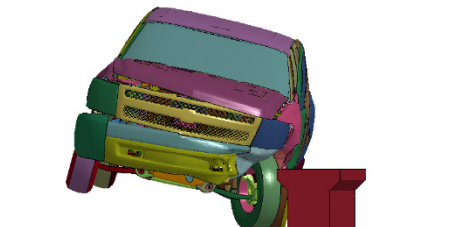
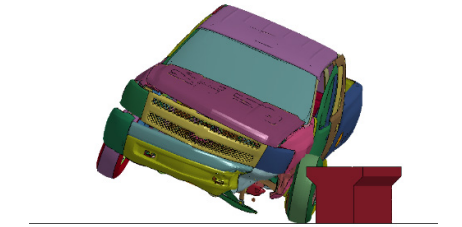
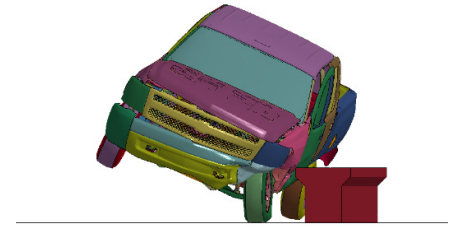
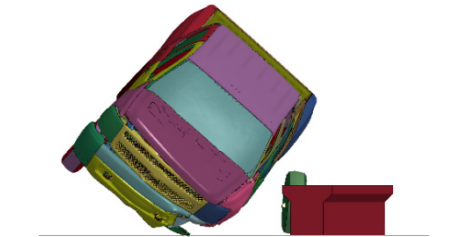
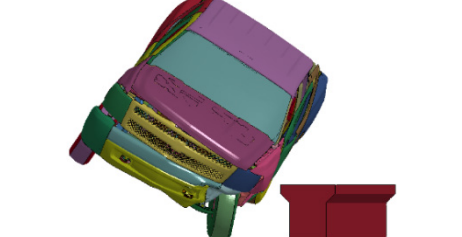
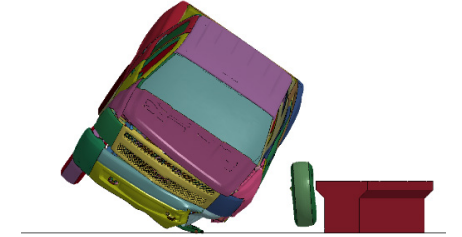
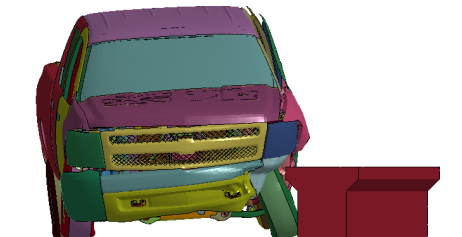
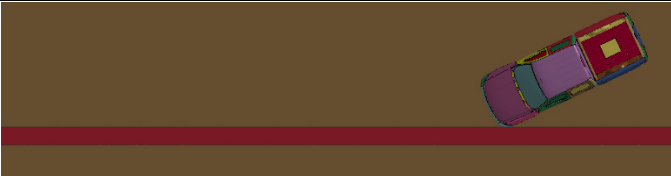

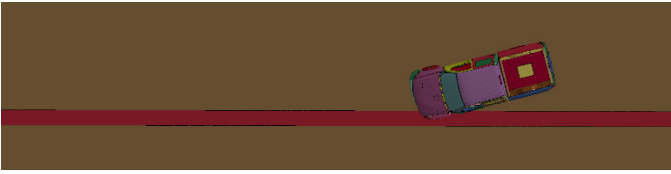
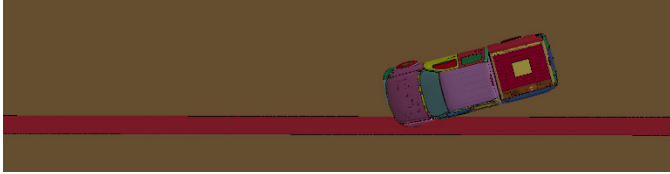
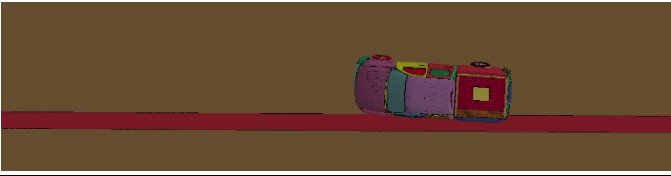
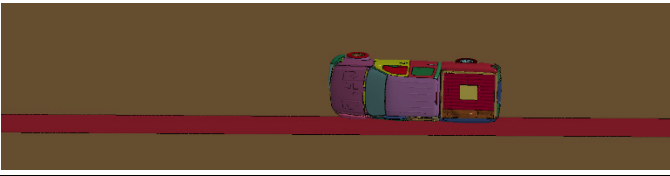
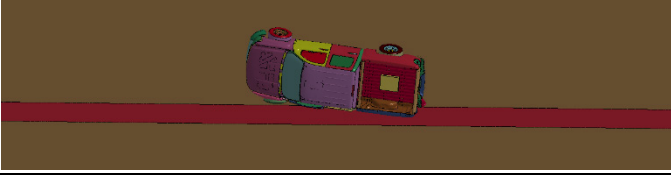
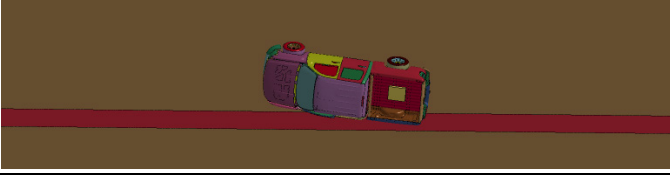

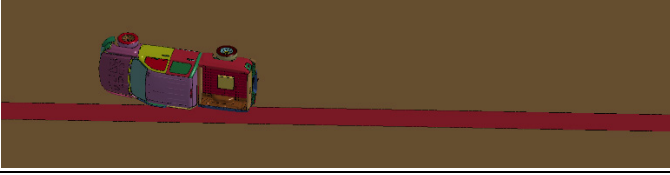


Time (seconds)	With impact tire disengagement	Without impact tire disengagement
0.0		
0.1		
0.2		
0.3		
0.6		
1.0		

Table 5.27 Sequential Images of Preliminary Simulations for 24-Inch Tall T Shaped PCB (Overhead View)

Time (seconds)	With impact tire disengagement	Without impact tire disengagement
0.0		
0.1		
0.2		
0.3		
0.6		
1.0		

5.5.5 24-Inch Tall T Shaped PCB with 1:20 Slope

In both cases, the pickup truck remained upright during and after the collision events. Figure 5.23 and Figure 5.24 show vehicle roll, pitch and yaw angles throughout the impact events against the 24-inch tall T shaped PCB with 1:20 slope in both cases, respectively. Maximum roll angle resulted to be -43.1 degrees in case 1 and -37.6 degrees in case 2. Table 5.28 compares the occupant risk values, which all remained in the limitation of MASH criteria. Table 5.29 and Table 5.30 show the sequential images of the two cases in front view and overhead view, respectively.

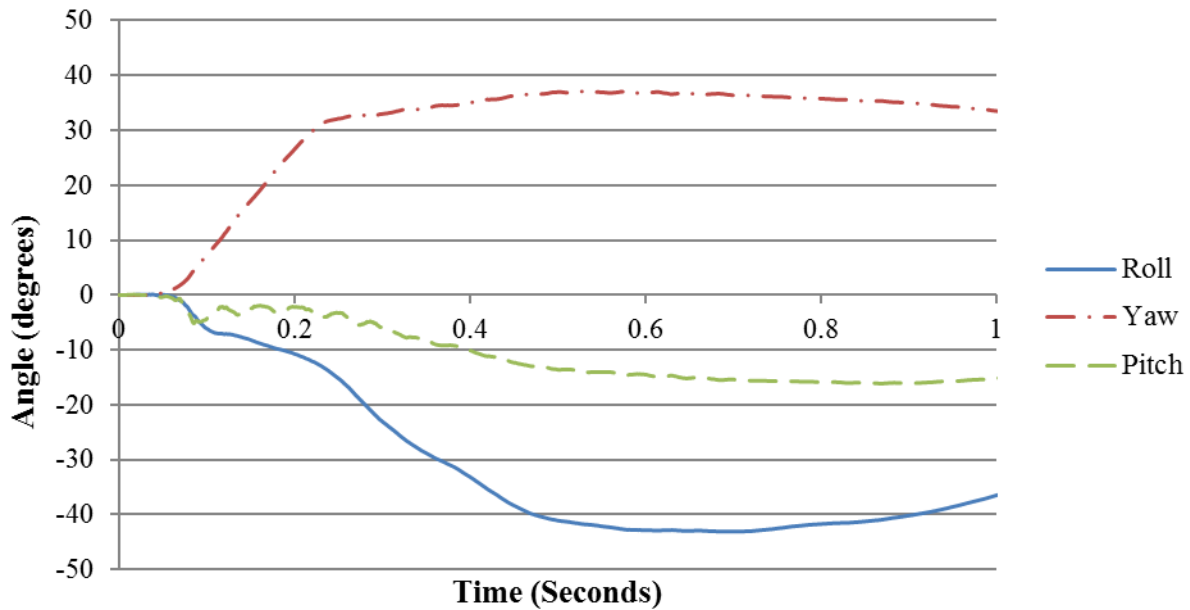


Figure 5.23 Angular Displacements of the Vehicle in Preliminary Simulation of 24-Inch Tall T Shaped PCB with 1:20 slope (Case 1)

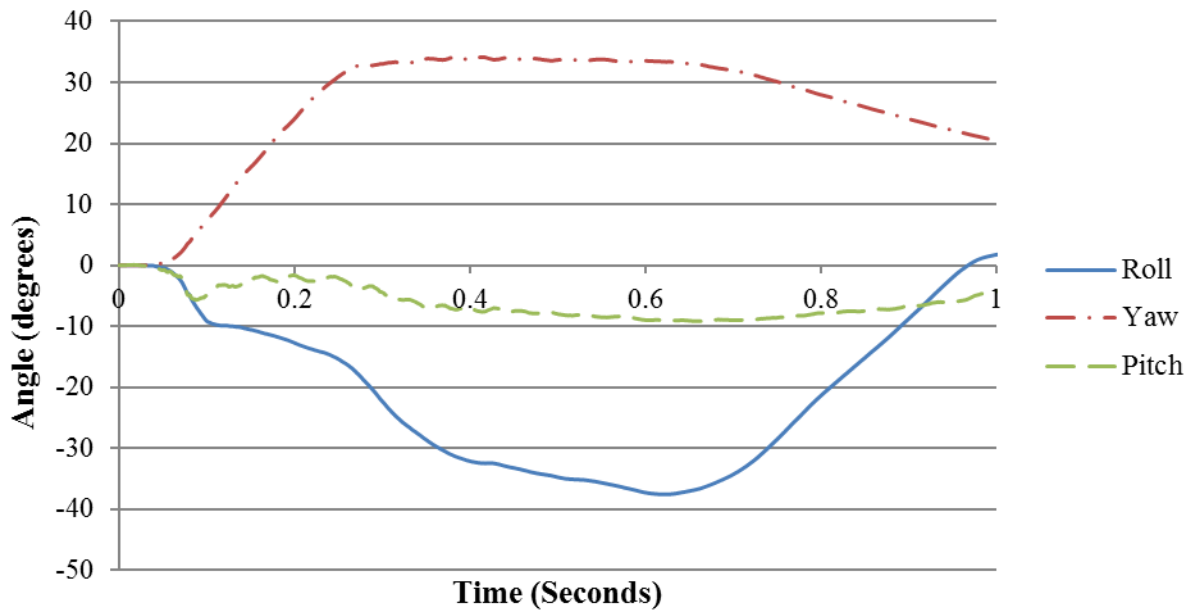


Figure 5.24 Angular Displacements of the Vehicle in Preliminary Simulation of 24-Inch Tall T Shaped PCB with 1:20 Slope (Case 2)

Table 5.28 Occupant Risk Values Comparison between Case 1 and Case 2 (24-Inch Tall T Shaped PCB with 1:20 Slope)

Occupant risk factors and Maximum Angular Displacement		Case 1 - With Impact Tire Disengagement	Case 2 - Without Impact Tire Disengagement
Impact Velocity (ft/s)	x-direction	15.1	22.3
	y-direction	-26.5	-23.3
Ridedown Acceleration (G)	x-direction	-6.5	-9.0
	y-direction	13.3	9.4
Maximum Angular Displacement (Degrees)	Roll	-43.1	-37.6
	Pitch	-16.1	-9.2
	Yaw	37.2	34.1

Table 5.29 Sequential Images of Preliminary Simulations for 24-Inch Tall T Shaped PCB with 1:20 Slope (Front View)



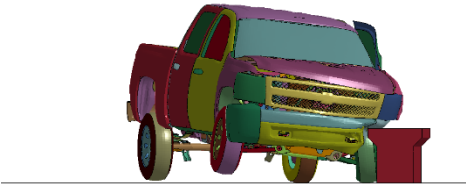
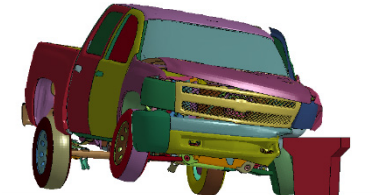
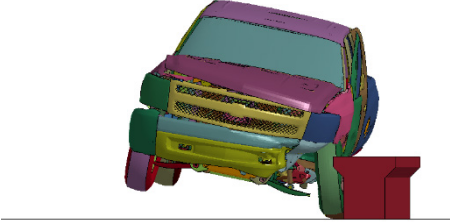
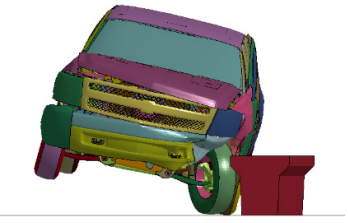
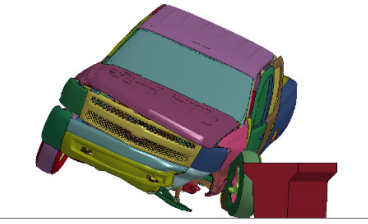
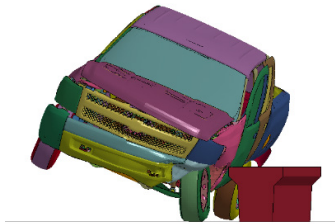
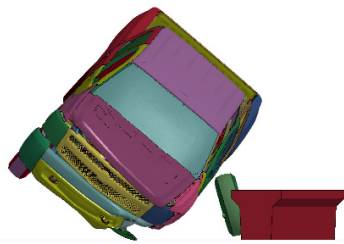
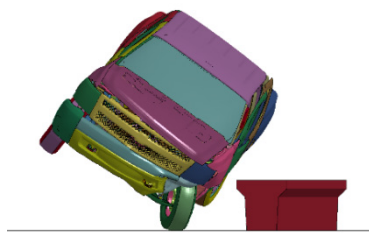
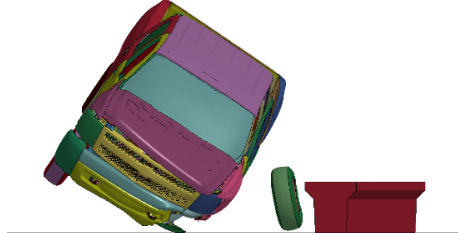
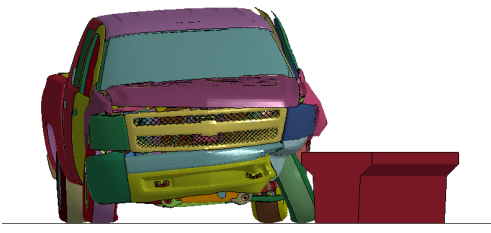



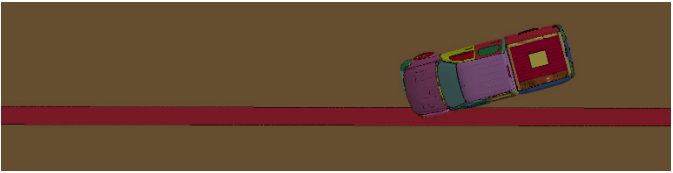

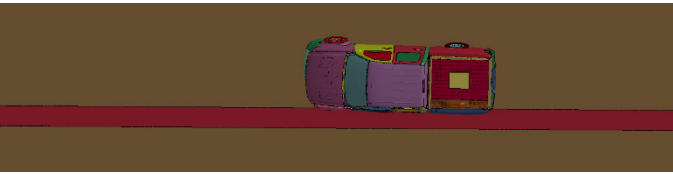
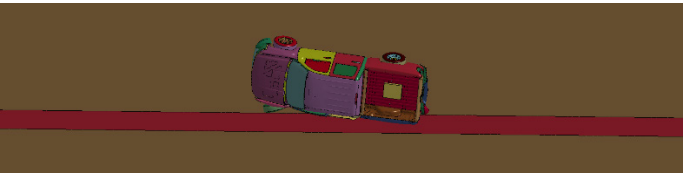
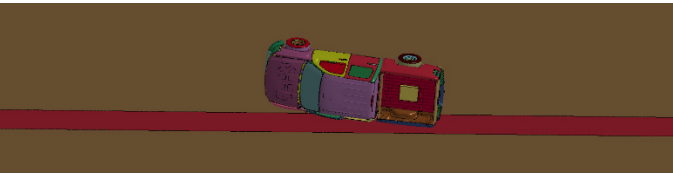
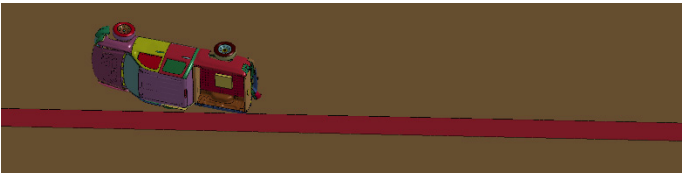



Time (seconds)	With Impact Tire Disengagement	Without Impact Tire Disengagement
0.0		
0.1		
0.2		
0.3		
0.6		
1.0		

Table 5.30 Sequential Images of Preliminary Simulations for 24-Inch Tall T Shaped PCB with 1:20 Slope (Overhead View)

Time (seconds)	With impact tire disengagement	Without impact tire disengagement
0.0		
0.1		
0.2		
0.3		
0.6		
1.0		

5.5.6 24-Inch Tall I Shaped PCB

In both cases, the pickup truck remained upright during and after the collision events. Figure 5.25 and Figure 5.26 show vehicle roll, pitch and yaw angles throughout the impact events against the 24-inch tall I shaped PCB in both cases, respectively. Maximum roll angle resulted to be -46 degrees in case 1 and -33.9 degrees in case 2. Table 5.31 compares the occupant risk values, which all remained in the limitation required by MASH criteria. Table 5.32 and Table 5.33 include the sequential images of the two cases in front and overhead view, respectively.

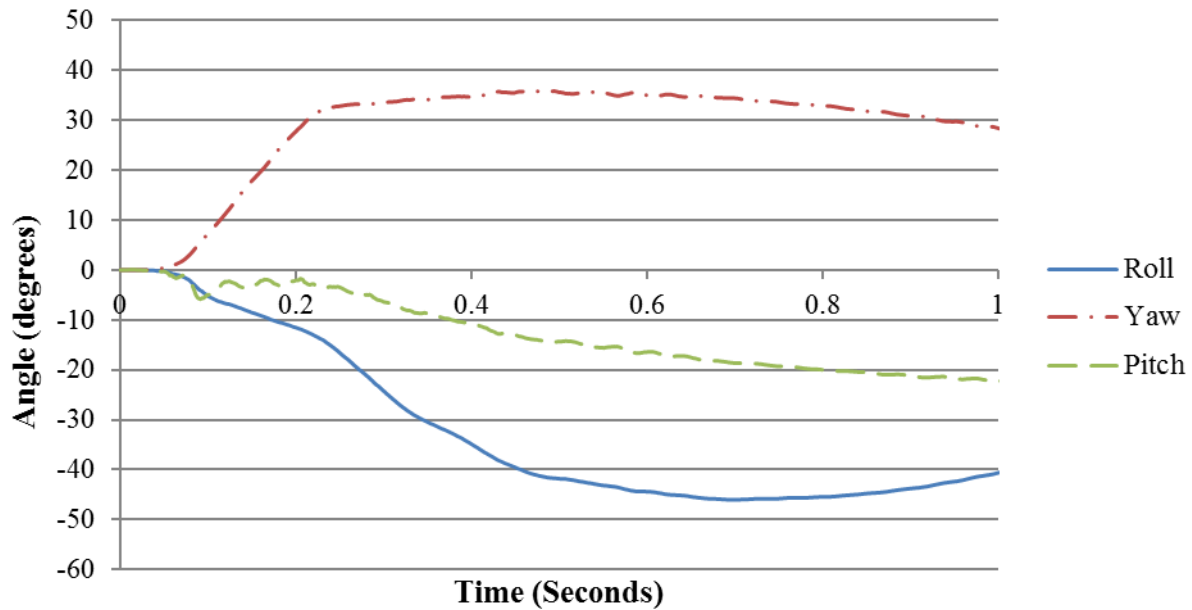


Figure 5.25 Angular Displacements of the Vehicle in Preliminary Simulation of 24-Inch Tall I Shaped PCB (Case 1)

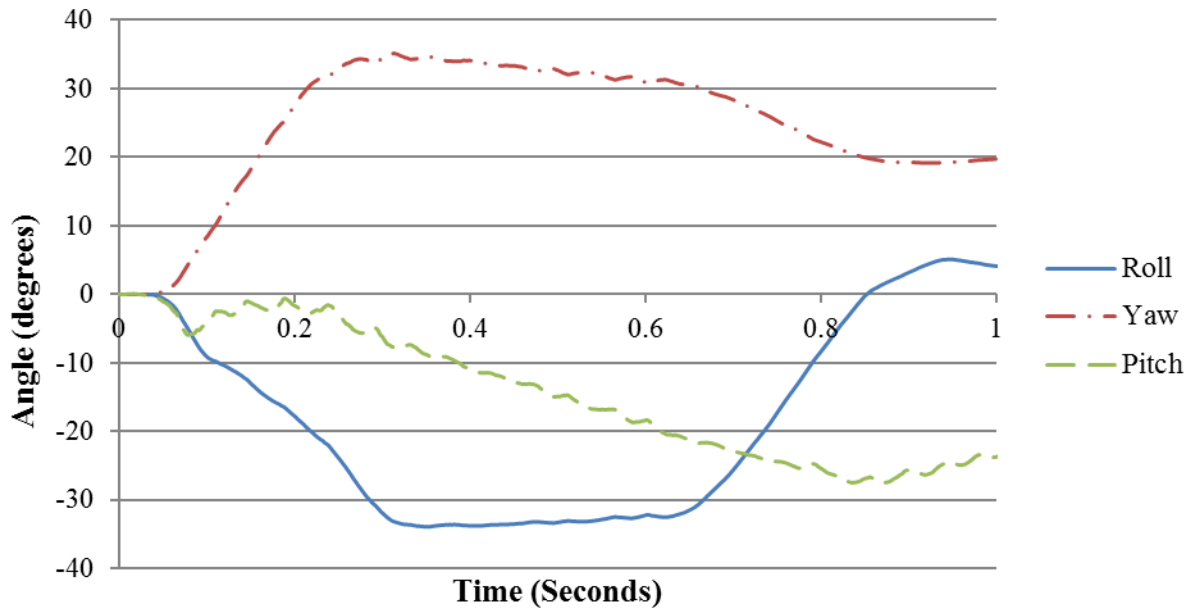


Figure 5.26 Angular Displacements of the Vehicle in Preliminary Simulation of 24-Inch Tall I Shaped PCB (Case 2)

Table 5.31 Occupant Risk Values Comparison between Case 1 and Case 2 (24-Inch Tall I Shaped PCB)

Occupant risk factors and Maximum Angular Displacement		Case 1 - With Impact Tire Disengagement	Case 2 - Without Impact Tire Disengagement
Impact Velocity (ft/s)	x-direction	16.1	14.8
	y-direction	-26.2	-27.2
Ridedown Acceleration (G)	x-direction	-5.4	-10.4
	y-direction	12.6	12.3
Maximum Angular Displacement (Degrees)	Roll	-46.0	-33.9
	Pitch	-23.3	-27.5
	Yaw	35.9	35.1

**Table 5.32 Sequential Images of Preliminary Simulations for 24-Inch Tall I Shaped PCB
(Front View)**

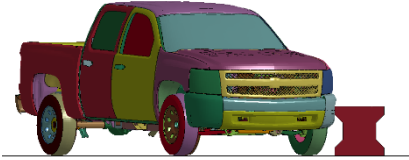
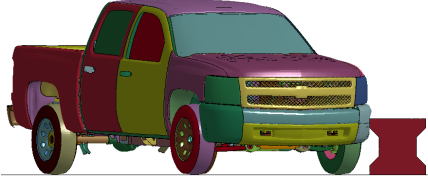
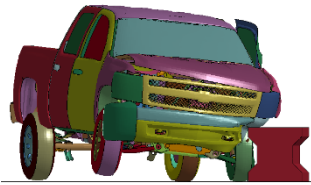
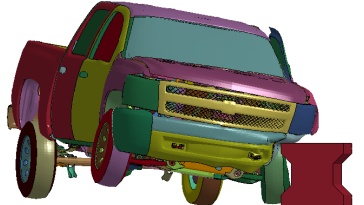
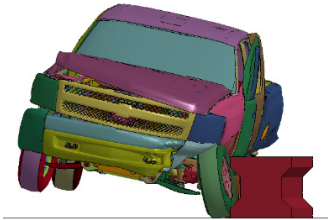

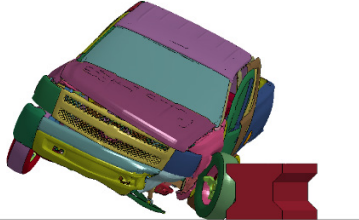
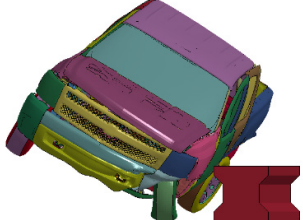
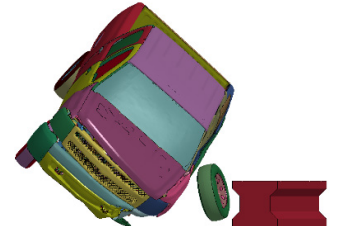
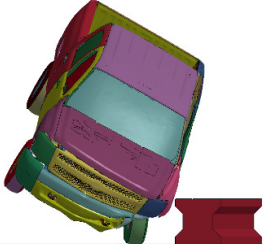
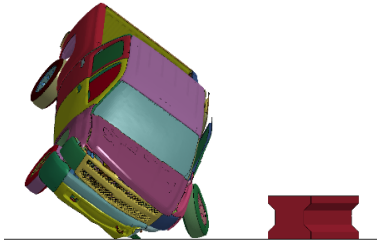

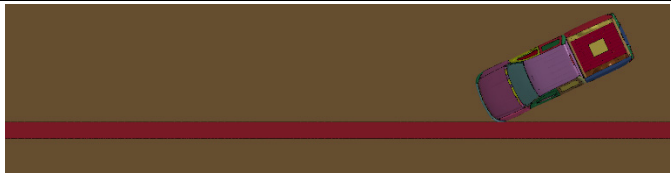


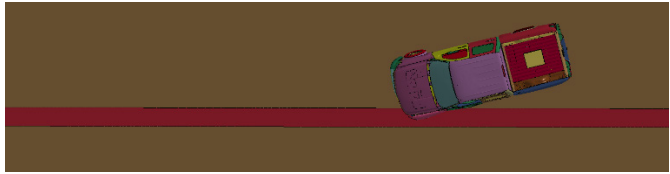
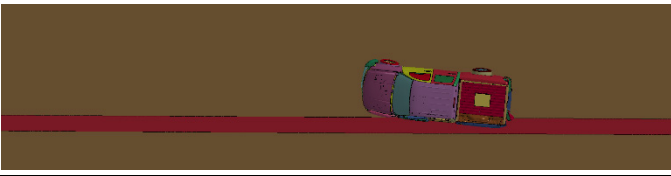
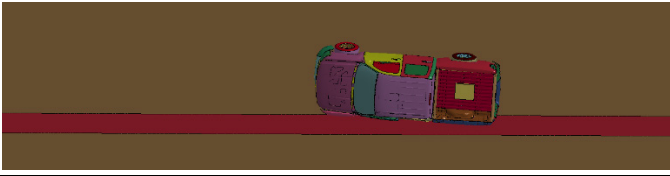
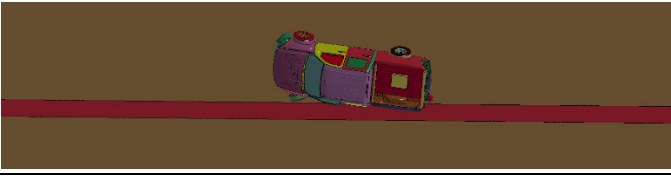


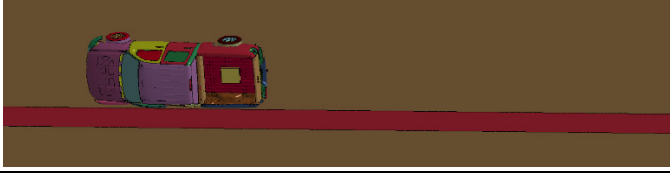


Time (seconds)	With Impact Tire Disengagement	Without Impact Tire Disengagement
0.0		
0.1		
0.2		
0.3		
0.6		
1.0		

Table 5.33 Sequential Images of Preliminary Simulations for 24-Inch Tall I Shaped PCB (Overhead View)

Time (seconds)	With impact tire disengagement	Without impact tire disengagement
0.0		
0.1		
0.2		
0.3		
0.6		
1.0		

5.5.7 24-Inch Tall I Shaped PCB with 1:20 Slope

The pickup truck was redirected and remained upright during and after the collision events in both cases. Figure 5.27 and Figure 5.28 show vehicle roll, pitch and yaw angles throughout the impact event against the 24-inch tall I shaped PCB with 1:20 slope in both cases, respectively. Maximum roll angle resulted to be -38.8 degrees in case 1 and -36.4 degrees in case 2. Table 5.16 compares the occupant risk values, which all remained in the limitation required by MASH criteria. Table 5.34 and Table 5.35 include the sequential images of the two cases in front view and overhead view, respectively.

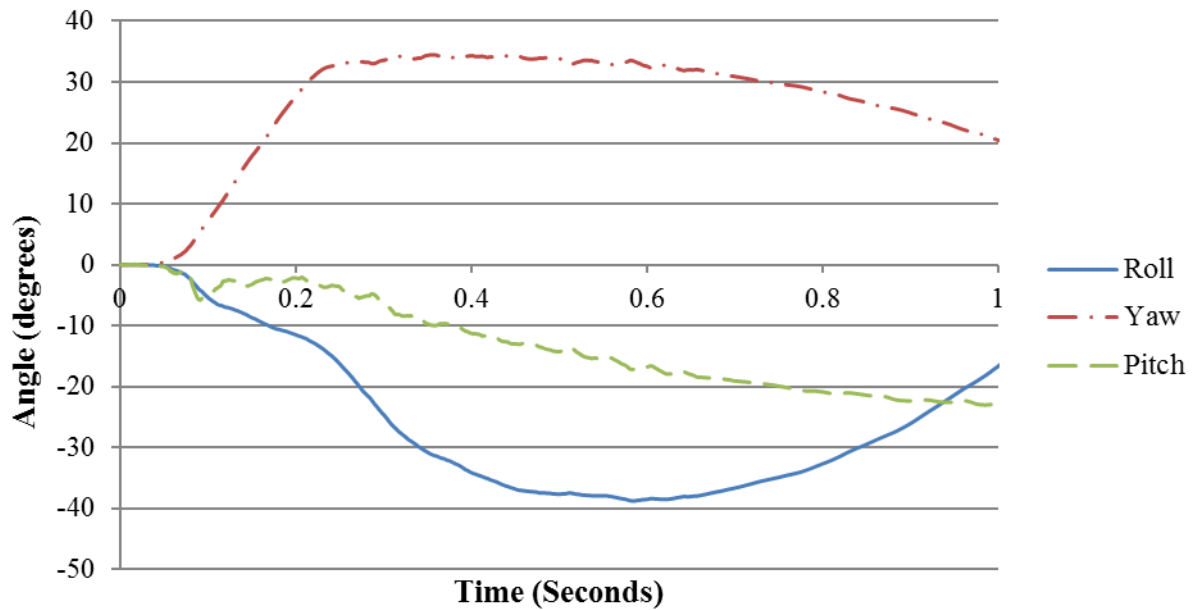


Figure 5.27 Angular Displacements of the Vehicle in Preliminary Simulation of 24-Inch Tall I Shaped PCB with 1:20 slope (Case 1)

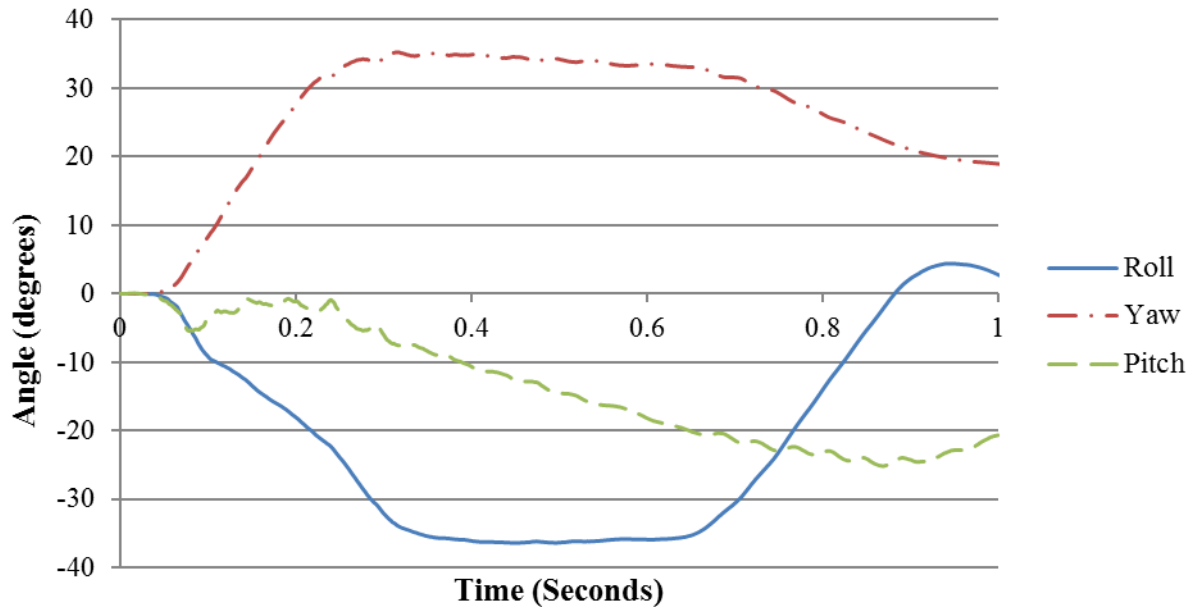


Figure 5.28 Angular Displacements of the Vehicle in Preliminary Simulation of 24-Inch Tall I Shaped PCB with 1:20 Slope (Case 2)

Table 5.34 Occupant Risk Values Comparison between Case 1 and Case 2 (24-Inch Tall I Shaped PCB with 1:20 Slope)

Occupant Risk Factors and Maximum Angular Displacement		Case 1 - With Impact Tire Disengagement	Case 2 - Without Impact Tire Disengagement
Impact Velocity (ft/s)	x-direction	16.4	16.4
	y-direction	-23.3	-22.3
Ridedown Acceleration (G)	x-direction	-5.7	-10.5
	y-direction	13.9	17.7
Maximum Angular Displacement (Degrees)	Roll	-38.8	-36.4
	Pitch	-23.0	-25.2
	Yaw	34.5	35.3

Table 5.35 Sequential Images of Preliminary Simulations for 24-Inch Tall I Shaped PCB with 1:20 Slope (Front View)

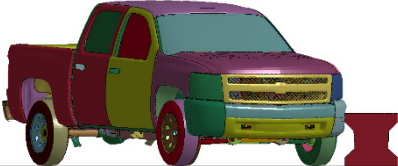

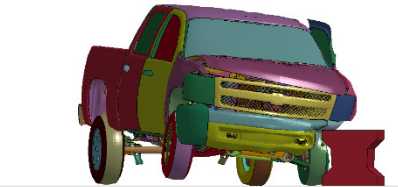
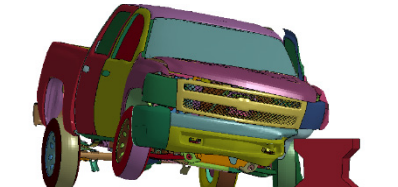
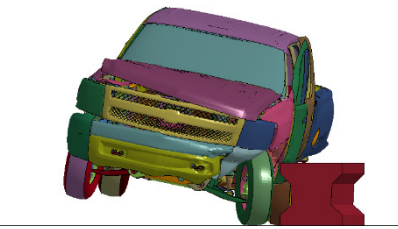
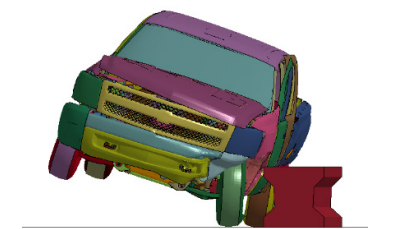
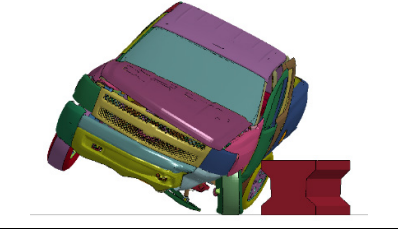
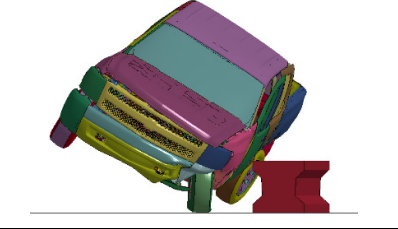
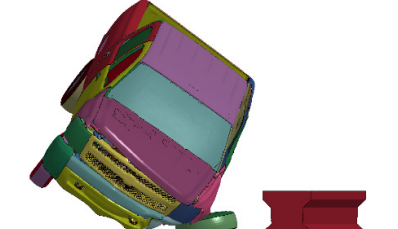
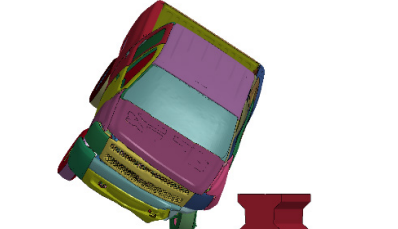
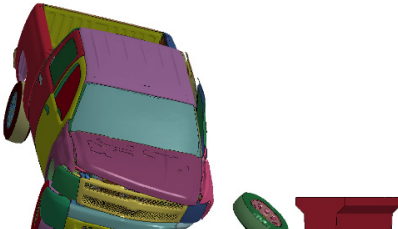
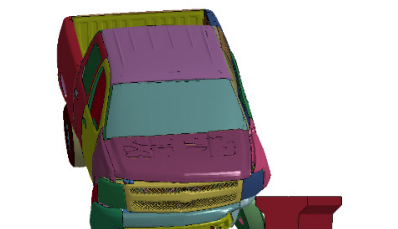
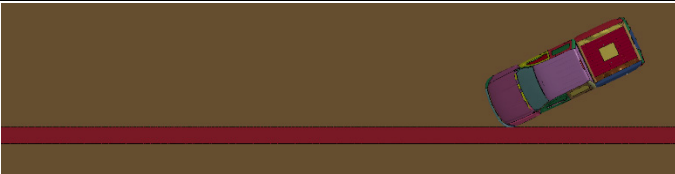


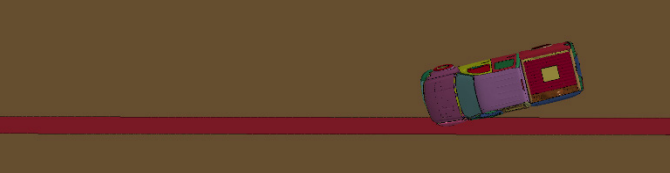
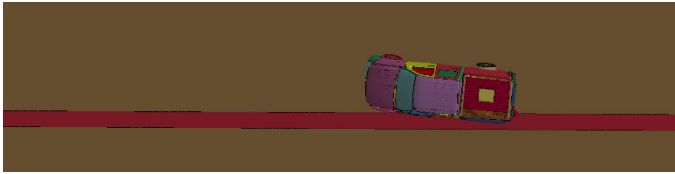
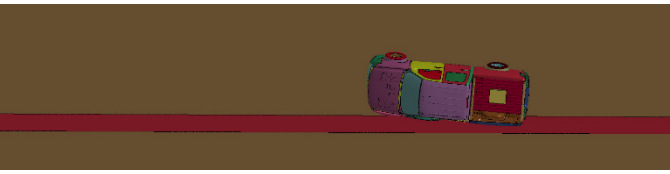


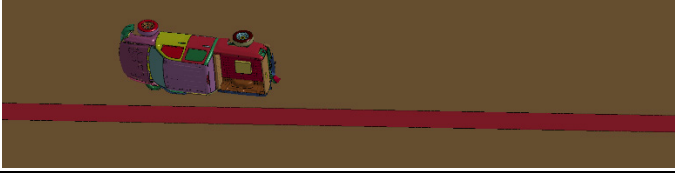



Time (seconds)	With Impact Tire Disengagement	Without Impact Tire Disengagement
0.0		
0.1		
0.2		
0.3		
0.6		
1.0		

Table 5.36 Sequential Images of Preliminary Simulations for 24-Inch Tall I Shaped PCB with 1:20 Slope (Overhead View)

Time (seconds)	With Impact Tire Disengagement	Without Impact Tire Disengagement
0.0		
0.1		
0.2		
0.3		
0.6		
1.0		

5.6 Summary and Comparison of 24 and 26-Inch Tall Barrier Simulations

5.6.1 Simulations with 26-Inch Tall Barriers

Simulations were conducted with the pickup truck vehicle impacting the PCB system at a speed of 62 mi/h and an angle of 25 degrees. Impact location was roughly at 1/3 of the 120-ft long, 26-inch tall concrete rigid block. Evaluated PCB systems included proposed PCB profile concepts of 1:15 slope, 1:20 slope, T shaped, T shaped with 1:20 slope, I shaped, I shaped with 1:20 slope. For all the simulated cases, the pickup truck was contained and redirected by the 26-inch tall PCB systems. Recorded occupant risks for each of these simulations against 26-inch tall PCB systems were all well within MASH limits.

Figure 5.29 summarizes the vehicle roll angular displacements recorded during the impact events, for those simulations which were modeled with impact tire disengagement. Figure 5.30 summarizes the vehicle roll angular displacements recorded during the impact events, for those simulations which were modeled without impact tire disengagement.

Preliminary simulations suggest that the vehicle maintained its stability during the impact event when evaluated against the proposed barrier profile concepts. The vehicle roll angular displacement was contained between roughly 25 and 40 degrees when considering tire disengagement. When the tire disengagement option was not applied, the vehicle roll angular displacement was even more contained within roughly a 5-degree span (30 to 35 degrees). Interestingly, it seems that the vehicle maintained a very similar rolling behavior when impacting the two T shaped profiles (with and without slopes), with and without tire disengagement (27 to 31 degrees).

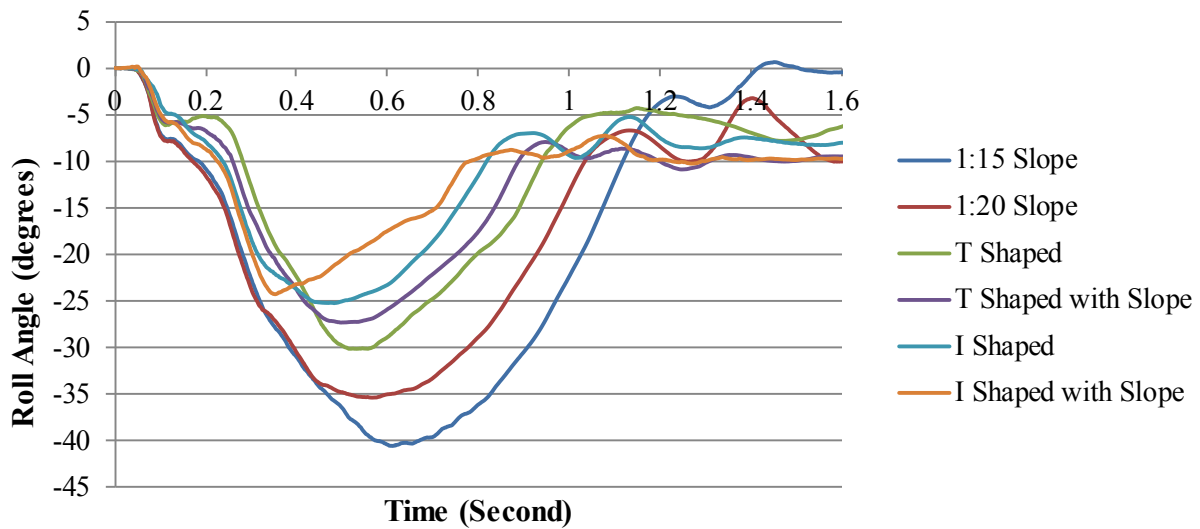


Figure 5.29 Roll Angle Comparison of 26-Inch Tall Barrier Concepts with Impact Tire Disengagement

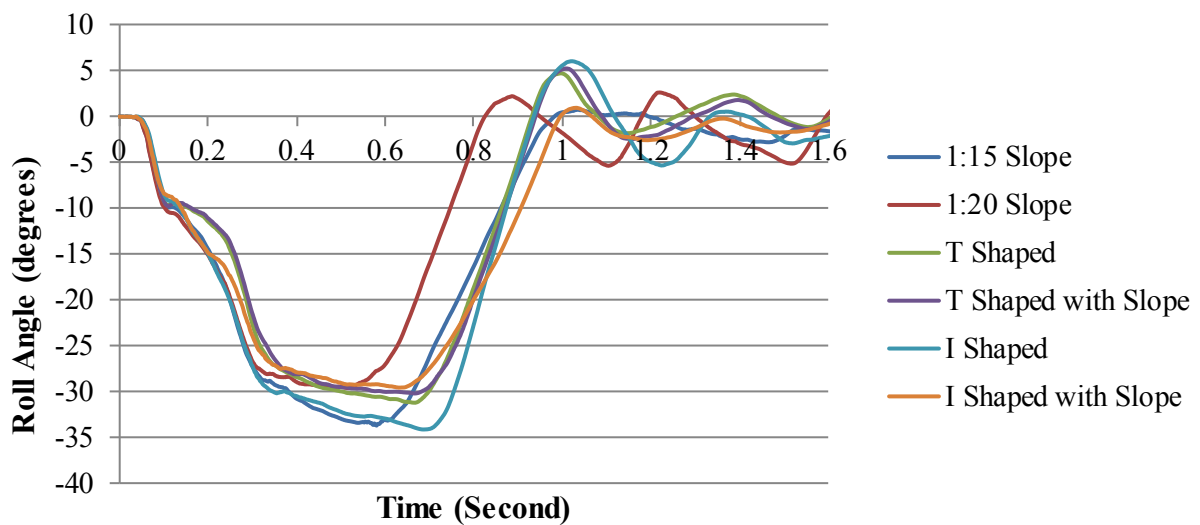


Figure 5.30 Roll Angle Comparison of 26-Inch Tall Barriers without Impact Tire Disengagement

Figure 5.31 summarizes the maximum roll angular displacements recorded in the preliminary simulations for the 26-inch tall barrier options. Values are reported per each evaluated profiles. For each profile, maximum roll values from parametric simulations with and

without tire disengagement are reported. Tire disengagement phenomena during a crash test cannot be easily predicted. Therefore, these two simulated cases – with and without tire disengagement – mean to represent the extremes of a number of vehicle tire behaviors which could potentially be experienced during a crash test. Therefore, when the simulations predict maximum roll angles of 27.3 and 30.1 degrees for the two simulated extreme cases of impact against a T shaped PCB with sloped sides, it would be expected that during the crash test the vehicle might experience rolling approximately within this range of angular displacements, due a variety of possible interactions that could potentially occur between the vehicle’s tire and the barrier profile.

The conducted preliminary simulations on the 26-inch tall PCB systems suggested that 26 inches height appears to be adequate to contain, redirect, and maintain stability of the impacting 2270P vehicle.

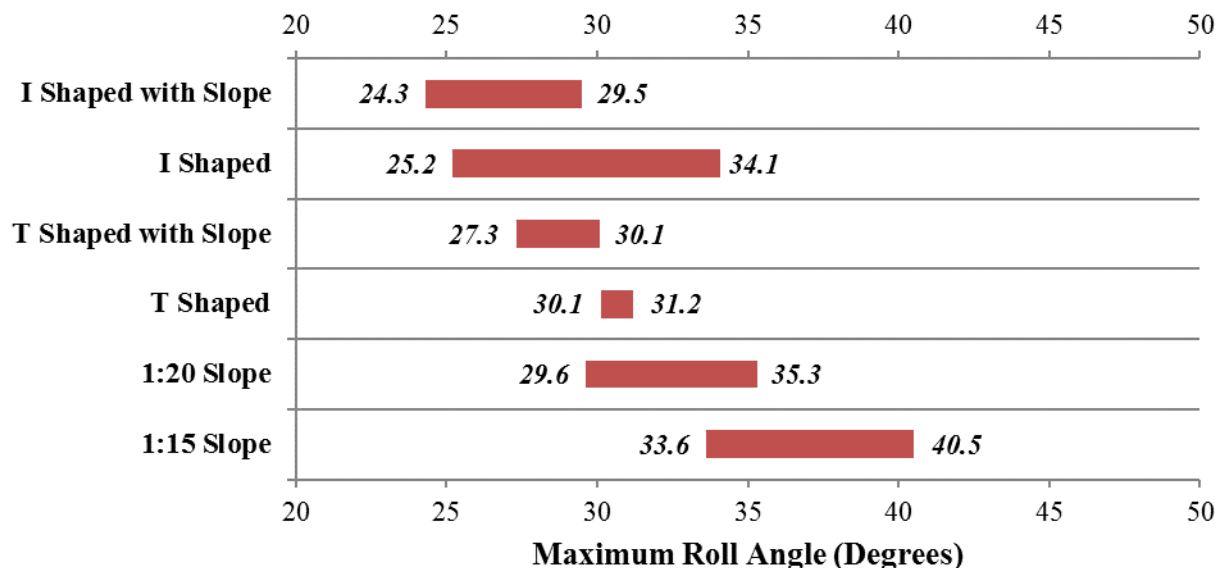


Figure 5.31 Range of Maximum Roll Angles of 26-Inch Tall Barrier Concepts

5.6.2 Simulations with 24-Inch Tall Barriers

Simulations were conducted with the pickup truck vehicle impacting the PCB system at a speed of 62 mi/h and an orientation of 25 degrees. Impact location was roughly at 1/3 of the 120-ft long, 24-inch tall concrete rigid block. Evaluated PCB systems included proposed PCB profile concepts of 1:15 slope, 1:20 slope, T shaped, T shaped with a 1:20 slope, I shaped, I shaped with a 1:20 slope. For all the 24-inch tall simulated profile concepts, the pickup truck was contained and redirected by the impacted PCB systems. Figure 5.32 summarizes the vehicle roll angular displacements recorded during the impact events, for those simulations which were modeled with impact tire disengagement. Figure 5.33 summarizes the vehicle roll angular displacements recorded during the impact events, for those simulations which were modeled without impact tire disengagement.

During the impact events against the 1:15 and 1:20 slope profiles (with impact tire disengagement), however, the 2270P pickup truck revealed unstable and unacceptable behavior. In both cases, the recorded maximum roll angular displacements were above the required MASH limits, failing the MASH requirements for vehicle stability. Figure 5.32 suggests that the vehicle maintained its stability during the impact events against the T Shaped and I Shaped low-profile PCBs with impact tire disengagement. For these cases, the vehicle roll angular displacement was contained between roughly 39 and 46 degrees when considering tire disengagement. When the tire disengagement option is not applied, the recorded maximum roll angular displacements were all contained within the required MASH limits, all below 38 degrees.

Recorded occupant risks for each of these simulations against 24-inch tall PCB systems were all well within MASH limits.

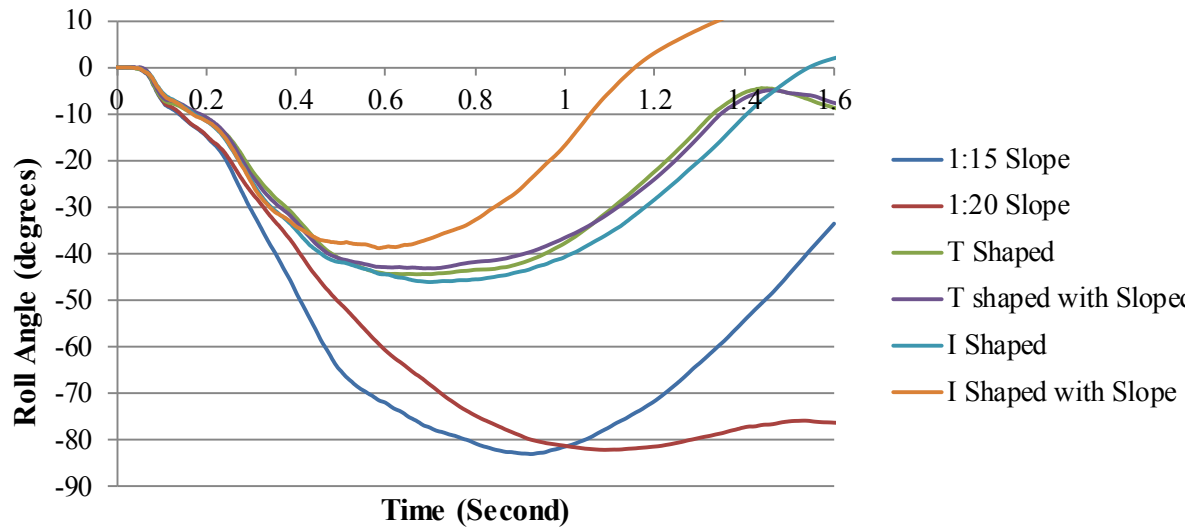


Figure 5.32 Roll Angle Comparison of 24-Inch Tall Barrier Concepts with Impact Tire Disengagement

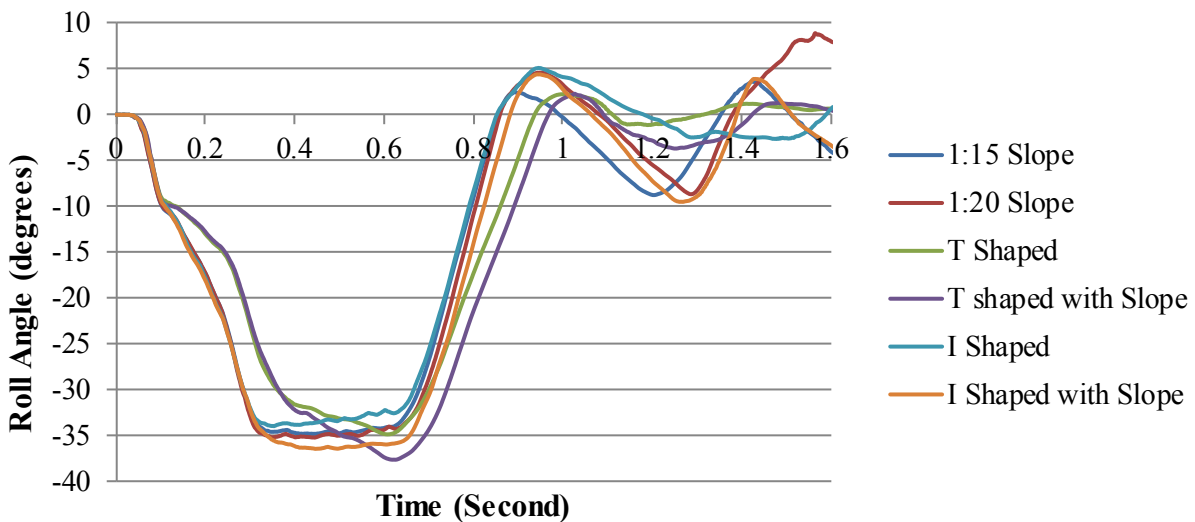


Figure 5.33 Roll Angle Comparison of 24-Inch Tall Barriers without Impact Tire Disengagement

Figure 5.34 summarizes the maximum roll angular displacements recorded in the preliminary simulations for the 24-inch tall barrier options. Values are reported per each evaluated profiles. For each profile, maximum roll values from parametric simulations with and

without tire disengagement are reported. These two simulated cases – with and without tire disengagement – mean to represent the extremes of a number of vehicle tire behaviors which could potentially be experienced during a crash test.

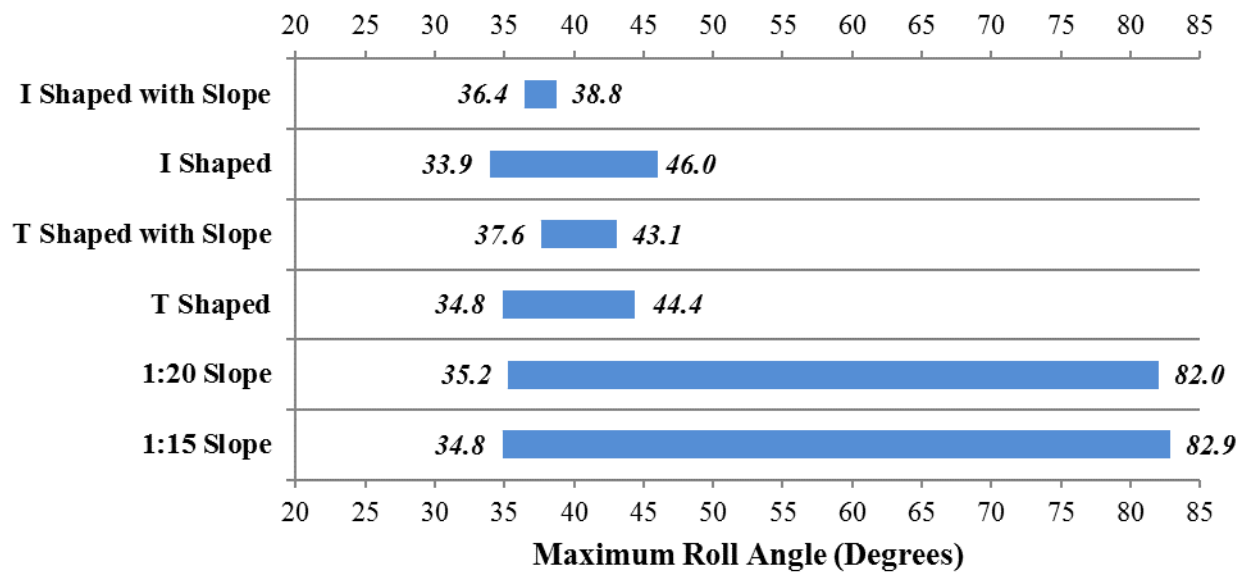


Figure 5.34 Range of Maximum Roll Angles of 24-Inch Tall Barrier Concepts

The conducted preliminary simulations on the 24-inch tall PCB systems suggested that not all the proposed barrier profiles might be able to adequately contain, redirect and stabilize the impacting 2270P vehicle. For the case of the sloped profiles (1:15 and 1:20), it appears that the systems might not be result crashworthy options due to the likely high instability of the 2270P vehicle.

5.7 Conclusion of Preliminary Simulations

For all the 26-inch tall simulated profile concepts, the 2270P vehicle was contained and redirected by the impacted PCB systems. For all the 24-inch tall simulated profile concepts, the 2270P vehicle was contained and redirected by the impacted PCB systems. During the impact events against the 1:15 and 1:20 slope profiles (with impact tire disengagement), however, the 2270P vehicle revealed unstable and unacceptable behavior. In both cases, the recorded maximum roll angular displacements were above the required MASH limits, failing the MASH requirements for vehicle stability.

Table 5.37 summarizes the occupant risk and angular displacements recorded in the preliminary simulations. Recorded occupant risks for each of these simulations were all well within MASH limits.

Based on these preliminary simulation results, it was decided to further investigate the behavior of the T Shaped low-profile PCB option, with consideration of specific barrier segment length, as well as detailed modeling of barrier segment connections. A height of 26 inches rather than 24 inches would guarantee more vehicle stability during the impact event. It was also concluded that the T Shaped profile appeared to have demonstrated more consistent performance in either cases with vehicle tire disengagement and without vehicle tire disengagement. It also appeared that there is no significant barrier performance improvement by sloping the sides of the T Shaped system. Therefore, it was decided to conduct detailed computer modeling and simulations of MASH Test 3-11 impact conditions against a T Shaped PCB profile with the two heights.

Table 5.37 Occupant Risk and Maximum Angular Displacements of Preliminary Simulations

Name	Tire Disengagement	OIV (ft/s)		ORA (G)		Roll	Pitch	Yaw	Result
		Longitudinal	Lateral	Longitudinal	Lateral				
1:15 Slope 24"	With	14.1	24.9	5.9	12.6	82.9	35.0	40.9	Fail
	Without	14.1	20.0	11.0	11.1	34.8	24.2	34.6	Pass
1:15 Slope 26"	With	20.7	20.3	11.2	11.5	40.5	16.3	35.2	Pass
	Without	16.7	24.3	7.7	12.0	33.6	11.4	33.4	Pass
1:20 Slope 24"	With	13.8	26.9	5.7	12.2	82.0	18.6	42.5	Fail
	Without	16.7	25.3	15.1	14.8	35.2	28.1	35.4	Pass
1:20 Slope 26"	With	20.0	27.2	10.2	11.2	35.3	18.3	36.4	Pass
	Without	18.7	24.3	8.2	12.1	29.6	15.2	33.5	Pass
T Shape 24"	With	19.0	22.6	5.0	11.5	44.4	15.6	37.5	Pass
	Without	20.3	20.7	7.8	11.0	34.8	11.0	33.9	Pass
T Shape 26"	With	19.3	23.0	7.6	8.9	30.1	9.8	34.3	Pass
	Without	19.0	23.9	13.4	14.0	31.2	7.3	34.3	Pass
T Shape with Slope 24"	With	15.1	26.5	6.5	13.3	43.1	16.1	37.2	Pass
	Without	22.3	23.3	9.0	9.4	37.6	9.2	34.1	Pass
T Shape with Slope 26"	With	14.1	25.3	8.0	9.9	27.3	10.0	36.3	Pass
	Without	20.7	25.3	7.0	15.7	30.1	6.9	34.1	Pass
I Shape 24"	With	16.1	26.2	5.4	12.6	46	23.3	35.9	Pass
	Without	14.8	27.2	10.4	12.3	33.9	27.5	35.1	Pass
I Shape 26"	With	13.4	26.9	5.8	12.5	25.2	10.9	33.8	Pass
	Without	16.7	26.9	14.4	14.7	34.1	12.3	35.1	Pass
I Shape with Slope 24"	With	16.4	23.3	5.7	13.9	38.8	23.0	34.5	Pass
	Without	16.4	22.3	10.5	17.7	36.4	25.2	35.3	Pass
I Shape with Slope 26"	With	17.4	26.6	8.8	13.1	24.3	12.5	38.0	Pass
	Without	14.8	22.6	14.6	20.0	29.5	8.2	34.3	Pass

6. DETAILED FINITE ELEMENT ANALYSIS OF SELECTED CONCEPTS

6.1 Introduction

The section herein presents detailed design of 26-inch tall and 24-inch tall T shaped low-profile PCBs. Based on constructability feedback, it was decided to include a 1:18 slope on the stem of the T shaped barrier to accommodate construction forming. Detailed finite element computer modeling of the systems were performed and simulations were replicated with the new detailed models. The detailed FE model of the low-profile PCB included realistic replica of the barrier segment length, scuppers, and segment connection details, such as steel rods, plate washers, washers, and nuts. Simulations of MASH test 3-11 were conducted with a 2270P pickup truck impacting the free-standing barrier systems. Two simulation cases were considered for each height: Case 1, with impact tire disengagement from the vehicle suspension assembly; Case 2, without impact tire disengagement.

6.2 Detailed Finite Element Analysis 26-Inch Tall T Shaped PCB

6.2.1 Design of the 26-Inch Tall T Shaped PCB

The low-profile barrier was comprised of six segments of 26-inch tall, 30-ft long T shaped reinforced concrete barriers. The overall length of the barrier was 180 ft. Adjacent segments were joined with two connecting rods located in recessed rectangular cavities near the end of each barrier segment. There were minimal gaps between the sections.

Each T shaped barrier segment was symmetrically shaped about its vertical axis: 15 inches wide at the base sloping outward to 17-inches wide to a 45 degrees outward flare point (located 18 inches above grade) that transitioned to 25 inches wide at the top.

The connecting rods were $\frac{7}{8}$ -inch diameter \times 26-inch long threaded rod with $\frac{7}{8}$ -inch SAE hardened flat washers, $5\times 5\times\frac{1}{2}$ -inch plate washers, and $\frac{7}{8}$ -inch hex nuts on each end. The rods were inserted through two $1\frac{1}{2}$ -inch schedule 40 PVC pipe sleeves cast into the end of each segment. A 2×18 -inch drain scupper was located on the bottom near each end. Two 8×4 -inch forklift slots were located about the longitudinal centerline on 4-foot centers.

The compressive strength of the concrete for the barrier was specified as 3600 psi TxDOT Class H. The welded wire reinforcing steel was grade 70 material. The connecting rods met ASTM A193 B7 specifications, and the corresponding heavy hex nuts met Grade 5. Plate washers were ASTM A36 material. Forklift sleeves were fabricated from Hollow Structural Section (HSS) $8\times 4\times\frac{3}{16}$ -inch ASTM A500 grade B material.

Figure 6.1 presents overall information on the 26-inch tall PCB and Figure 6.2 shows the detailed geometry of the 26-inch tall PCB.

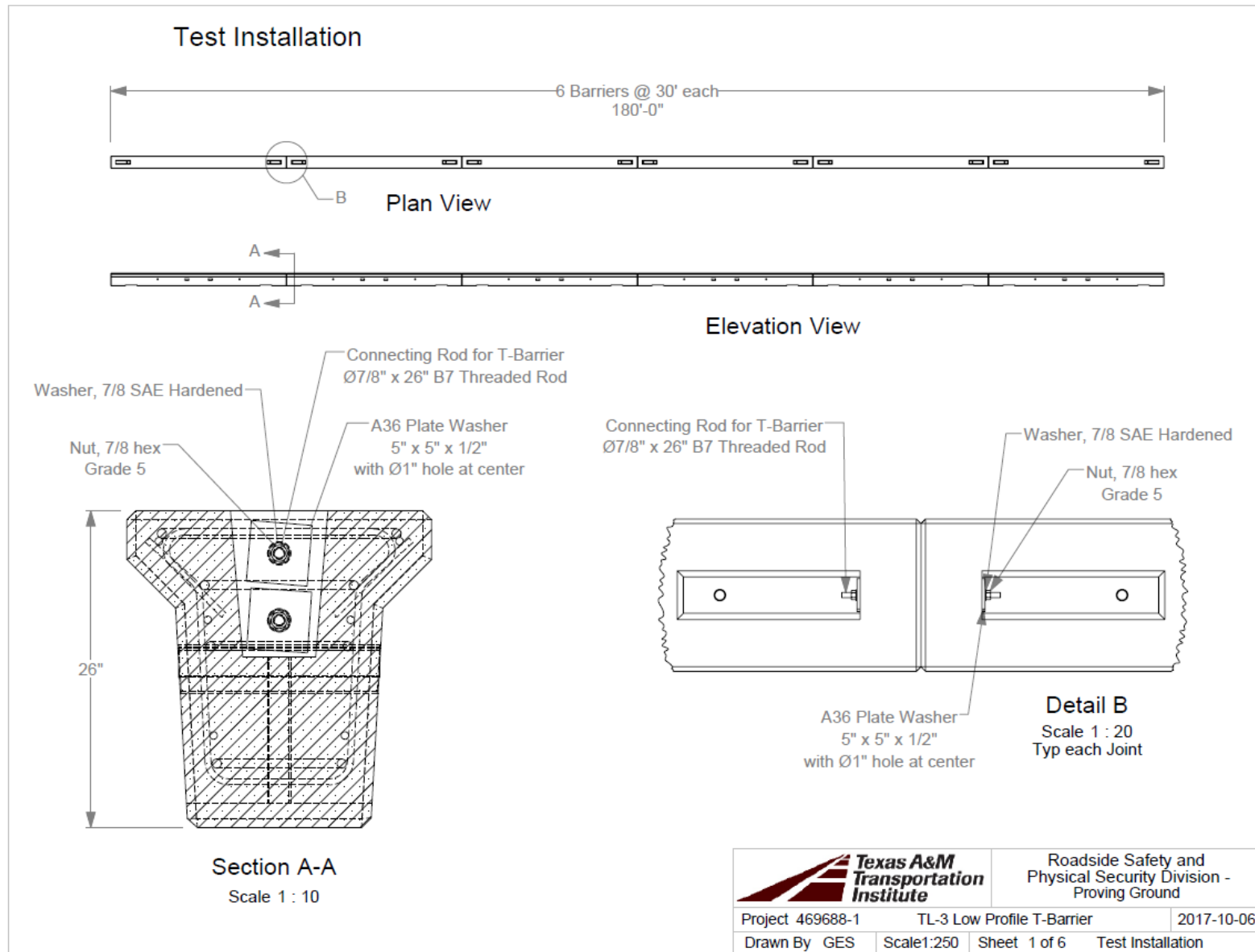


Figure 6.1 Overall Details of the 26-Inch Tall T Shaped PCB

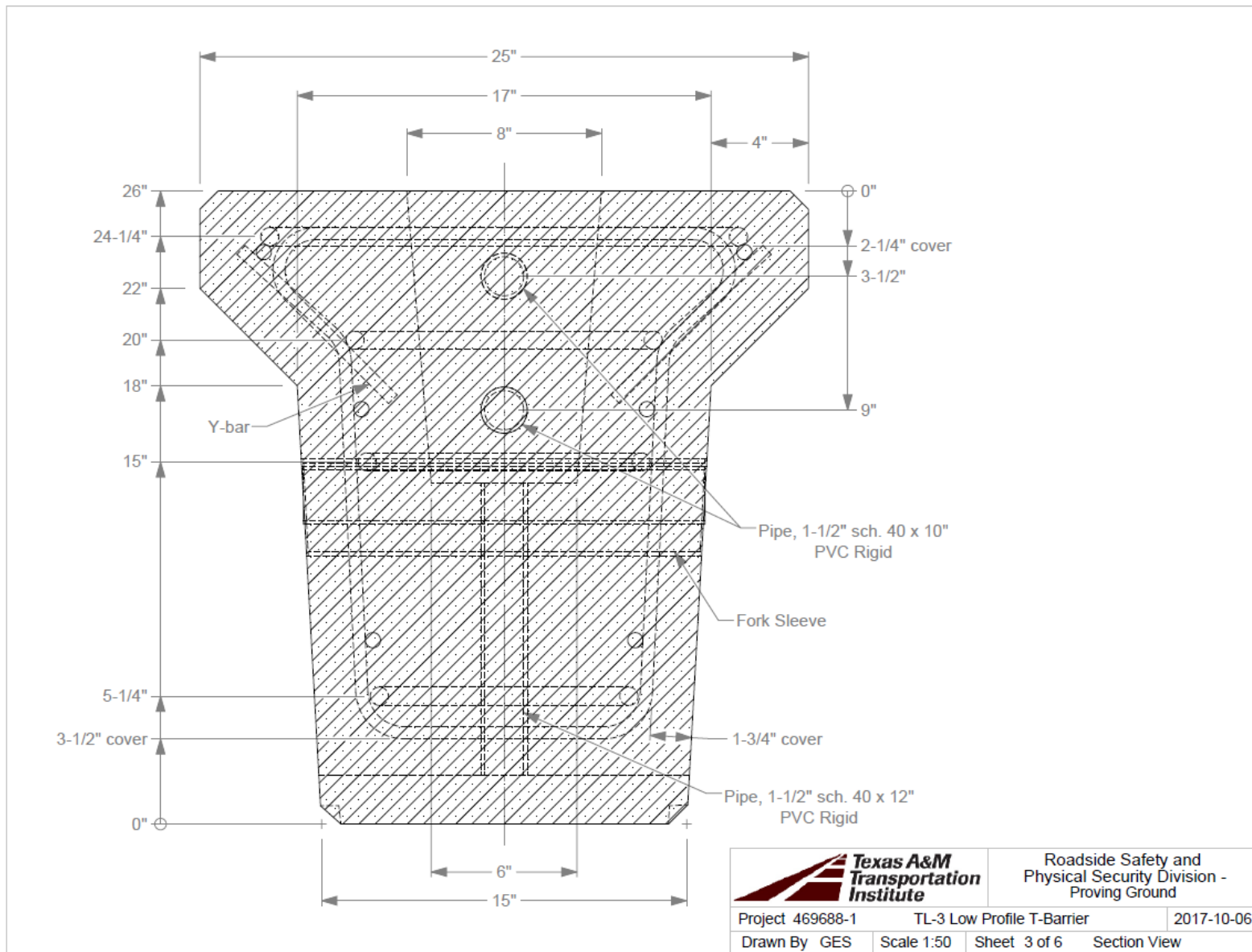


Figure 6.2 Detailed Geometry of the 26-Inch Tall T Shaped PCB

6.2.2 FE Model of the 26-Inch Tall T Shaped PCB

The detailed FE model of the 26-inch tall T shaped low-profile PCB included barrier segments, plate washers, washers, nuts, steel rods and the ground. The PCB model contains six 30-feet long barrier segments for a total length of 180 feet, and total number of 376360 elements. Eight-node solid brick elements and four-node shell elements were mainly used to build the model. It should be noted that no concrete failure was included in the detailed FE models. Therefore, the developed model did not have the ability to predict fracture or spalling of concrete which might happen during the full-scale crash test. Solid elements were used to build the concrete barrier segments, the density of the concrete was determined to be 150 psf, Young modulus was 3400 ksi and the Poisson's ratio was 0.2. Steel components were modeled using MAT_PIECEWISE_LINEAR_PLASTICITY material card in LS-DYNA. The threaded steel rods were modeled using elastic solid brick elements with the property of A193 B7 steel. The steel plate washers were modeled using elastic shell elements with the property of A36 steel. Similarly, the washers and nuts were modeled using four-node, elastic, shell elements with Grade 5 steel properties. The ground was modeled with rigid shell elements. Figure 6.3 contains different views for the FE model of one segment, Figure 6.4 illustrates the connection within the FE model.

Contact type SURFACE-TO-SURFACE was placed between the nut and washer, washer and plate washer, washer and threaded steel rod, plate washer and barrier, plate washer and threaded steel rod. Barrier segments contact with each other with an applied frictional coefficient of 0.45. The static frictional coefficient between the ground and barriers was 0.63 while the dynamic frictional coefficient was 0.26.

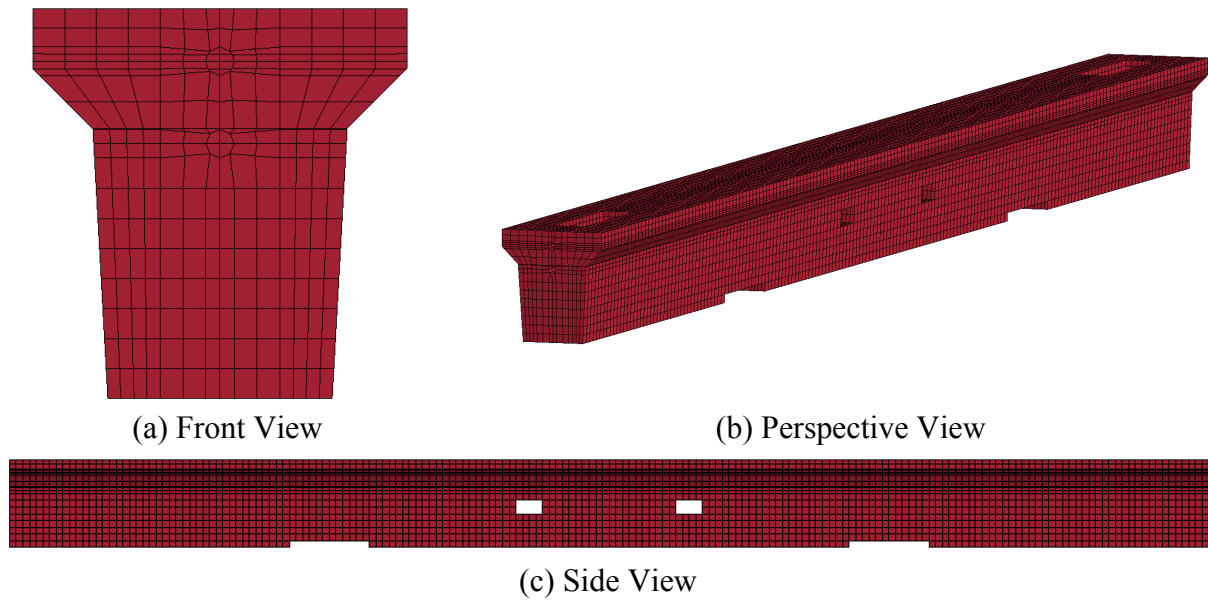


Figure 6.3 Front, Perspective and Side Views of a Segment of the 26-Inch Tall Model

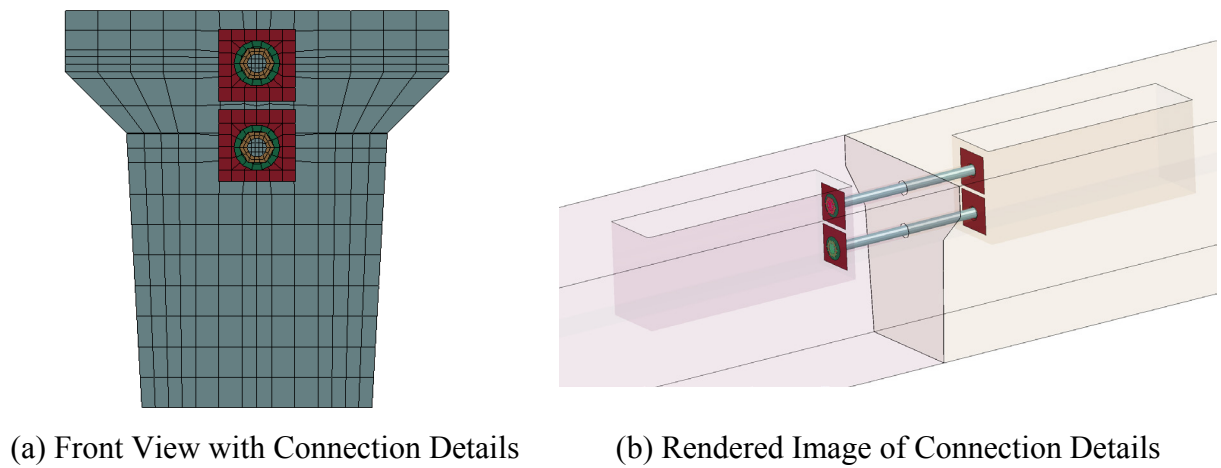


Figure 6.4 Images of the 26-Inch Tall Barrier FE Model with Connection Details

The 180-ft, free-standing, low-profile PCB was impacted by the 2270P vehicle at a speed of 62 mi/h and with an angle of 25 degrees. Based on MASH requirements, the vehicle impacted the system 4.3-feet upstream of a connection, roughly around one-third of the system length. Two cases were considered in the simulation, case 1 was “with impact tire disengagement” and case 2 was “without impact tire disengagement”.

6.2.3 Case 1 Detailed Simulation with Impact Tire Disengagement

6.2.3.1 Vehicle Stability and Barrier Performance

A force-based ability for front impact tire disengagement was applied for this simulation, giving the opportunity to the impacting front tire to detach from the vehicle suspension assembly if condition occurs.

After 0.03 seconds from the initial impact of the pickup truck, the front impact tire began to disengage from the suspension. At 0.05 seconds, the vehicle began to redirect. The vehicle was traveling parallel with the barrier at 0.23 seconds and the rear of the vehicle impacted the barrier at 0.25 seconds.

The 2270P pickup truck remained upright during and after the modeled collision event. Figure 6.5 shows vehicle roll, pitch and yaw angles throughout the impact event against the 26-inch tall low-profile PCB. Maximum roll, pitch, and yaw angles resulted to be -19.2, -8.8, and 35.9 degrees respectively, they all remained in the range required by MASH criteria.

Figure 6.6 contains images of the barrier at the beginning of impact and at final configuration. A maximum barrier deformation of 29.8 inches (2.5 feet) was reached at approximately 0.60 seconds.

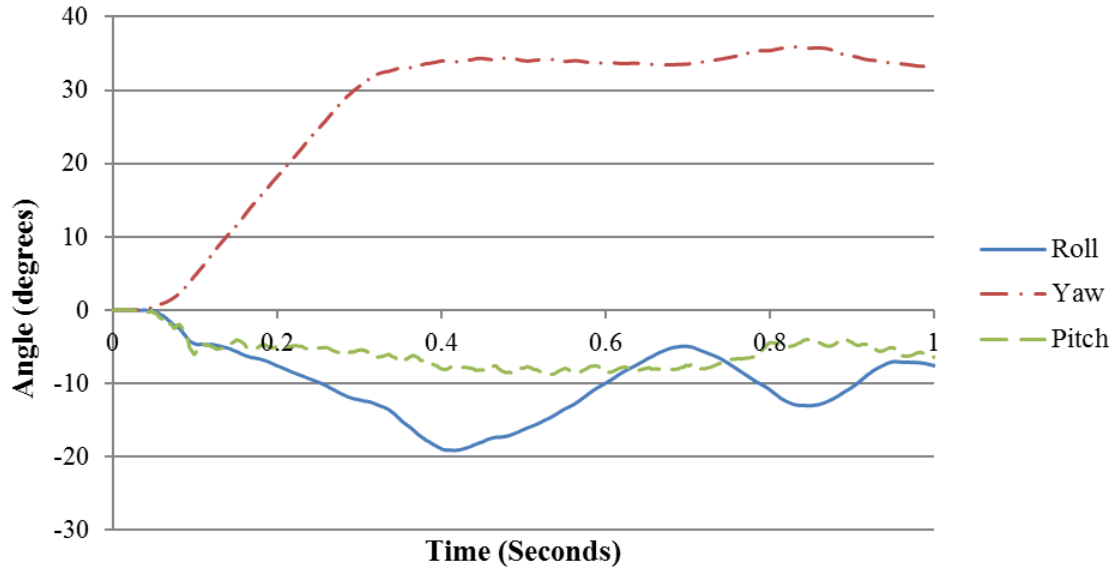
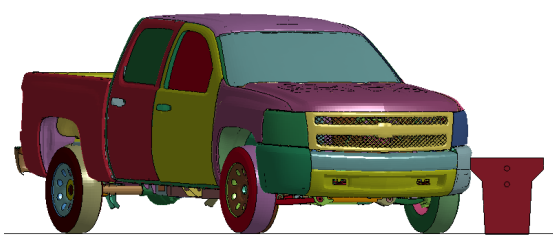
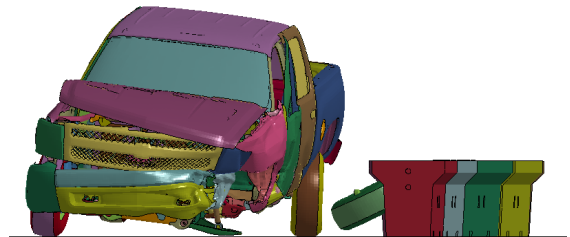


Figure 6.5 Angular Displacements of the Vehicle in Case 1 of 26-Inch Tall PCB Simulation



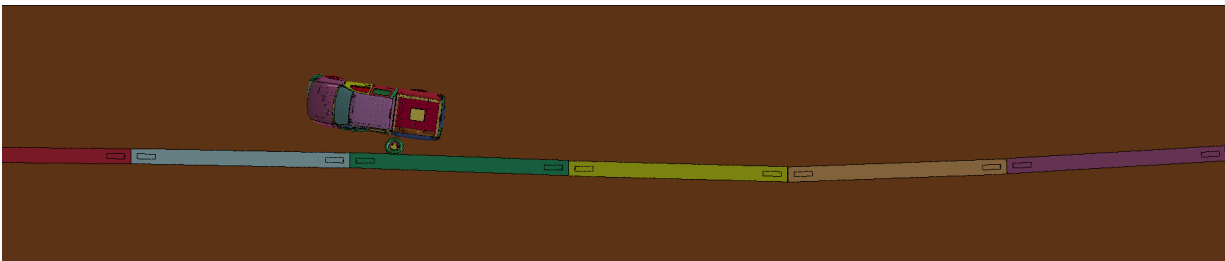
(a) Front View at Impact



(b) Front View at Final Configuration



(c) Overhead View at Impact



(d) Overhead View at Final Configuration

Figure 6.6 Initial and Deflected Shape of the 26-Inch Tall T Shaped PCB in Case 1

6.2.3.2 Occupant Risk Assessment

TRAP program [27] was used to evaluate occupant risk factors based on the applicable MASH safety evaluation criteria. Data acquired from the accelerometer, located at the vehicle center of gravity, were digitized for evaluation of occupant risk. In the longitudinal direction, the occupant impact velocity was 22.0 ft/s at 0.122 seconds, the highest 10-ms occupant ridedown acceleration was -5.0 G from 0.139 to 0.149 seconds, and the maximum 50-ms average acceleration was -11.1 G between 0.059 and 0.109 seconds. In the lateral direction, the occupant impact velocity was -19.0 ft/s at 0.122 seconds, the highest 10-ms occupant ridedown acceleration was 6.0 g from 0.312 to 0.322 seconds, and the maximum 50-ms average was 9.6 g between 0.045 and 0.095 seconds. Theoretical Head Impact Velocity (THIV) was 28.4 ft/s at 0.117 seconds; Post-Impact Head Decelerations (PHD) was 6.0 G between 0.312 and 0.322 seconds; and Acceleration Severity Index (ASI) was 1.42 between 0.074 and 0.124 seconds. All of which were within the preferred limits in accordance with MASH.

6.2.3.3 Energy Values

Energy values were evaluated in the detailed finite element simulations. The kinetic energy applied to the barrier by the impacting vehicle is dissipated by converting it into other forms of energy. Internal energy constitutes any energy stored in a component through plastic and elastic deformation (strains) or a change in temperature. Sliding energy represents any energy dissipated due to friction between components. Hourglass energy is an unreal numerical energy dissipated by LS-DYNA. Hourglass energy should be minimized as much as possible (less than 5 percent in any significant part, and less than 10 percent in other parts preferred).

As shown in Figure 6.7, approximately 18 percent of the initial kinetic energy of the impacting vehicle was converted into internal energy (damage or deformation of the vehicle and

barrier components). Approximately 2 percent of the initial kinetic energy was converted into hourglass energy. Approximately 19 percent of the initial kinetic energy was converted into sliding interface energy. About 52 percent of the initial kinetic energy had yet to be dissipated by the system at the time of final impact configuration, mainly due to the remaining velocity of the vehicle. The 9 percent reduction in total energy of the system was due to numerical computation and loss of energy in the deformation of the barrier and connections.

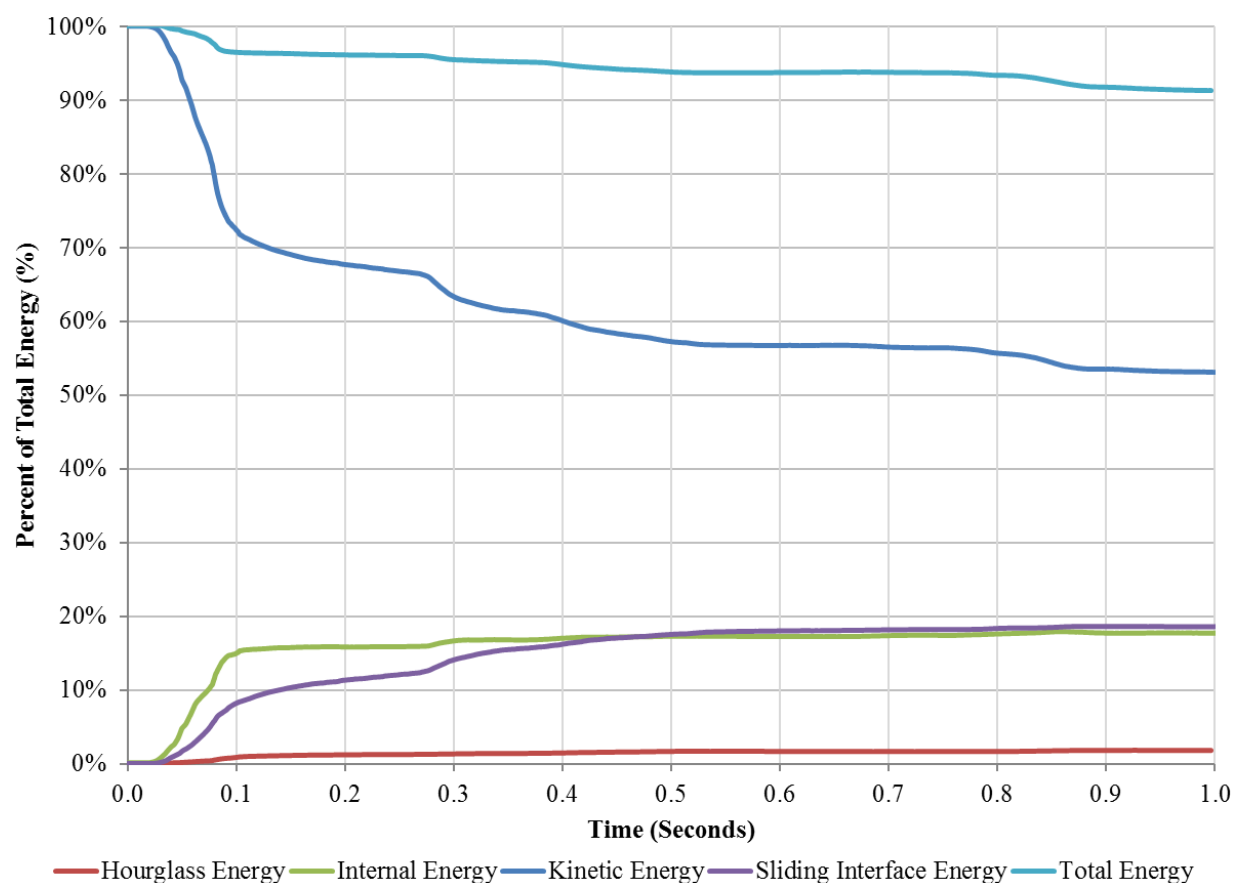
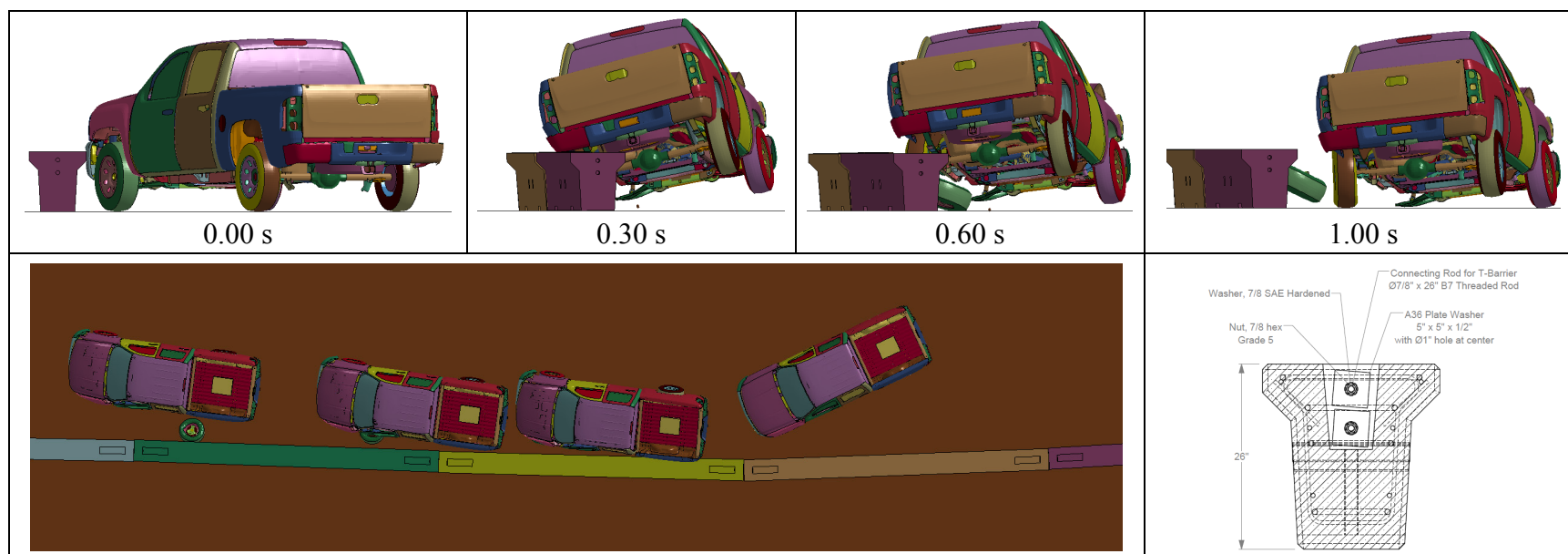


Figure 6.7 Energy Distribution History in Case 1 (26-Inch Tall T Shaped PCB Simulation)

6.2.3.4 Summary

Figure 6.8 summarizes results for MASH Test 3-11 simulation with a 2270P vehicle (with impact tire disengagement) impacting a 26-inch tall low-profile PCB. Results shows that the 26-inch tall PCB performed adequately by containing and redirecting the impacting 2270P vehicle. The free-standing barrier had a maximum deflection about 29.8 inches from its initial position during the impact event. The barrier did not show any potential for tipping over or allowing the impacting vehicle for intrusion in the opposing lane. Also, simulation indicated that the 2270P vehicle maintained stability during the MASH Test 3-11 impact condition.



General Information

Test Agency Texas A&M Transportation Institute (TTI)
 Test Standard Test No. MASH Test 3-11

Test Article

Type Longitudinal Barrier - Concrete
 Name MASH TL-3 Low-Profile Barrier
 Installation Length 180 ft
 Material or Key Elements Six segments of 26-inch tall, 30-ft long "T" shaped reinforced concrete barrier
 Soil Type Concrete Pavement,

Test Vehicle

Type/Designation 2270P
 Make and Model Finite Element Silverado Pickup
 Curb 4877 lb
 Test Inertial 5033 lb
 Dummy No dummy
 Gross Static 5033 lb

Impact Conditions

Speed 62.0 mi/h
 Angle 25.0 degrees
 Location/Orientation One Third of Barrier Length

Exit Conditions

Speed 44.9 mi/h
 Angle 3.6 degrees

Occupant Risk Values

Longitudinal OIV 22.0 ft/s
 Lateral OIV -19.0 ft/s
 Longitudinal Ridedown -5.0 G
 Lateral Ridedown 6.0 G
 THIV 28.4 ft/s
 PHD 6.0 G
 ASI 1.42
 Max. 0.050-s Average
 Longitudinal -11.1 G
 Lateral -9.6 G
 Vertical -2.9 G

Post-Impact Trajectory

Stopping Distance N/A

Vehicle Stability

Maximum Roll Angle -19.2 degrees
 Maximum Pitch Angle -8.8 degrees
 Maximum Yaw Angle 35.9 degrees
 Vehicle Snagging No
 Vehicle Pocketing No

Test Article Deflections

Dynamic 29.8 inches
 Permanent 29.1 inches
 Working Width N/A

Figure 6.8 Summary of Detailed Simulation Results of 26-inch Tall T Shaped PCB (With Impact Tire Disengagement)

6.2.4 Case 2 Detailed Simulation without Impact Tire Disengagement

6.2.4.1 Vehicle Stability and Barrier Performance

Tire disengagement was not applied in this case. The front impact tire kept attaching to the vehicle suspension assembly during the impact event. At 0.06 seconds, the impacting vehicle began to redirect. The vehicle was traveling parallel with the barrier at 0.23 seconds and the rear of the vehicle impacted the barrier at 0.25 seconds.

The modeled 2270P vehicle remained upright during and after the modeled collision event. Figure 6.9 shows vehicle roll, pitch and yaw angles throughout the impact event against the 26-inch tall low-profile PCB. Maximum roll, pitch, and yaw angles resulted to be -13.5, -6.3, and 32.7 degrees respectively, they all remained in the range required by MASH criteria.

Figure 6.10 contains images of the barrier at the beginning of impact and at final configuration. A maximum barrier deformation of 29.4 inches (2.5 feet) was reached at approximately 0.61 seconds.

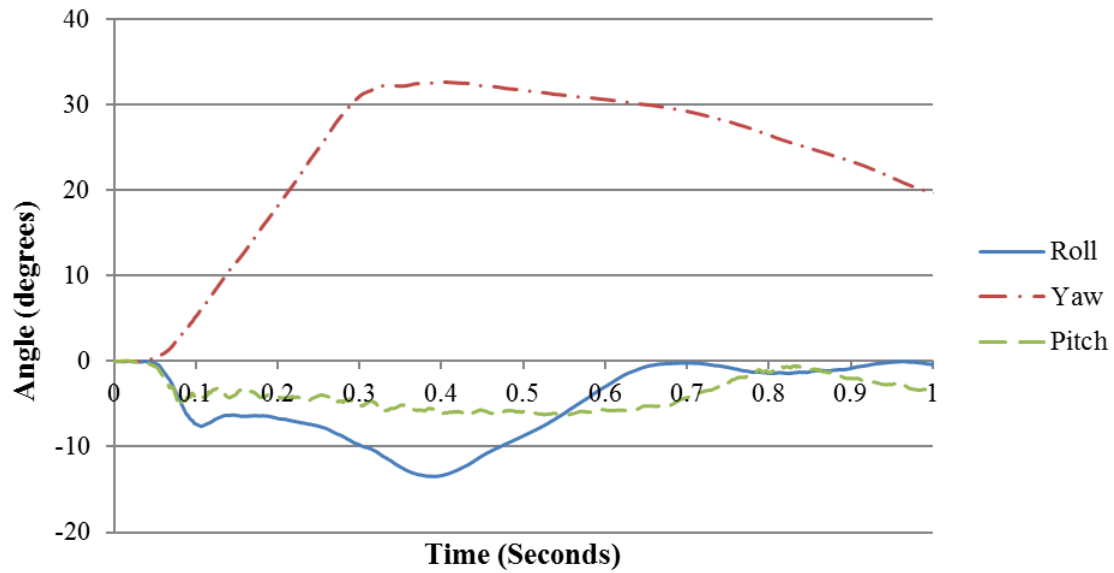
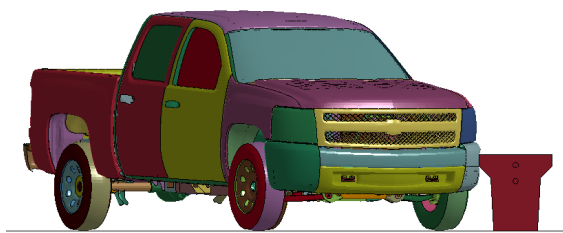
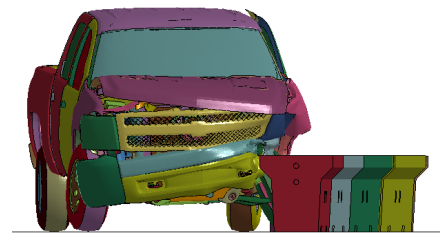


Figure 6.9 Angular Displacements of the Vehicle in Case 2 of 26-inch Tall PCB Simulation



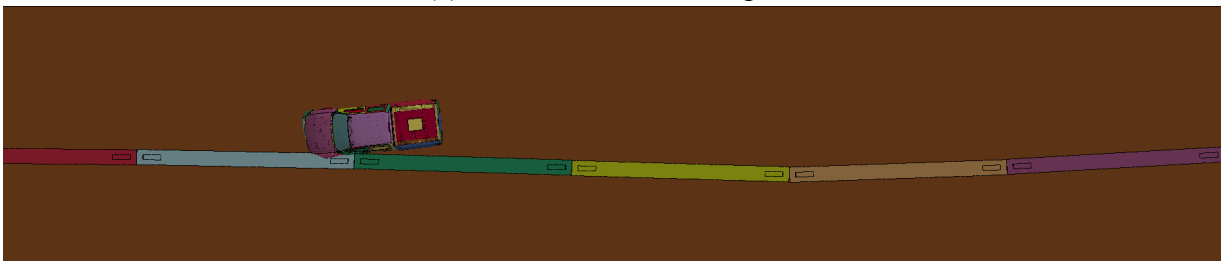
(a) Front View at Impact



(b) Front View at Final Configuration



(c) Overhead View at Impact



(d) Overhead View at Final Configuration

Figure 6.10 Initial and Deflected Shape of the 26-Inch Tall PCB in Case 2

6.2.4.2 Occupant Risk Assessment

In the longitudinal direction, the occupant impact velocity was 22.3 ft/s at 0.117 seconds, the highest 10-ms occupant ridedown acceleration was -6.0 g from 0.134 to 0.144 seconds, and the maximum 50-ms average acceleration was -12.1 g between 0.032 and 0.082 seconds. In the lateral direction, the occupant impact velocity was -17.4 ft/s at 0.117 seconds, the highest 10-ms occupant ridedown acceleration was 7.6 g from 0.304 to 0.314 seconds, and the maximum 50-ms average was 11.5 g between 0.034 and 0.084 seconds. All of which were within the preferred limits in accordance with MASH. THIV was 27.9 ft/s at 0.112 seconds; PHD was 7.9 g between 0.304 and 0.314 seconds; and ASI was 1.66 between 0.068 and 0.118 seconds.

6.2.4.3 Energy Values

Energy values were evaluated in this detailed finite element simulation. As shown in Figure 6.11, approximately 20 percent of the initial kinetic energy of the impacting vehicle was converted into internal energy. Approximately 2 percent of the initial kinetic energy was converted into hourglass energy. Approximately 18 percent of the initial kinetic energy was converted into sliding interface energy. About 51 percent of the initial kinetic energy had yet to be dissipated by the system at the time of final impact configuration, mainly due to the remaining velocity of the vehicle. The 9 percent reduction in total energy of the system is due to numerical computation and loss of energy in the deformation of the barrier and connections.

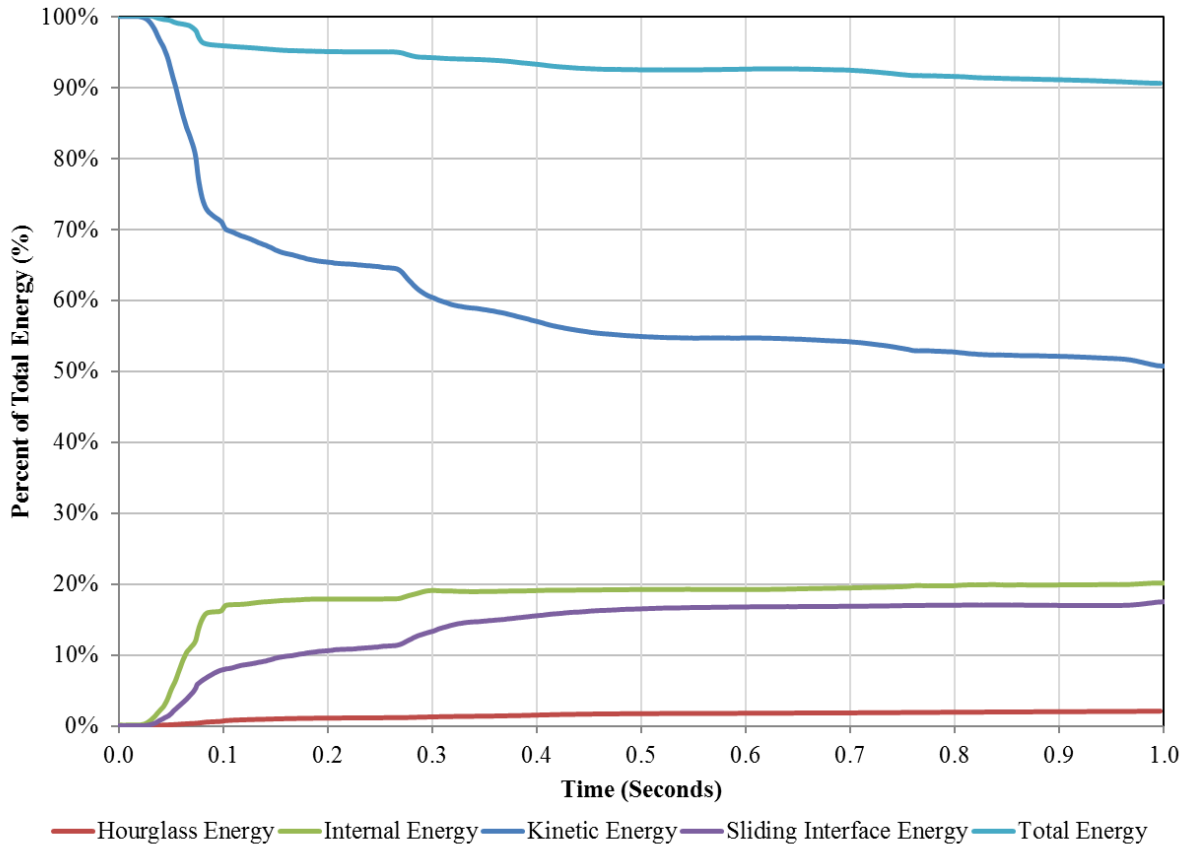
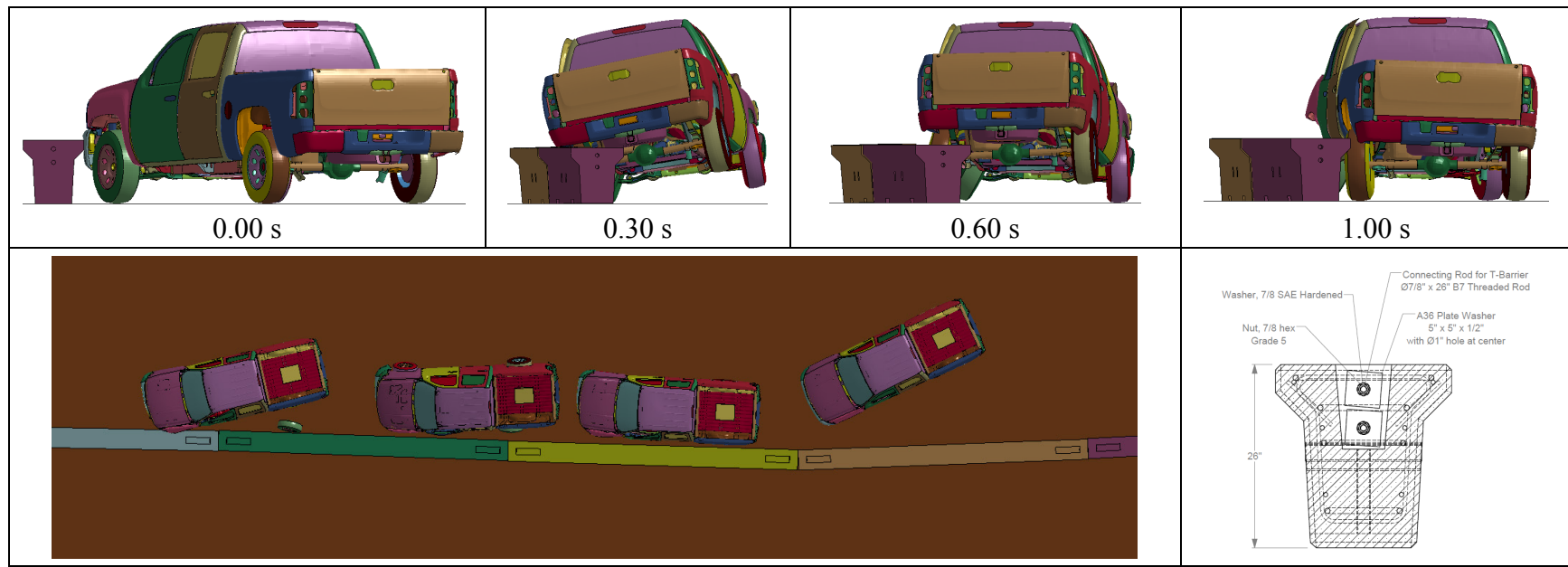


Figure 6.11 Energy Distribution History in Case 2 (26-Inch Tall PCB Simulation)

6.2.4.4 Summary

Figure 6.12 summarizes results for MASH Test 3-11 simulation with a 2270P vehicle (without impact tire disengagement) impacting a 26-inch tall low-profile PCB. Results shows that the 26-inch tall PCB performed adequately by containing and redirecting the impacting 2270P vehicle. The free-standing barrier had a maximum deflection about 29.4 inches from its initial position during the impact event. The barrier did not show any potential for tipping over or allowing the impacting vehicle for intrusion in the opposing lane. Also, simulation indicated that the 2270P vehicle maintained stability during the MASH TL 3-11 impact conditions event.



General Information

Test Agency Texas A&M Transportation Institute (TTI)
 Test Standard Test No. MASH Test 3-11

Test Article

Type Longitudinal Barrier - Concrete
 Name MASH TL-3 Low-Profile Barrier
 Installation Length 180 ft
 Material or Key Elements Six segments of 26-inch tall, 30-ft long "T" shaped reinforced concrete barrier

Soil Type

Concrete Pavement,

Test Vehicle

Type/Designation 2270P
 Make and Model Finite Element Silverado Pickup
 Curb 4877 lb
 Test Inertial 5033 lb
 Dummy No dummy
 Gross Static 5033 lb

Impact Conditions

Speed 62.0 mi/h
 Angle 25.0 degrees
 Location/Orientation One Third of Barrier Length

Exit Conditions

Speed 45.2 mi/h
 Angle 3.8 degrees

Occupant Risk Values

Longitudinal OIV 22.3 ft/s
 Lateral OIV -17.4 ft/s
 Longitudinal Ridedown -6.0 G
 Lateral Ridedown 7.6 G
 THIV 27.9 ft/s
 PHD 7.9 G
 ASI 1.66

Max. 0.050-s Average

Longitudinal -12.1 G
 Lateral -11.5 G
 Vertical -2.8 G

Post-Impact Trajectory

Stopping Distance N/A

Vehicle Stability

Maximum Roll Angle -13.5 degrees
 Maximum Pitch Angle -6.3 degrees
 Maximum Yaw Angle 32.7 degrees
 Vehicle Snagging No
 Vehicle Pocketing No

Test Article Deflections

Dynamic 31.5 inches
 Permanent 30.8 inches
 Working Width N/A

Figure 6.12 Summary of Detailed Simulation Results of 26-inch Tall Low-Profile PCB (Without Impact Tire Disengagement)

6.2.5 Results Comparison between Case 1 and Case 2 of 26-Inch Tall T Shaped PCB

Results of the two detailed FE simulations cases were compared to determine the performance envelope of the 26-inch tall low-profile barrier. Table 6.1 compares the occupant risk values and maximum angular displacements. Table 6.2 and Table 6.3 include the sequential images of the two cases in front view and overhead view, respectively.

Occupant risk values were very comparable between the two cases. The impact velocity increased slightly in lateral direction (y-direction) for case 1 (+1.6 ft/s). However, the predicted ridedown acceleration was reduced for case 1 (there is a decrease of 1.0 G and 1.6 G in longitudinal and lateral direction, respectively). Case 1 had greater roll, pitch and yaw angles than case 2. Comparing the sequential images of both simulations, tire disengagement had a tendency to increase the instability of the vehicle.

To sum up, the crashworthiness of the free-standing 26-inch tall low-profile PCB was evaluated through finite element computer simulations according to MASH test 3-11. Two different cases were performed, vehicle behaved more instable in the case with impact tire disengagement. Simulation results indicated that the 26-inch tall low-profile PCB maintained occupant risks well within the limiting values according to MASH criteria.

Table 6.1 Occupant Risk Values Comparison between Case 1 and Case 2 (26-Inch Height)

Occupant Risk Factors and Maximum Angular Displacement		Case 1 - With Impact Tire Disengagement	Case 2 - Without Impact Tire Disengagement
Impact Velocity (ft/s)	x-direction	22.0	22.3
	y-direction	-19.0	-17.4
Ridedown Acceleration (G)	x-direction	-5.0	-6.0
	y-direction	6.0	7.6
Maximum Angular Displacement (Degrees)	Roll	-19.2	-13.5
	Pitch	-8.8	-6.3
	Yaw	35.9	32.7

Table 6.2 Sequential Images of Case 1 and Case 2 of 26-Inch Tall PCB (Front View)

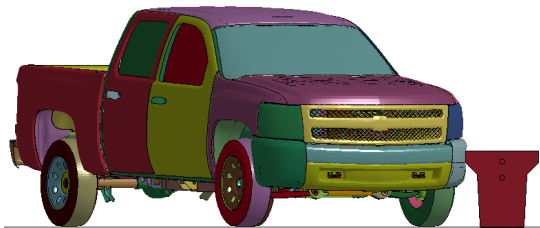
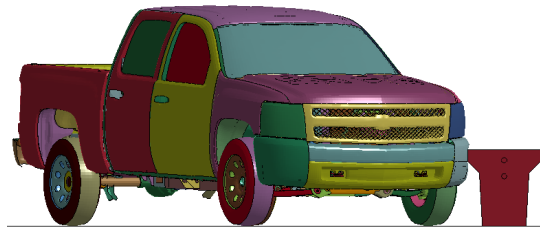
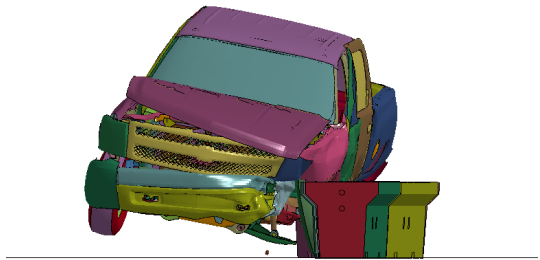
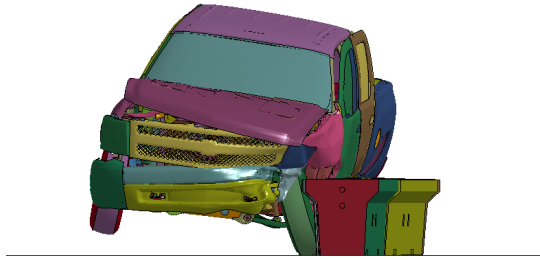
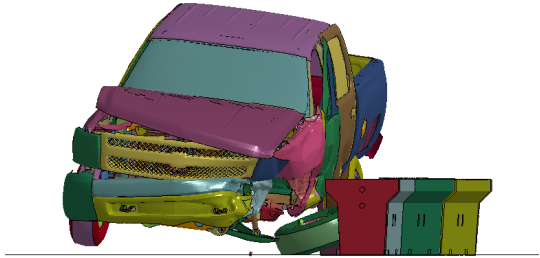
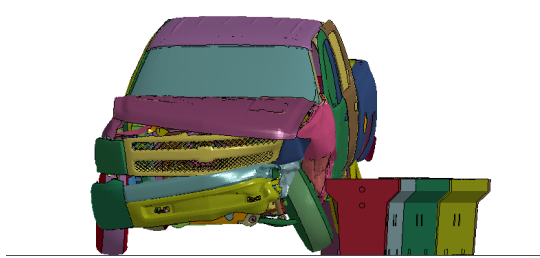
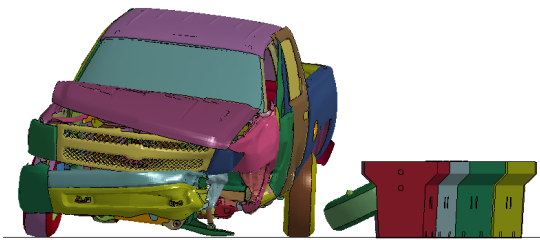
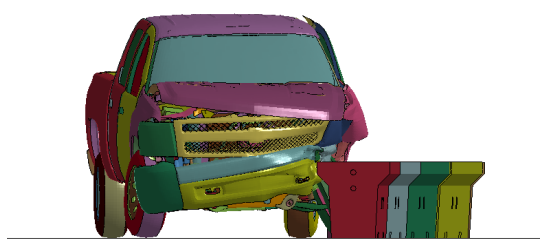
Time (seconds)	Case 1 With Impact Tire Disengagement	Case 2 Without Impact Tire Disengagement
0.0		
0.3		
0.6		
1.0		

Table 6.3 Sequential Images of Case 1 and Case 2 of 26-Inch Tall PCB (Overhead View)

Time (seconds)	Case 1 With Impact Tire Disengagement	Case 2 Without Impact Tire Disengagement
0.0		
0.3		
0.6		
1.0		

6.3 Detailed Finite Element Analysis 24-Inch Tall T Shaped PCB

6.3.1 Design of 24-Inch Tall T Shaped PCB

The design of the 24-inch tall low-profile PCB was identical to the 26-inch tall PCB, except for the height. The 24-inch tall low-profile PCB was comprised of six segments of 30-ft long T shaped reinforced concrete barriers. The overall length of the barrier was 180 feet. Each T barrier segment was symmetrically shaped about its vertical axis: 15 inches wide at the base sloping outward to 17-inches wide to a 45° outward flare point (located 16 inches above grade) that transitioned to 25 inches wide at the top.

6.3.2 Finite Element Model of the 24-Inch Tall T Shaped PCB

The detailed FE model of the 24-inch tall T shaped low-profile PCB included barrier segments, plate washers, washers, nuts, steel rods and the ground. The PCB model contains six 30-ft long barrier segments for a total length of 180 feet, and total number of 361240 elements. The materials and contacts used in this model were identical to the 26-inch tall barrier model. Figure 6.13 shows different views for the FE model of one segment, Figure 6.14 illustrates the connection within the FE model.

The 180-ft, free-standing, low-profile PCB was impacted by the pickup truck at a speed of 62 mi/h and with an angle of 25 degrees. Based on MASH requirements, the vehicle impacted the system 4.3-feet upstream of a connection, roughly around one-third of the system length. Two cases were considered in the simulation, case 1 was “with impact tire disengagement” and case 2 was “without impact tire disengagement”.

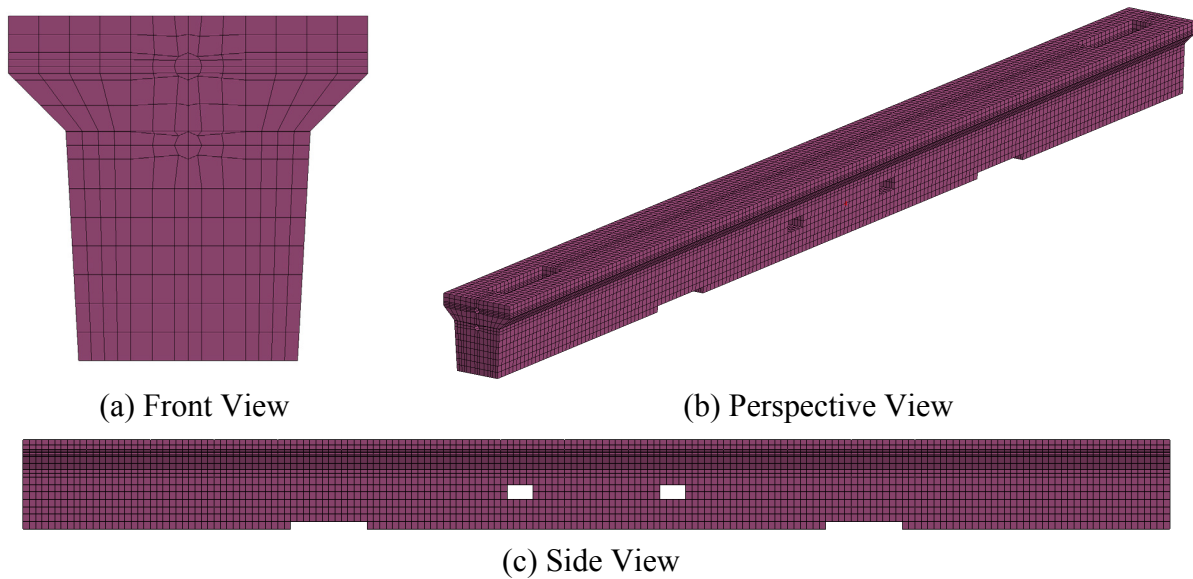


Figure 6.13 Front, Perspective and Side Views of a Segment of the 24-Inch Tall PCB Model

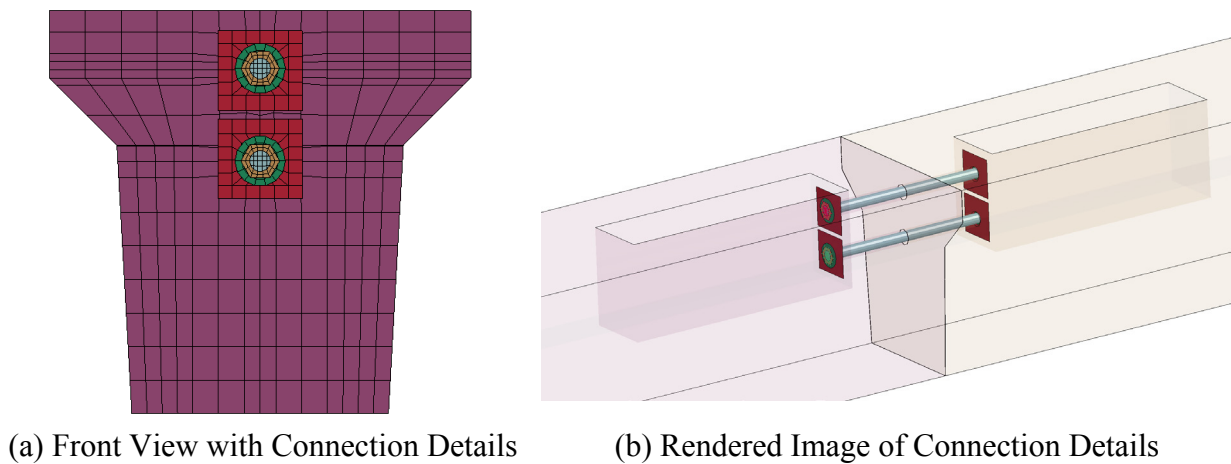


Figure 6.14 Images of the 24-Inch tall barrier FE Model with Connection Details

6.3.3 Case 1 Detailed Simulation with Impact Tire Disengagement

6.3.3.1 Vehicle Stability and Barrier Performance

A force-based ability for front impact tire disengagement was applied for this simulation, giving the opportunity to the impacting front tire to detach from the vehicle suspension assembly if condition occurs.

After 0.03 seconds from the initial impact of the pickup truck, the front impact tire began to disengage from the suspension. At 0.05 second, the vehicle began to redirect. The vehicle was traveling parallel with the barrier at 0.24 second and the rear of the vehicle contacted the barrier at 0.26 second.

The 2270P pickup truck remained upright during and after the modeled collision event. Figure 6.15 shows vehicle roll, pitch and yaw angles throughout the impact event against the 24-inch tall low-profile PCB. Maximum roll, pitch, and yaw angles resulted to be -20.6, -6.9, and 29.3 degrees respectively, they all remained in the range required by MASH criteria.

Figure 6.15 contains images of the barrier at the beginning of impact and at final configuration. A maximum barrier deformation of 31.5 inches (2.6 feet) was reached at approximately 0.60 seconds.

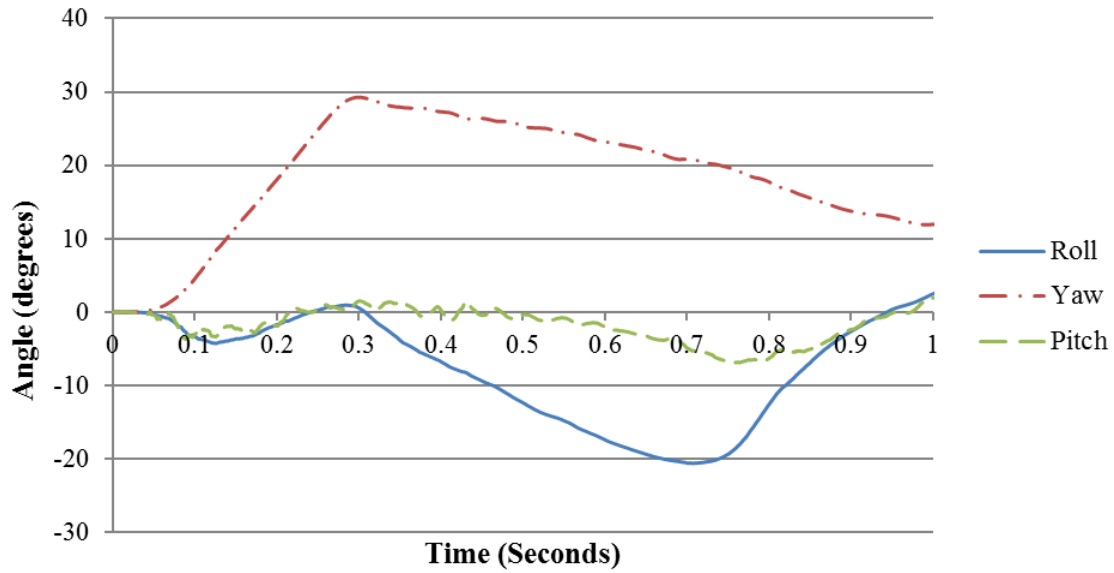
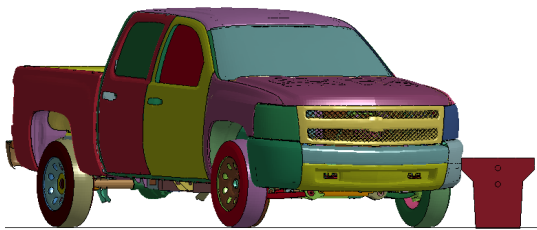
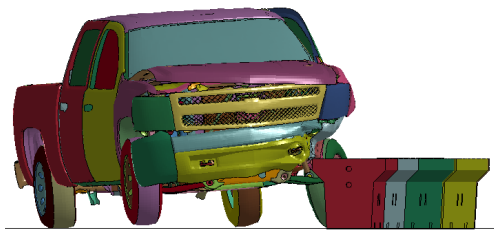


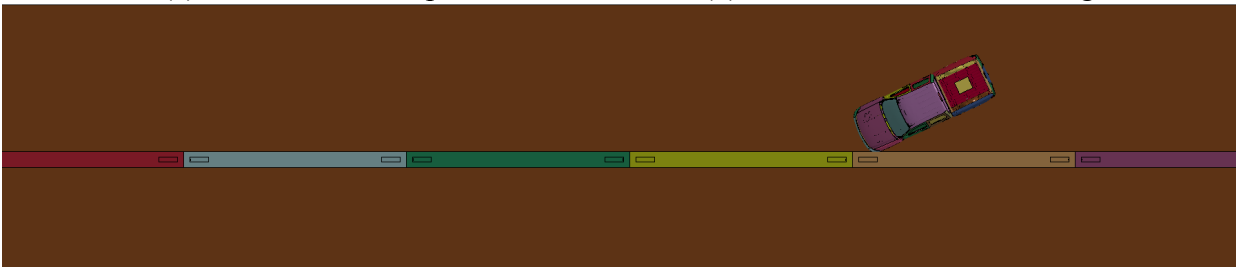
Figure 6.15 Angular Displacements of the Vehicle in Case 1 (24-Inch Tall PCB Simulation)



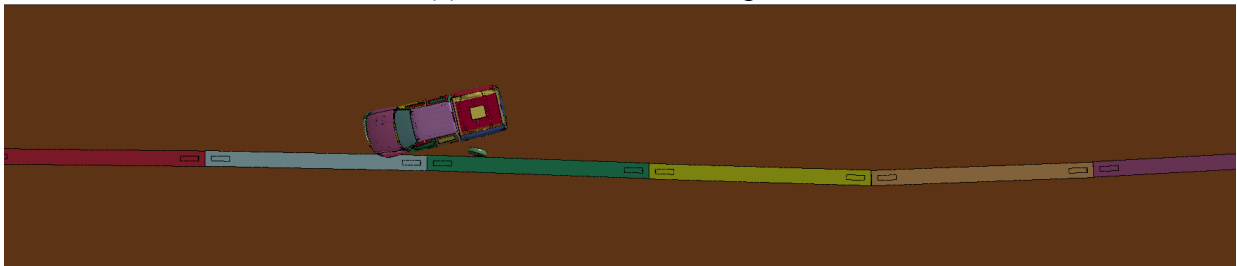
(a) Front View at Impact



(b) Front View at Final Configuration



(c) Overhead View at Impact



(d) Overhead View at Final Configuration

Figure 6.16 Initial and Deflected Shape of the 24-Inch Tall T Shaped PCB in Case 1

6.3.3.2 Occupant Risk Assessment

In the longitudinal direction, the occupant impact velocity was 20.0 ft/s at 0.124 seconds, the highest 0.010-s occupant ridedown acceleration was -5.2 G from 0.759 to 0.769 seconds, and the maximum 0.050-s average acceleration was -10.0 G between 0.054 and 0.104 seconds. In the lateral direction, the occupant impact velocity was -19.0 ft/s at 0.124 seconds, the highest 0.010-s occupant ridedown acceleration was 13.9 G from 0.286 to 0.296 seconds, and the maximum 0.050-s average acceleration was -9.2 G between 0.039 and 0.089 seconds. THIV was 27.2 ft/s at 0.120 seconds; PHD was 14.1 G between 0.286 and 0.296 seconds; and ASI was 1.41 between 0.076 and 0.126 seconds. All of which were within the preferred limits in accordance with MASH criteria.

6.3.3.3 Energy Values

Energy values were evaluated in the detailed finite element simulations. As shown in Figure 6.17, approximately 21 percent of the initial kinetic energy of the impacting vehicle was converted into internal energy. Approximately 2 percent of the initial kinetic energy was converted into hourglass energy. Approximately 16 percent of the initial kinetic energy was converted into sliding interface energy. About 51 percent of the initial kinetic energy had yet to be dissipated by the system at the time of final impact configuration, mainly due to the remaining velocity of the vehicle. The 8 percent reduction in total energy of the system was due to numerical computation and loss of energy in the deformation of the barrier and connections.

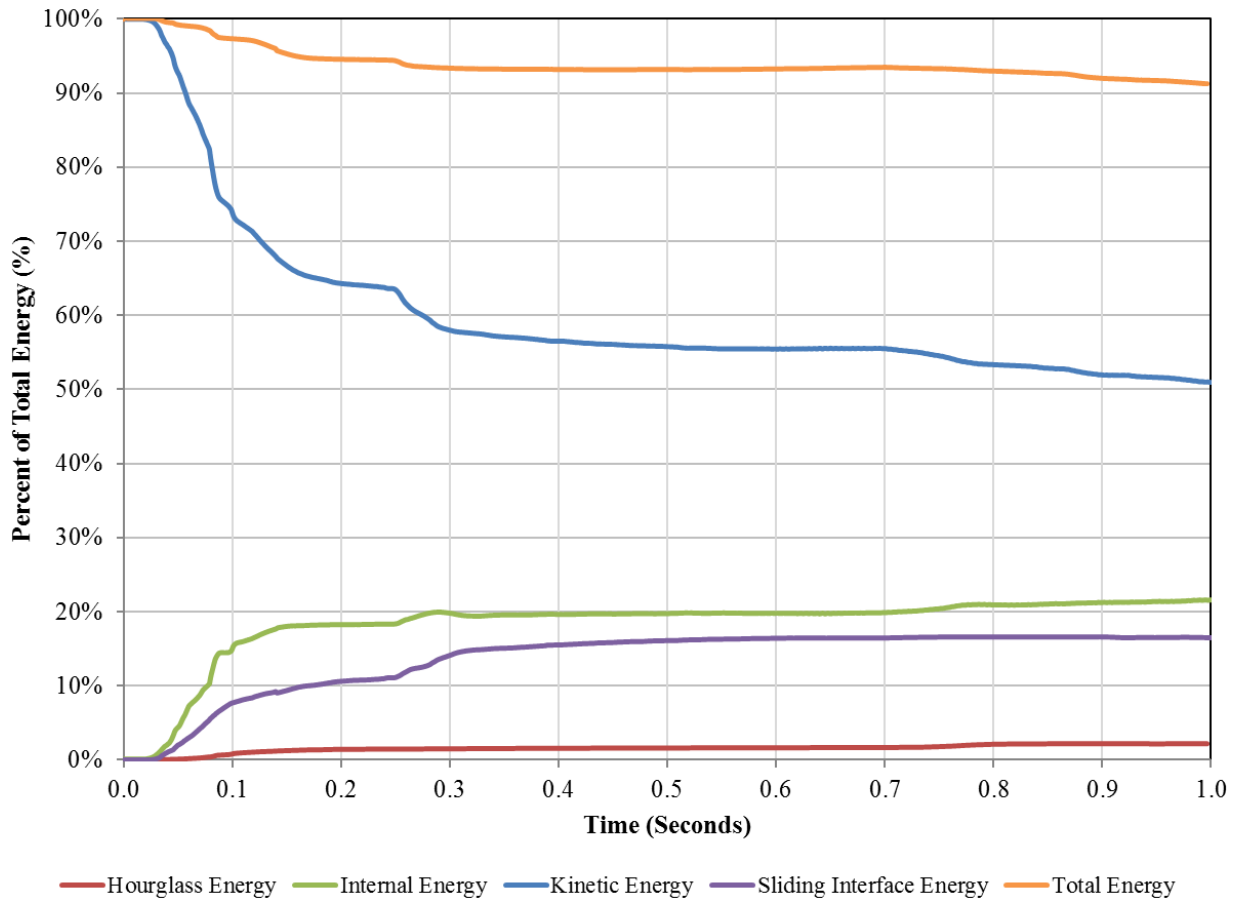
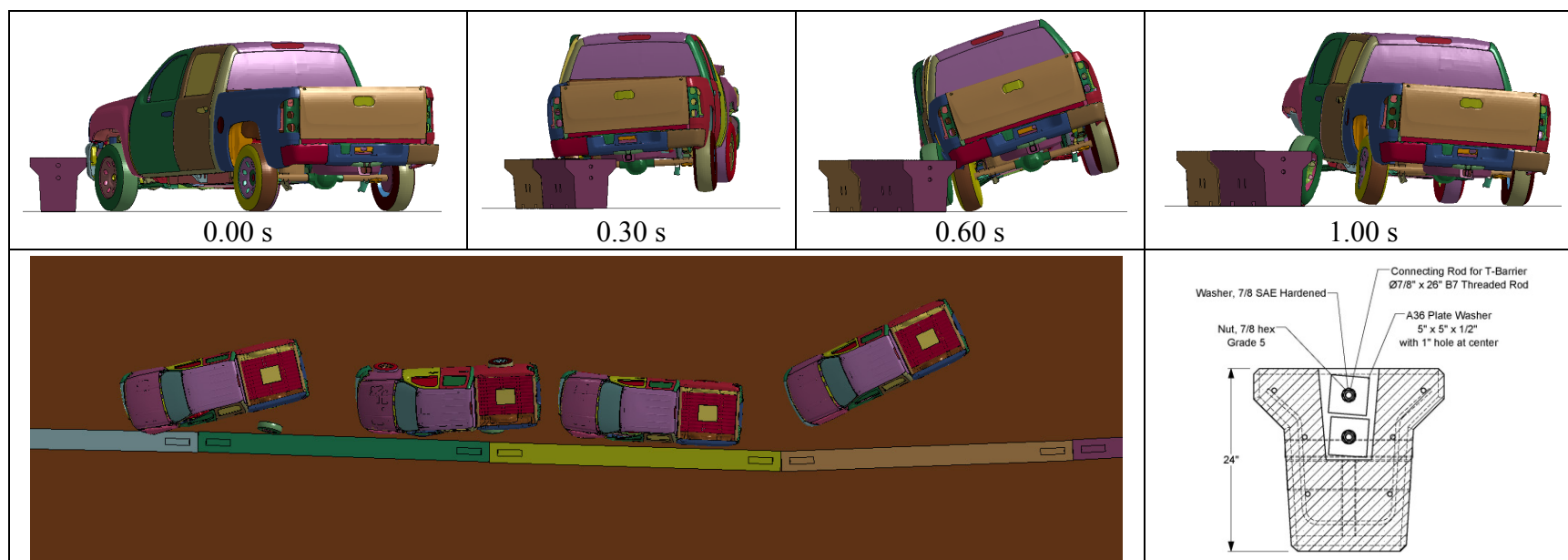


Figure 6.17 Energy Distribution History in Case 1 (24-Inch Tall PCB Simulation)

6.3.3.4 Summary

Figure 6.18 summarizes results for MASH Test 3-11 simulation with a 2270P vehicle (with impact tire disengagement) impacting a 24-inch tall low-profile PCB. Results showed that the 24-inch tall PCB performed adequately by containing and redirecting the impacting 2270P vehicle. The free-standing barrier had a maximum deflection about 31.5 inches from its initial position during the impact event. However, the barrier did not show any potential for tipping over and allowing the impacting vehicle for intrusion in the opposing lane. In addition, simulations indicate the 2270P vehicle maintaining stability during the MASH TL 3-11 impact conditions.



General Information

Test Agency Texas A&M Transportation Institute (TTI)
 Test Standard Test No. MASH Test 3-11

Test Article

Type Longitudinal Barrier - Concrete
 Name MASH TL-3 Low-Profile Barrier
 Installation Length 180 feet
 Material or Key Elements Six segments of 24-inch tall, 30-ft long T shaped reinforced concrete barrier

Soil Type Concrete Pavement

Test Vehicle

Type/Designation 2270P
 Make and Model Finite Element Silverado Pickup
 Curb 4877 lb
 Test Inertial 5033 lb
 Dummy No dummy
 Gross Static 5033 lb

Impact Conditions

Speed 62.0 mi/h
 Angle 25.0 degrees
 Location/Orientation One Third of Barrier Length

Exit Conditions

Speed 47.4 mi/h
 Angle 3.8 degrees

Occupant Risk Values

Longitudinal OIV 20.0 ft/s
 Lateral OIV 19.0 ft/s
 Longitudinal Ridedown -5.2 G
 Lateral Ridedown -13.9 G
 THIV 29.8 km/h
 PHD 14.1 G
 ASI 1.41
 Max. 0.050-s Average
 Longitudinal -10.0 G
 Lateral -9.2 G
 Vertical -4.3 G

Post-Impact Trajectory

Stopping Distance N/A

Vehicle Stability

Maximum Roll Angle -20.6 degrees
 Maximum Pitch Angle -6.9 degrees
 Maximum Yaw Angle 20.6 degrees
 Vehicle Snagging No
 Vehicle Pocketing No

Test Article Deflections

Dynamic 31.5 inches
 Permanent 30.8 inches
 Working Width N/A

Figure 6.18 Summary of Detailed Simulation Results of 24-inch Tall Low-Profile PCB (With Impact Tire Disengagement)

6.3.4 Case 2 Detailed Simulation without Impact Tire Disengagement

6.3.4.1 Vehicle Stability and Barrier Performance

Tire disengagement was not applied in this case. The front impact tire kept attaching to the vehicle suspension assembly during the impact event. At 0.05 second, the vehicle began to redirect. The vehicle was traveling parallel with the barrier at 0.23 second and the rear of the vehicle contacted the barrier at 0.25 second.

The 2270P pickup truck remained upright during and after the modeled collision event. Figure 6.19 shows vehicle roll, pitch and yaw angles throughout the impact event against the 24-inch tall low-profile PCB. Maximum roll, pitch, and yaw angles resulted to be -19.8, -12.2, and 32.9 degrees respectively, they all remained in the range required by MASH criteria.

Figure 6.20 contains images of the barrier at the beginning of impact and at final configuration. A maximum barrier deformation of 30.9 inches (2.57 feet) was reached at approximately 0.60 seconds.

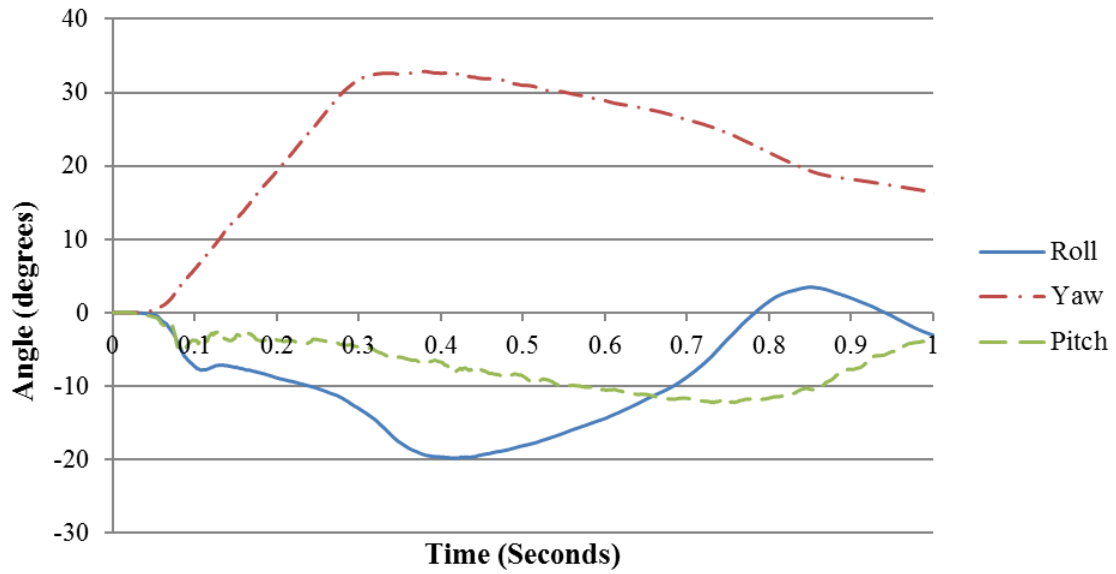
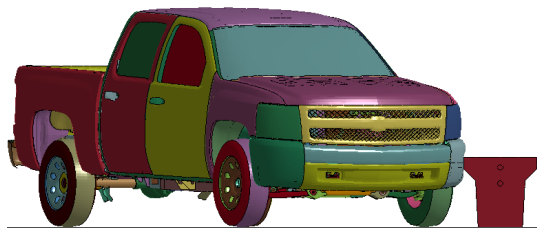
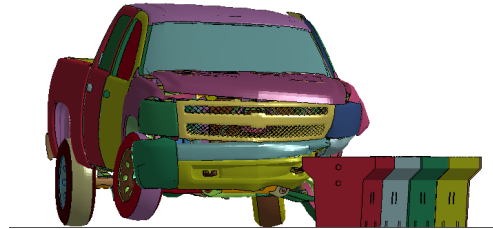


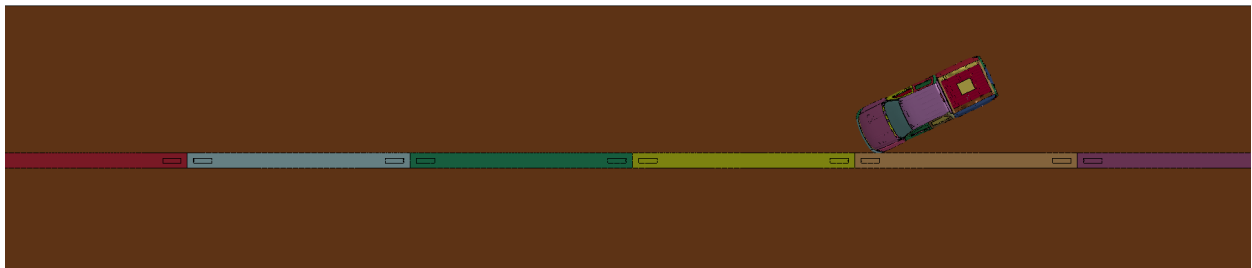
Figure 6.19 Angular Displacements of the Vehicle in Case 2 (24-Inch Tall PCB Simulation)



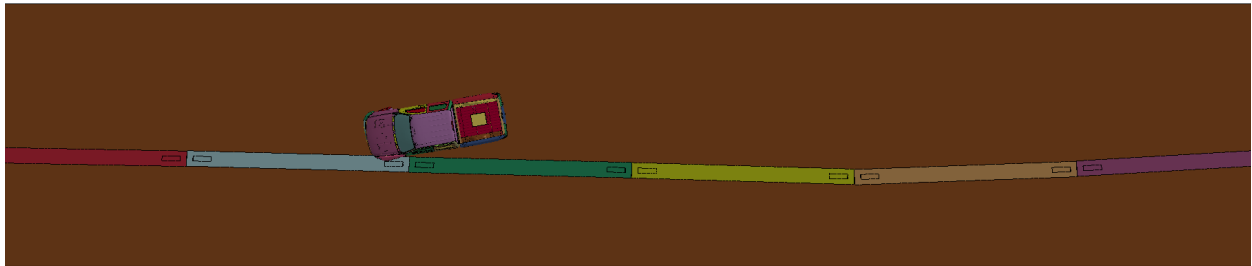
(a) Front view at impact



(b) Front view at final configuration



(c) Overhead view at impact



(d) Overhead view at final configuration

Figure 6.20 Initial and Deflected Shape of the 24-Inch Tall T Shaped PCB in Case 2

6.3.4.2 Occupant Risk Assessment

Occupant risk factors were evaluated based on the applicable MASH safety evaluation criteria. In the longitudinal direction, the occupant impact velocity was 22.9 ft/s at 0.117 seconds, the highest 0.010-s occupant ridedown acceleration was -6.2 G from 0.133 to 0.143 seconds, and the maximum 0.050-s average acceleration was -11.0 G between 0.051 and 0.101 seconds. In the lateral direction, the occupant impact velocity was 16.7 ft/s at 0.117 seconds, the highest 0.010-s occupant ridedown acceleration was -9.0 G from 0.301 to 0.311 seconds, and the maximum 0.050-s average acceleration was -11.8 G between 0.034 and 0.084 seconds. THIV was 26.9 ft/s at 0.111 seconds; PHD was 9.0 G between 0.301 and 0.311 seconds; and ASI was 1.66 between 0.067 and 0.117 seconds. All of which were within the preferred limits in accordance with MASH.

6.3.4.3 Energy Values

Energy values were evaluated. As shown in Figure 6.21, approximately 17 percent of the initial kinetic energy of the impacting vehicle was converted into internal energy. Approximately 2 percent of the initial kinetic energy was converted into hourglass energy. Approximately 21 percent of the initial kinetic energy was converted into sliding interface energy. About 50 percent of the initial kinetic energy had yet to be dissipated by the system at the time of final impact configuration, mainly due to the remaining velocity of the vehicle. The 10 percent reduction in total energy of the system was due to numerical computation and loss of energy in the deformation of the barrier and connections.

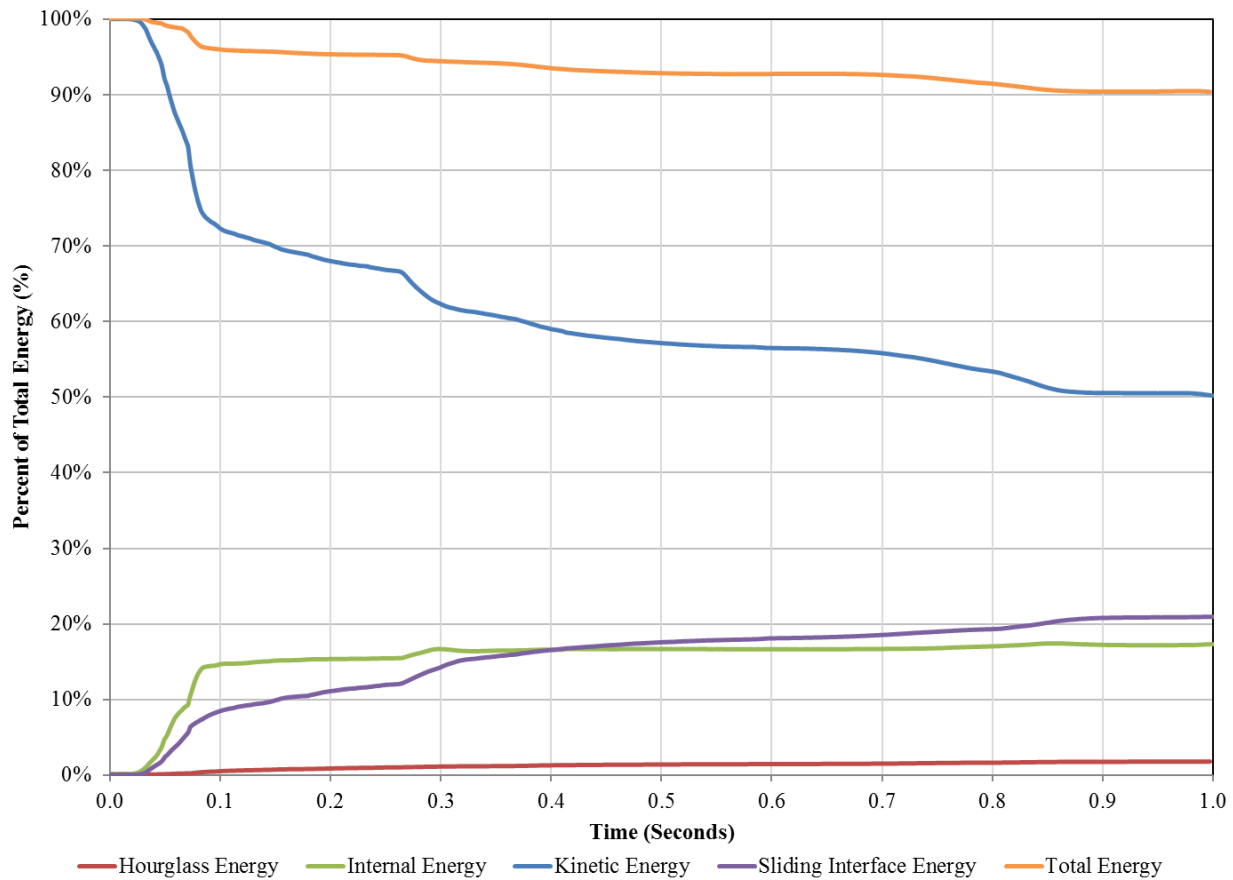
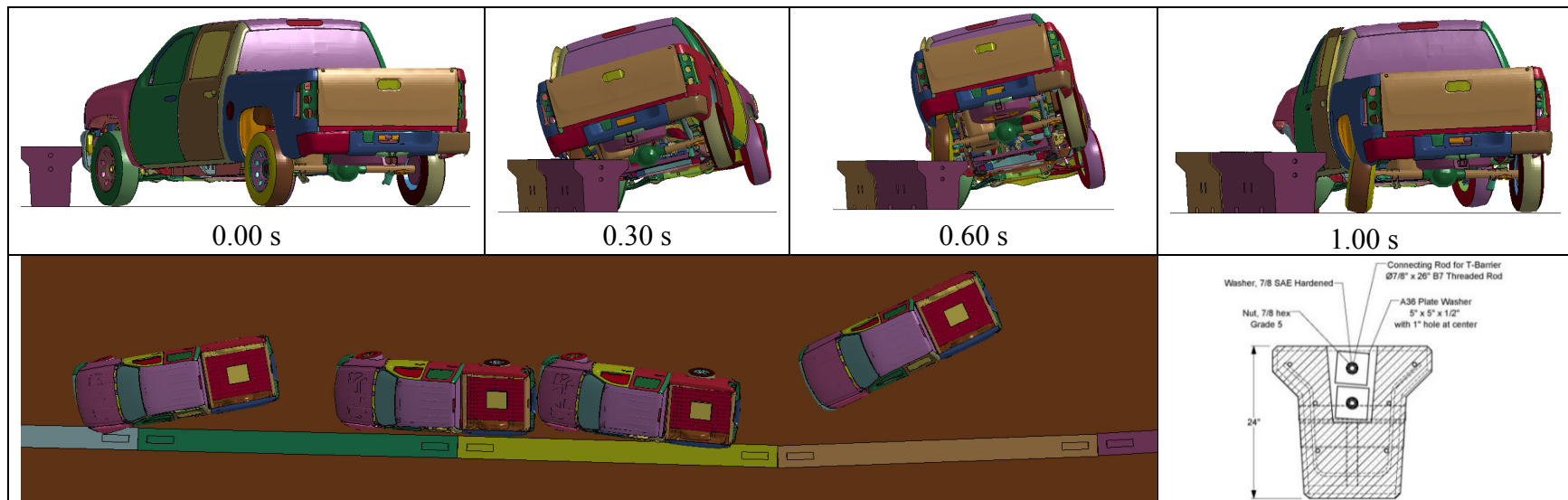


Figure 6.21 Energy Distribution History in Case 2 (24-Inch Tall PCB Simulation)

6.3.4.4 Summary

Figure 6.22 summarizes results for MASH Test 3-11 simulation with a 2270P vehicle (without impact tire disengagement) impacting a 24-inch tall low-profile PCB. Results showed that the 24-inch tall PCB performed adequately by containing and redirecting the impacting 2270P vehicle. The free-standing barrier had a maximum deflection about 30.9 inches from its initial position during the impact event. The vehicle was redirected and did not penetrate, underide, or override the installation. Simulation indicated that the 2270P vehicle maintained stability during the MASH TL 3-11 impact conditions event.



General Information

Test Agency Texas A&M Transportation Institute (TTI)
Test Standard Test No. MASH Test 3-11

Test Article

Type Longitudinal Barrier - Concrete
Name MASH TL-3 Low-Profile Barrier
Installation Length 180 ft
Material or Key Elements Six segments of 24-inch tall, 30-ft long "T" shaped reinforced concrete barrier
Soil Type Concrete Pavement,

Test Vehicle

Type/Designation 2270P
Make and Model Finite Element Silverado Pickup
Curb 4877 lb
Test Inertial 5033 lb
Dummy No dummy
Gross Static 5033 lb

Impact Conditions

Speed 62.0 mi/h
Angle 25.0 degrees
Location/Orientation One Third of Barrier Length

Exit Conditions

Speed 45.2 mi/h
Angle 5.6 degrees

Occupant Risk Values

Longitudinal OIV 23.0 ft/s
Lateral OIV 16.7 ft/s
Longitudinal Ridedown -6.2 G
Lateral Ridedown -9.0 G
THIV 29.7 km/h
PHD 9.0 G
ASI 1.66

Max. 0.050-s Average

Longitudinal -11.0 G
Lateral -11.8 G
Vertical 3.1 G

Post-Impact Trajectory

Stopping Distance N/A

Vehicle Stability

Maximum Yaw Angle -32.9 degrees
Maximum Pitch Angle 12.2 degrees
Maximum Roll Angle -19.8 degrees
Vehicle Snagging No
Vehicle Pocketing No

Test Article Deflections

Dynamic 30.9 inches
Permanent 30.0 inches
Working Width N/A

Figure 6.22 Summary of Simulation Results of 24-Inch Tall Low-Profile PCB (Without Impact Tire Disengagement)

6.3.5 Results Comparison between Case 1 and Case 2 of 24-Inch Tall T Shaped PCB

Results of the two detailed FE simulations cases were compared to determine the performance envelope of the 24-inch tall T Shaped low-profile PCB. Table 6.4 compares the occupant risk values and maximum angular displacements. Table 6.5 and Table 6.6 include the sequential images of the two cases in front view and overhead view, respectively.

Occupant risk values were very comparable between the two cases. The impact velocity increased slightly in lateral direction (y-direction) for case 1 (+2.3 ft/s). The predicted ridedown acceleration was increased for case 1 (there is an increase of 4.9 G in lateral direction). Case 1 had similar roll and yaw angles with case 2, but the vehicle experienced much more pitch in Case 2.

Overall, the crashworthiness of the free-standing 24-inch tall low-profile PCB was evaluated through finite element computer simulations according to MASH test 3-11. Two different cases were performed, vehicle behaved more instable in the case with impact tire disengagement. Simulation results indicated that the 24-inch tall low-profile PCB maintained occupant risks well below the limiting values according to MASH criteria.

Table 6.4 Occupant Risk Values Comparison between Case 1 and Case 2 (24-Inch Height)

Occupant Risk Factors and Maximum Angular Displacement		Case 1 - With Impact Tire Disengagement	Case 2 - Without Impact Tire Disengagement
Impact Velocity (ft/s)	x-direction	20.0	22.9
	y-direction	-19.0	-16.7
Ridedown Acceleration (G)	x-direction	-5.2	-6.2
	y-direction	-13.9	-9.0
Maximum Angular Displacement (Degrees)	Roll	-20.6	-19.8
	Pitch	-6.9	-12.2
	Yaw	29.3	32.9

Table 6.5 Sequential Images of Case 1 and Case 2 of 24-Inch Tall PCB (Front View)

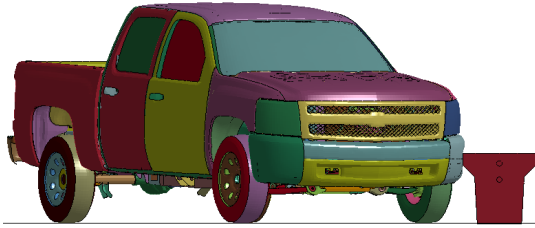
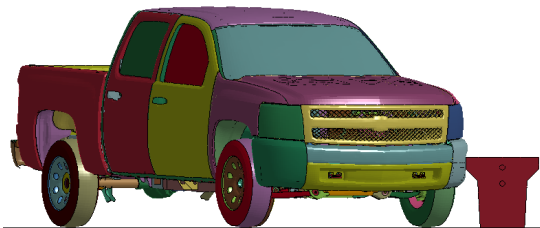
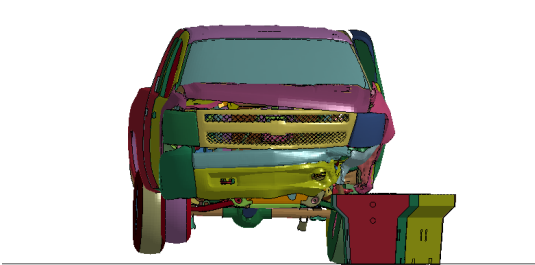
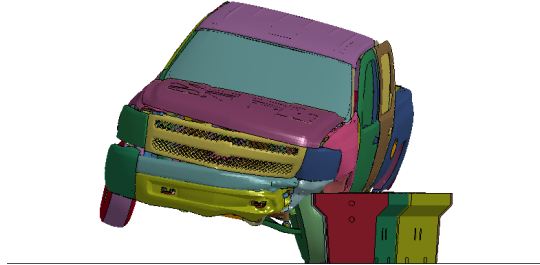
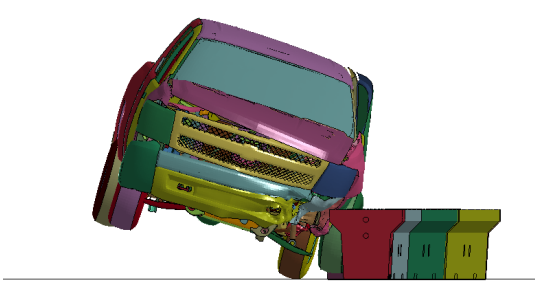
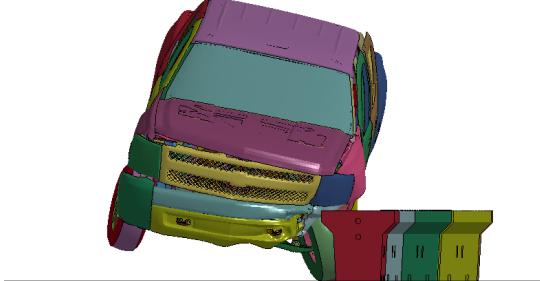
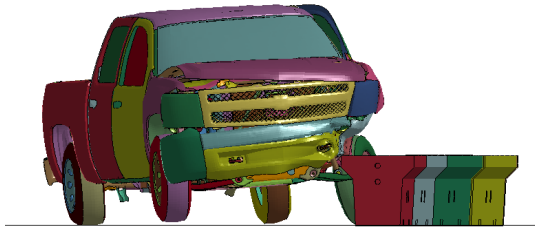
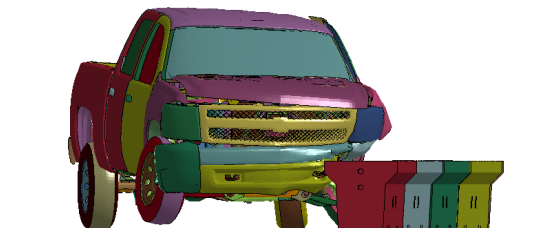
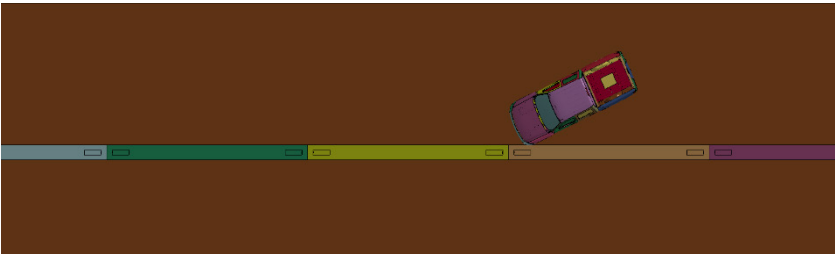
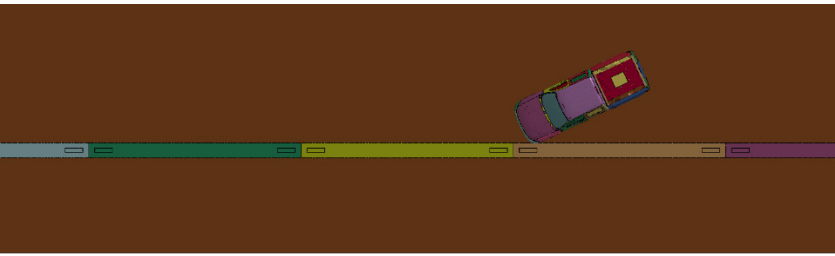

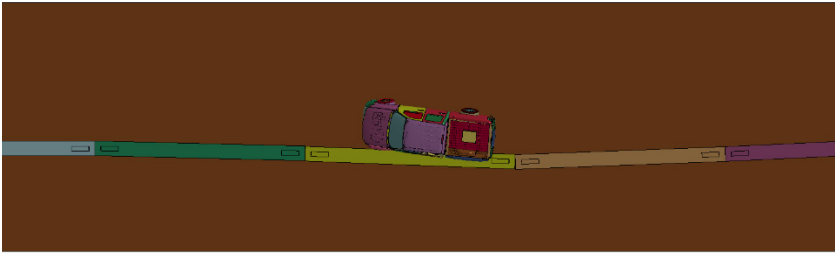
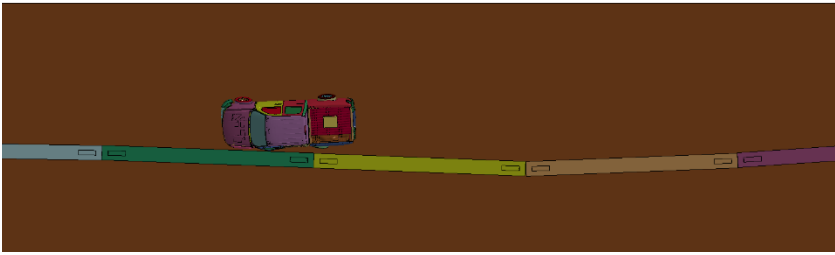
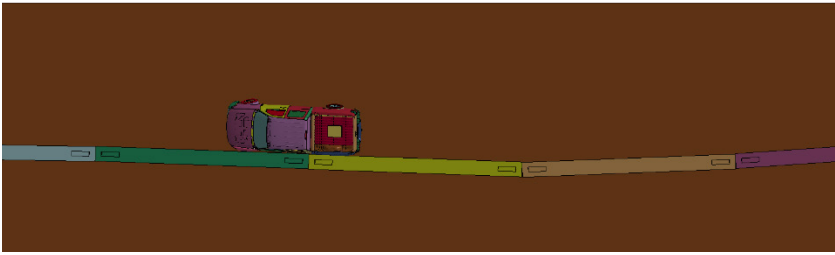
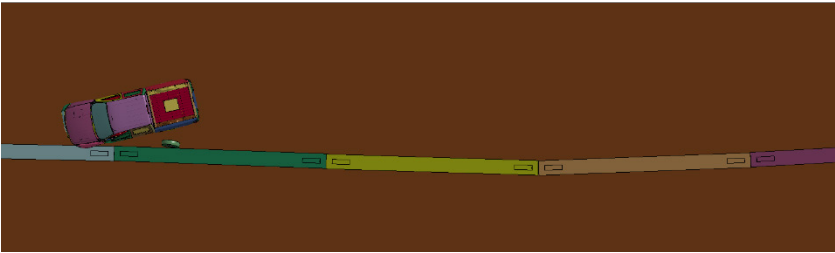
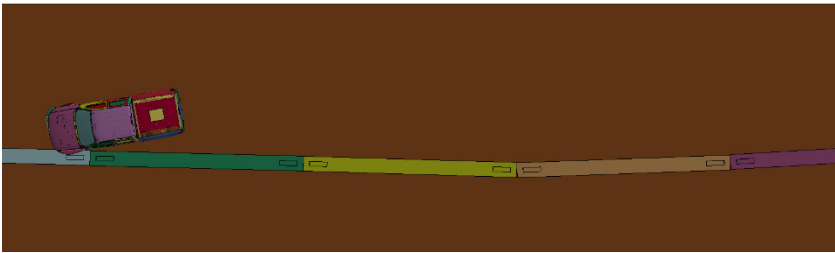
Time (seconds)	Case 1 With Impact Tire Disengagement	Case 2 Without Impact Tire Disengagement
0.0		
0.3		
0.6		
1.0		

Table 6.6 Sequential Images of Case 1 and Case 2 of 24-Inch Tall PCB (Overhead View)

Time (seconds)	Case 1 With impact tire disengagement	Case 2 Without impact tire disengagement
0.0		
0.3		
0.6		
1.0		

6.4 Conclusion of Detailed Simulations

Detailed finite element simulations were conducted to predict the performance of the T shaped low-profile PCB with heights of 24 and 26 inches. To allow for easiness of construction forming, it was decided to modify the straight side of the barrier to 1:18 slope. Detailed FE models were developed with segments and connection details based on the designs.

MASH test 3-11 impact conditions were replicated in the detailed simulations. The modeled 2270P pickup truck impacted the barrier at about 1/3 of the system length with a speed of 62 mi/h and an angle of 25 degrees. Different tire attachment cases were considered for each height (with and without impact tire disengagement). It should be noted that concrete failure options were not implemented in the FE model, so that the developed model did not have the ability to predict fracture or spalling of concrete which might happen during the full-scale crash test.

The crashworthiness of the 26-inch tall T shaped barrier was predicted to be acceptable by successfully contained and redirected the vehicle during the simulated impact event. Simulation results showed all the occupant risk values were below MASH limitation, and the barrier had a maximum dynamic deflection of 29.8 inches. The 24-inch tall barrier also had acceptable crashworthiness from the predicting simulations. Consider the failed full-scale crash tests and preliminary simulations, a height of 26 inches would guarantee more vehicle stability during the impact event. Therefore, 26-inch tall T shaped PCB was determined to be constructed and crash tested.

7. FULL-SCALE CRASH TEST

7.1 Introduction

The 26-inch tall T shaped low-profile PCB was constructed as designed. Two full-scale crash tests were implemented to evaluate the crashworthiness of the PCB. In the first test (MASH test 3-11), a 2270-kg pickup truck was used to impact the barrier at a speed of 62 mi/h and an angle of 25.0 degrees. This test designation was used to test the strength of the barrier system. In the second crash test (MASH test 3-10), barrier's ability to contain and redirect small passenger vehicles during the collision event was investigated. An 1100-kg passenger car impacted the barrier at a speed of 62mi/h and an angle of 25.0 degrees.

7.2 MASH Test 3-11

7.2.1 Barrier Installation Details and Test Vehicle

The test installation consisted of six free-standing reinforced concrete barriers, each 30 feet long, for a total length of 180 feet. Adjacent barriers were connected with two 26-inch long, 7/8-inch diameter B7 threaded rods, along with plate washers, SAE hardened washers, and Grade 5 hex nuts. The barriers were 15 inches wide at bottom, 25 inches wide at top, and 26 inches tall. Figure 7.1 provides images of the installation.

Figure 7.2 and Figure 7.3 show the 2013 Dodge RAM 1500 pickup truck used for the crash test. The vehicle's test inertia weight was 5012 lb, and its gross static weight was 5012 lb. The height to the lower edge of the vehicle bumper was 11.75 inches, and height to the upper edge of the bumper was 27.0 inches. The height to the vehicle's center of gravity was 29.0 inches. The vehicle was directed into the installation using the cable reverse tow and guidance system, and was released to be freewheeling and unrestrained just prior to impact.



Figure 7.1 Images of the 26-Inch Tall T Shaped Low-Profile PCB Prior to MASH Test 3-11



Figure 7.2 Test Vehicle Prior to MASH Test 3-11



Figure 7.3 Test Vehicle at Targeted Impact Point Prior to MASH Test 3-11

7.2.2 Test Description

The test vehicle was traveling at an impact speed of 62.4 mi/h as it contacted the 26-inch tall low-profile PCB 4.3 feet upstream of the joint between segments 2 and 3 at an impact angle of 24.5°. At approximately 0.072 seconds, the vehicle began to redirect, and at 0.089 s, the front left tire blew out and began to detach from the suspension assembly. The vehicle was traveling parallel with the barrier at 0.245 seconds. As the vehicle continued forward, it lost contact with barrier while traveling at 43.1 mi/h and 9.7 degrees. The vehicle yawed counterclockwise and came to rest 431 feet downstream of the impact and 81 feet toward the field side. Figure 7.4 presents a schematic of the crash test.

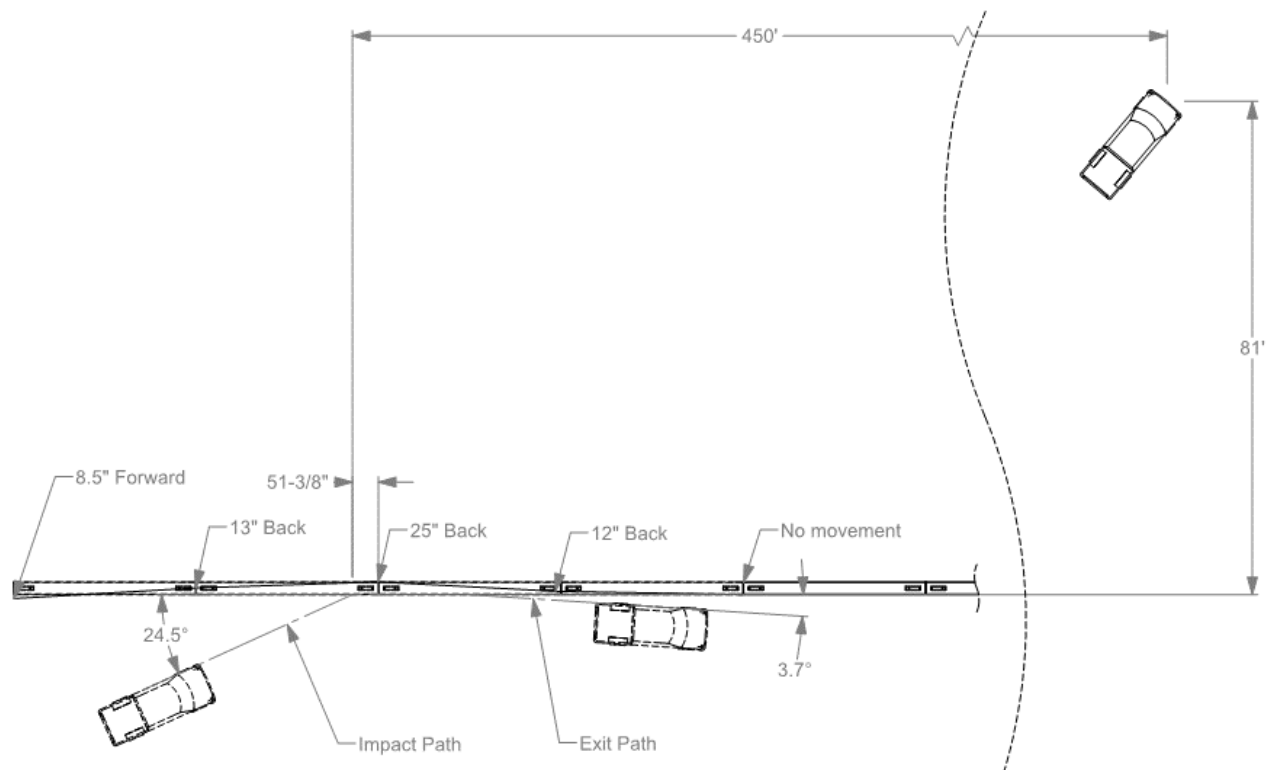


Figure 7.4 Test Schematic

7.2.3 Damage to the Barrier and Vehicle

Figure 7.5 shows the damage to the 26-inch tall PCB after crash test. The upstream end of segment 1 was displaced 8.5 inches toward traffic side and the downstream end was displaced 13.0 inches toward the field side. Joint 2-3 was displaced 25.0 inches toward field side, and joint 3-4 was displaced 12.0 inches toward the field side. No movement was noted at the downstream end of segment 4. Working width was 50.6 inches, and the height of maximum working width was 26.0 inches. Maximum dynamic deflection during the test was 25.0 inches, and maximum permanent deformation was 25.0 inches. Figure 7.6 and show the damage at joint 2-3. Concrete spalling was found along the impact area and on the field side at joint 2-3. The damage did not expose any reinforcing steel and was not considered to significantly affect the structural integrity of the barrier system. Additionally, the threaded steel rods were bent slightly as Figure 7.7 shows.

Figure 7.8 shows the damage that the vehicle had sustained. The front bumper, left frame rail, hood, grill, radiator and support, left front fender, left front tire and rim, left front upper and lower A-arms, left front upper and lower ball joints, front sway bar, tie rod ends, left front and rear doors, left rear cab corner, left rear exterior bed, left rear rim, and bumper were damaged. The windshield sustained a stress crack in the left lower corner radiating upward. Maximum exterior crush to the vehicle was 10.0 inches in the horizontal plane at the front bumper at bumper height. Maximum occupant compartment deformation was 2.0 inches in the driver side floor from the firewall to the driver seat.



Figure 7.5 Images of 26-Inch Tall T Shaped Low-Profile PCB after MASH Test 3-11



Figure 7.6 Concrete Spalling at Joint 2-3



Figure 7.7 Thread Rods Deformation at Joint 2-3



Figure 7.8 Test Vehicle after MASH Test 3-11

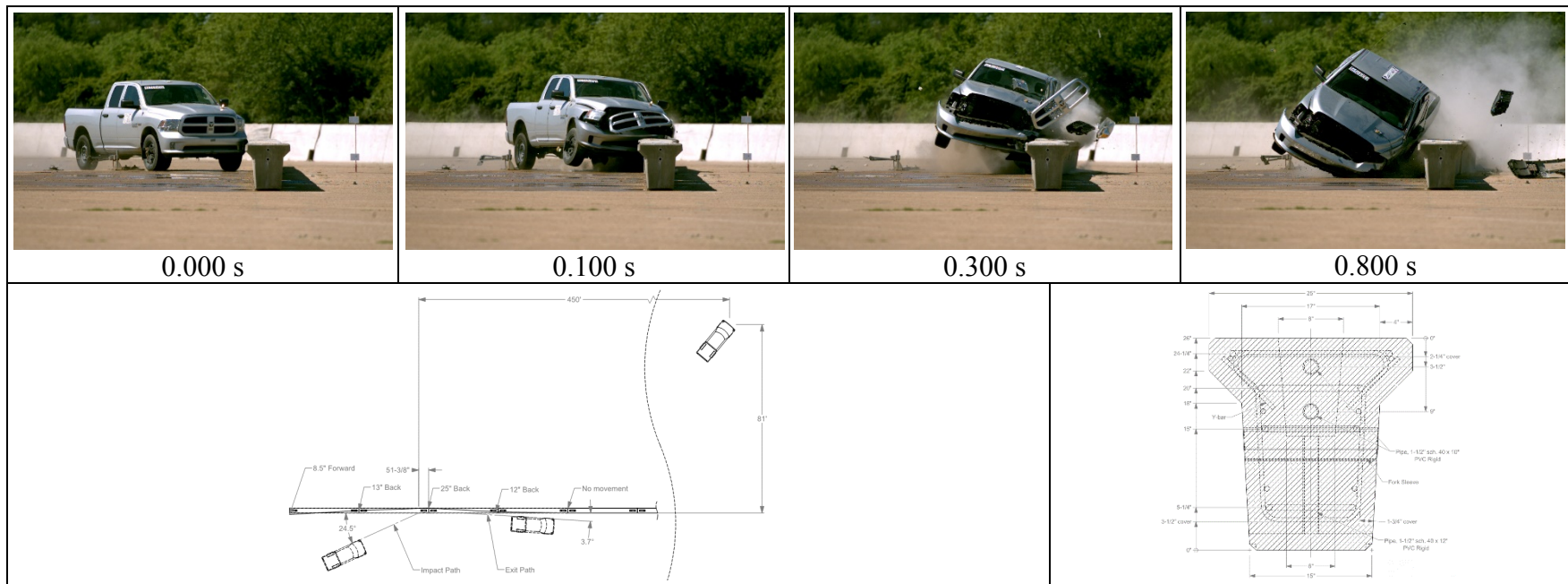
7.2.4 Occupant Risk Factors

Data acquired from the accelerometer, located at the vehicle center of gravity, were digitized for evaluation of occupant risk. In the longitudinal direction, the occupant impact velocity was 19.4 ft/s at 0.111 s, the highest 0.010-s occupant ridedown acceleration was 3.3 G from 0.592 to 0.602 s, and the maximum 0.050-s average acceleration was -9.4 G between 0.038 and 0.088 s. In the lateral direction, the occupant impact velocity was 20.7 ft/s at 0.111 s, the highest 0.010-s occupant ridedown acceleration was 6.5 G from 0.279 to 0.289 s, and the maximum 0.050-s average was 11.2 G between 0.039 and 0.089 s. THIV was 29.5 ft/s at 0.107 seconds; PHD was 6.9 G between 0.279 and 0.289 s; and ASI was 1.55 between 0.058 and 0.108 seconds. All of which were within the preferred limits in accordance with MASH.

Maximum roll, pitch, and yaw angles resulted to be -40, -10, and 36 degrees respectively, they all remained in the range required by MASH criteria.

7.2.5 Summary of the MASH Test 3-11

The 2270P vehicle was redirected and contained after impact. Vehicle did not penetrate, underide, or override the free-standing barrier system. The maximum lateral deflection of the barrier system was 25.0 inches and occurred at joint 2-3. There were no detached elements or debris to show potential for penetration of the occupant compartment or to present undue hazard to others in the area. The vehicle remained upright and stable during the impact and after exiting the installation. The results showed that the 26-inch tall free-standing T shaped low-profile PCB performed acceptably and met the evaluation criteria of MASH test 3-11. Figure 7.9 summarizes the data and other pertinent information from the test.



General Information

Test Agency Texas A&M Transportation Institute (TTI)
 Test Standard Test No. MASH Test 3-11
 TTI Test No. 469688-1-2
 Test Date..... 2018-04-16

Test Article

Type Portable Concrete Barrier
 Name..... Modified Low-Profile Barrier
 Installation Length..... 180 ft
 Material or Key Elements T-shaped concrete barrier 15 inches at base, 25 inches at top, 26 inches tall

Soil Type and Condition Placed on concrete surface, damp

Test Vehicle

Type/Designation 2270P
 Make and Model..... 2013 Dodge RAM Pickup
 Curb 5058 lb
 Test Inertial 5012 lb
 Dummy No dummy
 Gross Static..... 5058 lb

Impact Conditions

Speed 62.4 mi/h
 Angle 24.5 degrees
 Location/Orientation 4.3 ft upstream of joint 2&3

Impact Severity

..... 111.6 kip-ft

Exit Conditions

Speed 43.1 mi/h
 Angle 3.7 degrees

Occupant Risk Values

Longitudinal OIV..... 19.4 ft/s
 Lateral OIV 20.7 ft/s
 Longitudinal Ridedown 3.3 G
 Lateral Ridedown 6.5 G
 THIV 32.5 km/h
 PHD..... 6.9 G
 ASI 1.55

Max. 0.050-s Average

Longitudinal..... -9.4 G
 Lateral -11.2 G
 Vertical -3.2 G

Post-Impact Trajectory

Stopping Distance..... 431 ft downstream
 81 ft twd field side

Vehicle Stability

Maximum Roll Angle..... 40 degrees
 Maximum Pitch Angle 10 degrees
 Maximum Yaw Angle 36 degrees
 Vehicle Snagging No
 Vehicle Pocketing No

Test Article Deflections

Dynamic 25.0 inches
 Permanent 25.0 inches
 Working Width..... 50.6 inches
 Height of Working Width 26.0 inches

Vehicle Damage

VDS..... 10-LFQ-5
 CDC 10FLEW4
 Max. Exterior Deformation 10 inches
 OCDI LF0010000
 Max. Occupant Compartment Deformation 2.0 inches

Figure 7.9 Summary of Results for MASH Test 3-11 on the 26-Inch Tall T Shaped Low-Profile PCB

7.3 MASH Test 3-10

7.3.1 Test Article

To complete the crashworthiness evaluation of the TL-3 26-inch tall T shaped low-profile PCB, a crash test with A small car was conducted according to MASH test 3-10 criteria. MASH test 3-10 is deigned to investigate a barrier's ability to successfully contain and redirect small passenger vehicles during the collision event. The primary concerns are the potential for vehicle under-ride, wheel snag, rollover, and head-slap.

Figure 7.10 and Figure 7.11 show the 2011 Kia Rio used for the crash test. The vehicle's test inertia weight was 2423 lb, and its gross static weight was 2588 lb. The height to the lower edge of the vehicle bumper was 7.75 inches, and height to the upper edge of the bumper was 21.5 inches. The target critical impact point for MASH test 3-10 on the low-profile PCB was 3.6 feet upstream of the joint between segments 2 and 3.



Figure 7.10 Test Vehicle Prior to MASH Test 3-10



Figure 7.11 Test Vehicle at the Targeted Impact Point Prior to MASH Test 3-10

7.3.2 Test Result

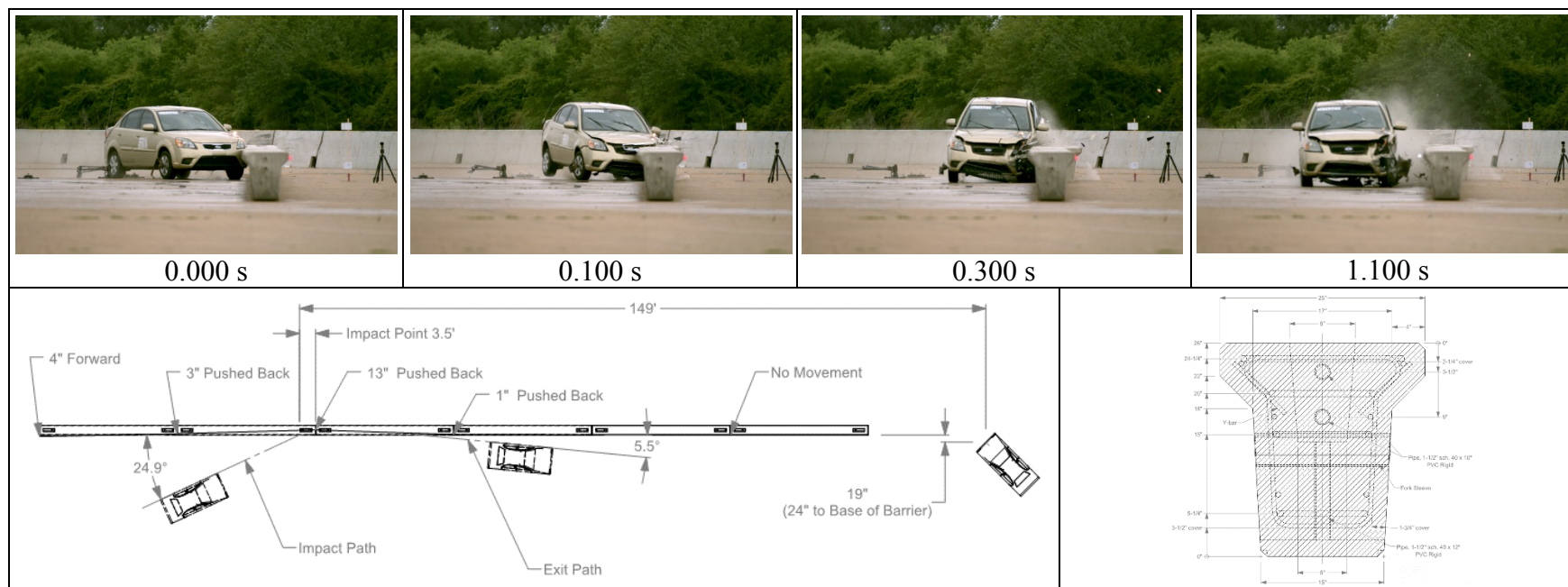
The actual impact speed and angle were 63.4 mi/h and 24.9 degrees, respectively. The actual impact point was 3.6 feet upstream of the joint between segments 2 and 3. Figure 7.12 includes images of the PCB after test. Small pieces of concrete broke off were found at joint 2-3. Maximum dynamic deflection during the test was 13.2 inches, and maximum permanent deformation was 13.0 inches. Figure 7.13 shows the damage that the vehicle sustained during the crash test. Maximum exterior crush to the vehicle was 12.0 inches in the side plane at the left front corner at bumper height. Maximum occupant compartment deformation was 1.0 inch in the left kick panel area. Occupant risk factors and other test results are summarized in Figure 7.14. The results showed that the 26-inch tall free-standing T shaped low-profile PCB performed acceptably and met the evaluation criteria of MASH test 3-10.



Figure 7.12 Images of 26-Inch Tall T Shaped Low-Profile PCB after MASH Test 3-10



Figure 7.13 Test Vehicle after MASH Test 3-10



General Information

Test Agency Texas A&M Transportation Institute (TTI)
 Test Standard Test No. MASH Test 3-10
 TTI Test No. 469688-1-1
 Test Date..... 2018-04-18

Test Article

Type Portable Concrete Barrier
 Name..... Modified Low-Profile Barrier
 Installation Length..... 180 ft
 Material or Key Elements T-shaped concrete barrier 15 inches at base, 25 inches at top, 26 inches tall

Soil Type and Condition Placed on concrete surface, damp

Test Vehicle

Type/Designation 1100C
 Make and Model..... 2011 Kia Rio
 Curb 2443 lb
 Test Inertial 2423 lb
 Dummy 165 lb
 Gross Static..... 2588 lb

Impact Conditions

Speed 63.4 mi/h
 Angle 24.9 degrees
 Location/Orientation 3.6 ft upstream of joint 2&3

Impact Severity

Exit Conditions 62 kip-ft
 Speed 46.0 mi/h
 Angle 5.7

Occupant Risk Values

Longitudinal OIV..... 23.0 ft/s
 Lateral OIV 24.9 ft/s
 Longitudinal Ridedown 4.7 G
 Lateral Ridedown 7.0 G
 THIV 36.7 km/h
 PHD 7.1 G
 ASI 2.1 G
 Max. 0.050-s Average
 Longitudinal..... -13.2 G
 Lateral 14.8 G
 Vertical 2.1 G

Post-Impact Trajectory

Stopping Distance 149 ft downstream
 2 ft toward traffic

Vehicle Stability

Maximum Roll Angle 4°
 Maximum Pitch Angle 7°
 Maximum Yaw Angle 31°
 Vehicle Snagging No
 Vehicle Pocketing No

Test Article Deflections

Dynamic 13.2 inches
 Permanent 13.0 inches
 Working Width..... 38.5 inches
 Height of Working Width 26.0 inches

Vehicle Damage

VDS..... 10-LFQ-5
 CDC 10FLEW3
 Max. Exterior Deformation 12 inches
 OCDI LF0000000
 Max. Occupant Compartment Deformation 1.0 inches

Figure 7.14 Summary Of Results For MASH Test 3-10 On The 26-Inch Tall T Shaped Low-Profile Barrier

8. FEA MODIFICATION AND VALIDATION

8.1 Introduction

In this section, the original finite element simulation results of the detailed 26-inch tall T shaped low-profile PCB were compared with the full-scale crash test results of MASH test 3-11. Significant differences were found in vehicle roll angle and barrier lateral deflection. Further analysis was conducted. After reviewing the crash test film and original FEA results, modifications were made to the pickup truck and low-profile PCB FE models for more accurate simulation results. A verification and validation program was used to validate the modified FEA.

8.2 Comparison between Original FEA and Full-Scale Crash Test

As shown in Figure 8.1, the front impact tire of the pickup truck was disengaged from the suspension assembly during the full-scale crash test. Therefore, the Case 1 (detailed simulation with impact tire disengagement) of the 26-inch tall barrier was used as original FEA to compare with the full-scale crash test.

Table 8.1 compares the occupant risk values between the original FEA and full-scale crash test. OIV, ORA values and pitch and yaw angles were very similar when comparing the original FEA and full-scale crash test. The significant difference was found in the maximum vehicle roll angle. The vehicle had a maximum roll angle of -40 degrees in the full-scale crash test, but only -19.2 degrees in the original FEA. Additionally, the FEA had greater maximum lateral deflection of the low-profile PCB (29.8 inches) than the full-scale crash test (25.0 inches).


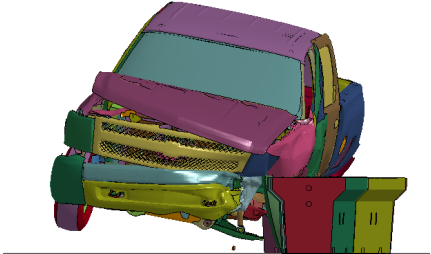

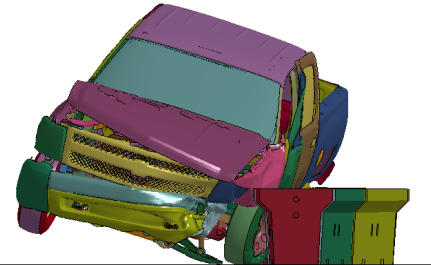

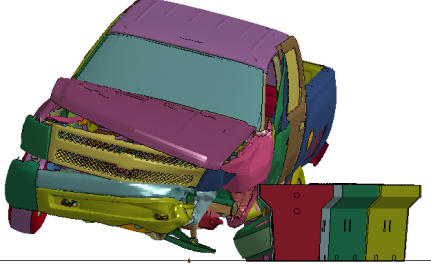


Figure 8.1 Front Impact Tire Disengagement

Table 8.1 Occupant Risk Factors Comparison between Original FEA and Crash Test

Occupant Risk Factors and Maximum Angular Displacements		Original FEA	Full-Scale Crash Test
Impact Velocity (ft/s)	x-direction	22.0	19.4
	y-direction	-19.0	-20.7
Ridedown Acceleration (G)	x-direction	-5.0	-3.3
	y-direction	6.0	6.5
Maximum Angular Displacements (Degrees)	Roll	-19.2	-40.0
	Pitch	-8.8	-10.0
	Yaw	35.9	36.0

Full-scale crash test film was analyzed and compared with original FEA as Table 8.2 shows. The pickup truck had different behavior after the front impact tire was detached from the suspension assembly. In the full-scale crash test, the disengaged tire blew out, turned to the horizontal direction and lost support for the pickup truck. However, tire blew out was very difficult to accomplish in FEA. In the FE simulations, the impact tire still had pressure after disengaged from the suspension assembly and prevented the pickup truck from further rolling to the barrier.

Time (Seconds)	Full-Scale Crash Test	Original FEA
0.3		
0.4		
0.5		

8.3 Modification and Validation

8.3.1 Modified FEA Results

Two main factors were considered for modification to get more accurate FEA results. The first one was the front impact tire and the second one was the friction coefficients between concrete portable barrier and ground. Since accurate tire blow out was not feasible to achieve in this study, the front impact tire was removed after it disengaged from the pickup truck. To get the right maximum barrier deflection, the static frictional coefficient between the ground and barriers was determined to be 0.83 and the dynamic frictional coefficient was 0.30, after a series of parametric finite element simulations were conducted.

The maximum barrier deflection was 25.3 inches in the modified FEA, the difference was only 1 percent compared with the full-scale crash test (25.0 inches). Figure 8.2 compares the vehicle angular displacements during the impact event, and the occupant risk factors were compared in Table 8.3.

Table 8.4 and Table 8.5 show frames from modified FEA and actual full-scale crash test against the 26-inch tall low-profile PCB. Generally, there was a good agreement between the vehicle stability and relative position between the vehicle and the barrier during the impact event. However, the vehicle presented more intrusion to the barrier and had greater roll angles in the full-scale crash test before it was redirected. The behavior differences could be a result of pickup truck FE model limitation.

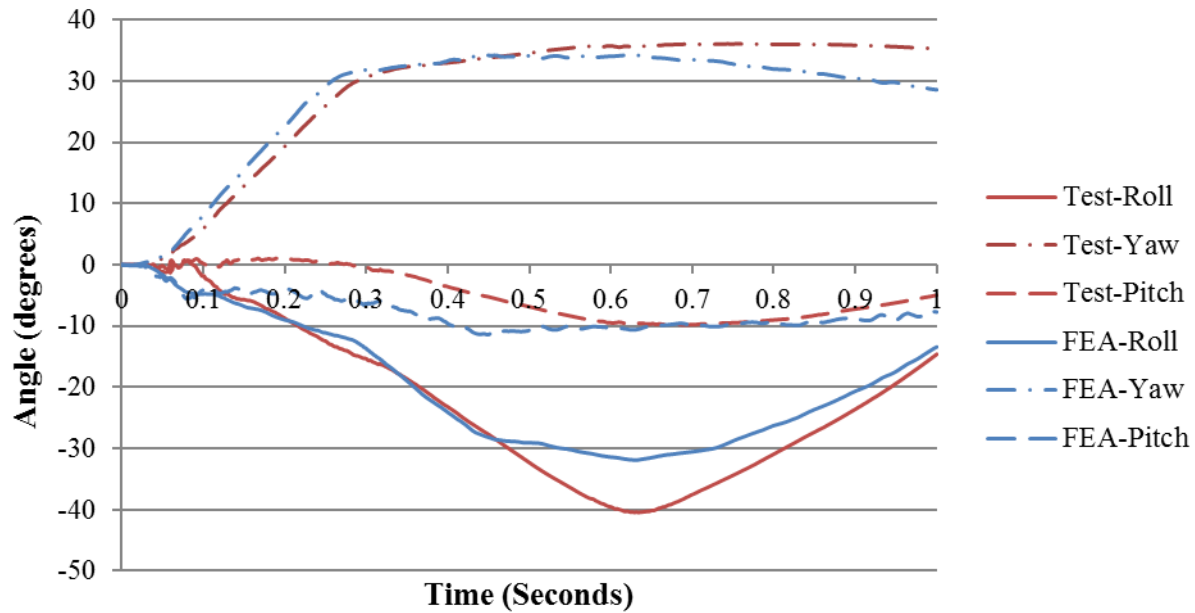


Figure 8.2 Roll, Yaw And Pitch Angles Comparison Between Modified Fea And Crash Test

Table 8.3 Occupant Risk Factors Comparison between Modified FEA and Crash Test

Occupant Risk Factors and Maximum Angular Displacements		Modified FEA	Full-Scale Crash Test
Impact Velocity (ft/s)	x-direction	20.3	19.4
	y-direction	-20.0	-20.7
Ridedown Acceleration (G)	x-direction	-5.3	-3.3
	y-direction	7.4	6.5
Maximum Angular Displacements (Degrees)	Roll	-31.9	-40.0
	Pitch	-11.4	-10.0
	Yaw	34.3	36.0

Table 8.4 Sequential Comparison between Modified FEA and Crash Test (Front View)

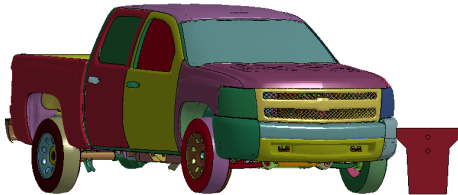

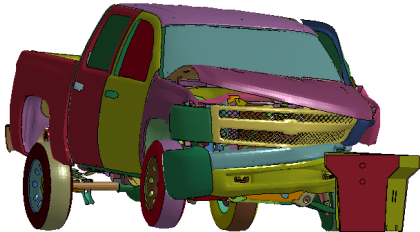

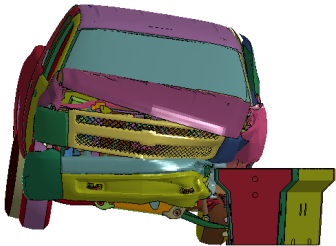

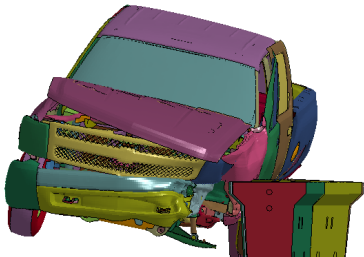

Time (Seconds)	Modified FEA	Full-Scale Crash Test
0		
0.1		
0.2		
0.3		

Table 8.4 Continued

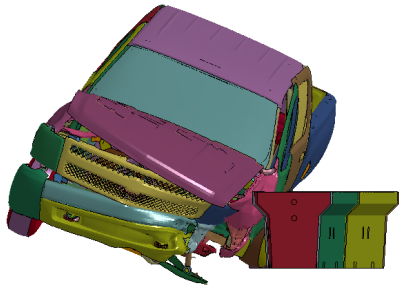

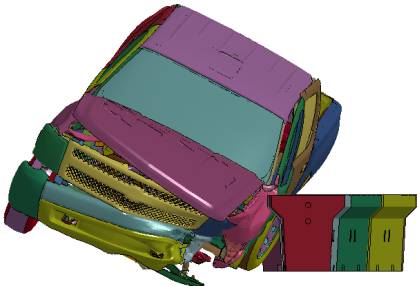

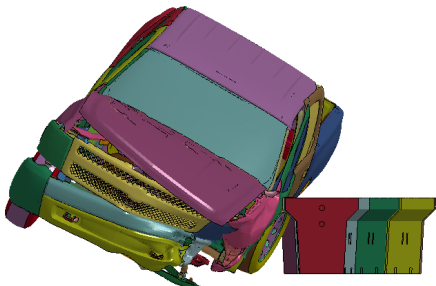

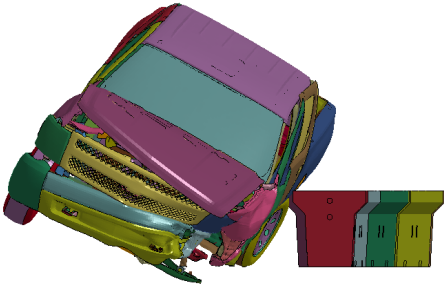

Time (Seconds)	Modified FEA	Full-Scale Crash Test
0.4		
0.5		
0.6		
0.7		

Table 8.5 Sequential Comparison between Modified FEA and Crash Test (Overhead View)







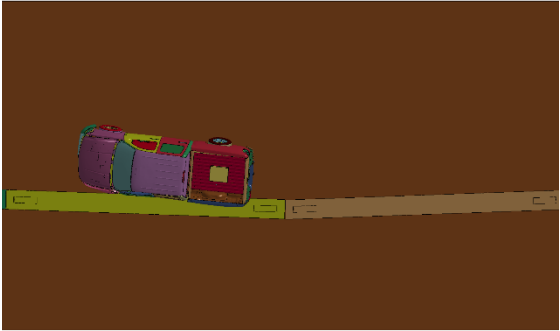

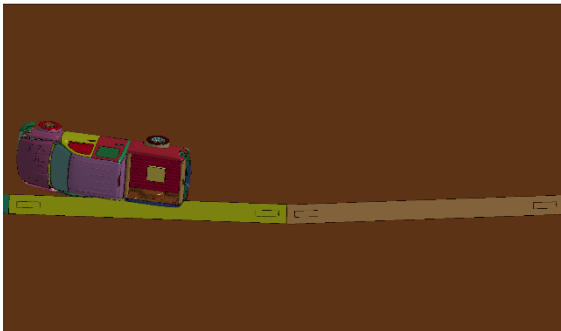

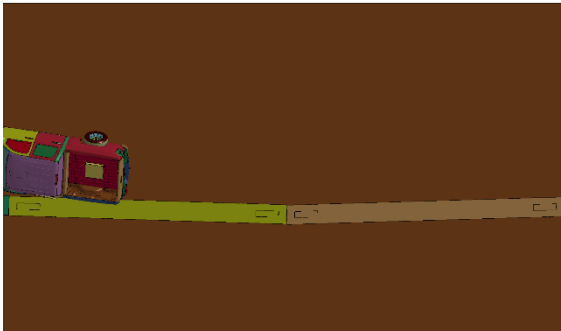

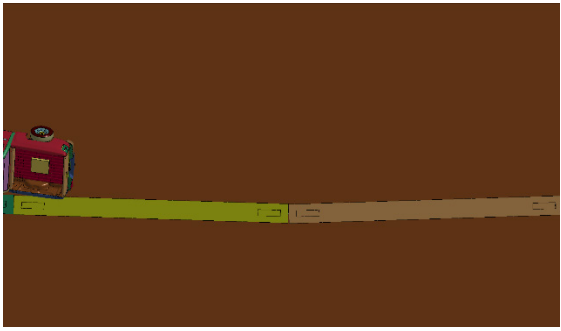

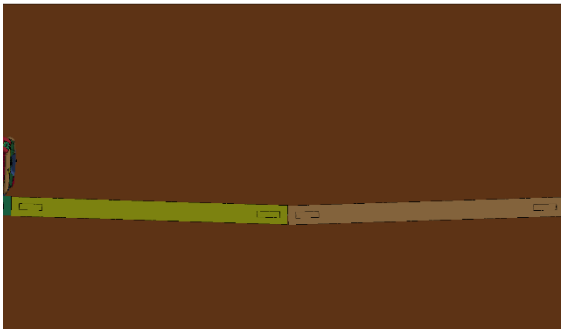

Time (Seconds)	Modified FEA	Full-Scale Crash Test
0		
0.1		
0.2		
0.3		

Table 8.5 Continued

Time (Seconds)	Modified FEA	Full-Scale Crash Test
0.4		
0.5		
0.6		
0.7		

8.3.2 RSVVP Validation

A program called the Roadside Safety Verification and Validation Program (RSVVP) was developed for validation of numerical models in roadside safety [28]. This program was used to compute the comparison metrics for a quantitative validation of the pickup truck FE impact model. This quantitative verification approach is based on the comparison of acceleration and angle curves from both simulation and test data according to Sprague and Geers (S&G) MPC and variance (ANOVA) metrics. The data from the simulation was filtered in LS-DYNA using SAE 180 filter. The evaluation was performed over a period of 1.0 second of impact event. The acceptance maximum values are 40% for S&G metrics, 5% for ANOVA mean and 35% for ANOVA standard deviation.

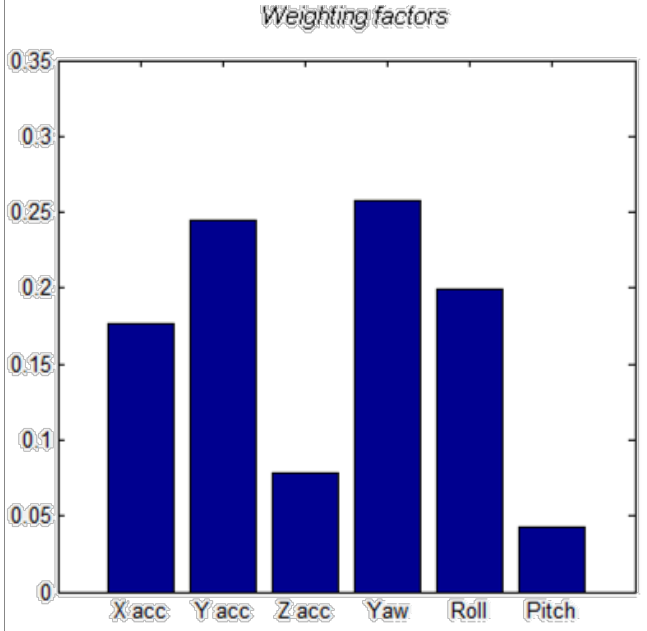
The results of the evaluation for the individual channels are shown in Table 8.6. Based on the Sprague-Geers metrics, the y acceleration and roll, pitch, yaw channels indicated that the numerical analysis was in agreement with the test, but the x acceleration and z acceleration channels were not. The ANOVA metrics indicated that the simulation was in good agreement with the test for all channels except the roll and pitch channels.

Since the metrics computed for the individual data channels did not all satisfy the acceptance criteria, the multi-channel option in RSVVP was used to calculate the weighted Sprague-Geer and ANOVA metrics for the six channels of data. The resulting weight factors computed for each channel are shown in both tabular form and graphical form in Table 8.7. The results indicated that the x and y acceleration, roll and yaw channels dominated the kinematics of the impact event. The weighted metrics computed in RSVVP using the Area II method in the multi-channel mode did satisfy the acceptance criteria. The time history comparison can be considered acceptable.

Table 8.6 Roadside Safety Validation Metrics Rating Table (Single-Channel Option)

Evaluation Criteria		Time Interval (0 to 1.0 second)		
O	<i>Sprague-Geer Metrics</i> List all the data channels being compared. Calculate the M and P metrics using RSVVP and enter the results. Values less than or equal to 40 are acceptable.	M (%)	P (%)	Pass?
	X acceleration	91.8	37.1	No
	Y acceleration	12.3	32.2	Yes
	Z acceleration	62.2	45.5	No
	Roll rate	13.4	3.1	Yes
	Pitch rate	32.8	14.1	Yes
	Yaw rate	4.9	2.8	Yes
P	<i>ANOVA Metrics</i> List all the data channels being compared. Calculate the ANOVA metrics using RSVVP and enter the results. Both of the following criteria must be met: <ul style="list-style-type: none"> The mean residual error must be less than five percent of the peak acceleration ($\bar{e} \leq 0.05 \cdot a_{Peak}$) and The standard deviation of the residuals must be less than 35 percent of the peak acceleration ($\sigma \leq 0.35 \cdot a_{Peak}$) 	Mean Residual	Standard Deviation of Residuals	Pass?
	X acceleration/Peak	-1.33	23.89	Yes
	Y acceleration/Peak	-1.00	13.48	Yes
	Z acceleration/Peak	-0.49	20.78	Yes
	Roll rate	5.95	8.28	No
	Pitch rate	30.6	23.11	No
	Yaw rate	-2.93	7.91	Yes

Table 8.7 Roadside Safety Validation Metrics Rating Table for Validation (Multi-Channel Option Using Area II Method)

Evaluation Criteria (time interval [0 to 1.0 second])																			
Channels (Select which were used)																			
<input checked="" type="checkbox"/> X Acceleration		<input checked="" type="checkbox"/> Y Acceleration		<input checked="" type="checkbox"/> Z Acceleration															
<input checked="" type="checkbox"/> Roll rate		<input checked="" type="checkbox"/> Pitch rate		<input checked="" type="checkbox"/> Yaw rate															
Multi-Channel Weights -Area (II) Method-	X Channel – 0.176666 Y Channel – 0.244870 Z Channel – 0.078464 Yaw Channel – 0.25711 Roll Channel – 0.19978 Pitch Channel- 0.04311		<div>Weighting factors</div>  <table><thead><tr><th>Channel</th><th>Weighting factor</th></tr></thead><tbody><tr><td>X'acc</td><td>0.176666</td></tr><tr><td>Y'acc</td><td>0.244870</td></tr><tr><td>Z'acc</td><td>0.078464</td></tr><tr><td>Yaw</td><td>0.25711</td></tr><tr><td>Roll</td><td>0.19978</td></tr><tr><td>Pitch</td><td>0.04311</td></tr></tbody></table>			Channel	Weighting factor	X'acc	0.176666	Y'acc	0.244870	Z'acc	0.078464	Yaw	0.25711	Roll	0.19978	Pitch	0.04311
			Channel	Weighting factor															
X'acc	0.176666																		
Y'acc	0.244870																		
Z'acc	0.078464																		
Yaw	0.25711																		
Roll	0.19978																		
Pitch	0.04311																		
O	Sprague-Geer Metrics Values less or equal to 40 are acceptable.			M (%)	P (%)	Pass?													
				29.5	20.0	Yes													
P	ANOVA Metrics Both of the following criteria must be met: • The mean residual error must be less than five percent of the peak acceleration ($e \leq 0.05 \cdot a_{Peak}$) • The standard deviation of the residuals must be less than 35 percent of the peak acceleration ($\sigma \leq 0.35 \cdot a_{Peak}$)			Mean Residual	Standard Deviation of Residuals	Pass?													
				-1.4	13.8	Yes													

8.4 Conclusion of the Modified FEA

Modifications were made to the FE models since discrepancy was found between the original detailed simulation and full-scale crash test. In the modified FEA, static and dynamic friction coefficients between barrier and ground were increased to 0.83 and 0.30, respectively. The front impact tire was removed after it detached from the vehicle suspension assembly. Modifications resulted in a nearly identical barrier performance and an improved vehicle behavior. The roll angle difference was only 8 degrees. In addition, the multi-channel option evaluation through the RSVVP program suggested that the modified FEA realistically replicated the results observed from the full-scale crash test.

9. CONCLUSION AND FUTURE WORK

A 26-inch tall T shaped low-profile portable concrete barrier was developed. This barrier was developed as a free standing system, which means quick installation, easy removal and no damage to the ground. Two full-scale crash tests were performed to evaluate the crashworthiness of this barrier. Crash tests showed acceptable results and demonstrated MASH TL-3 compliance of this T shaped low-profile PCB. In the MASH test 3-11, the freestanding barrier systems experienced a 25-inch maximum dynamic deflection, while the vehicle had a maximum roll angle of 40 degrees. This new low-profile barrier presents a major advance for work zones where the vehicle speeds are under 62 mi/h.

The sight-distance obstruction problem was evaluated and a simplified experiment was conducted. It is concluded that a barrier with a 26-inch height can provide sufficient visibility of both headlights to allow seeing the upcoming vehicle at nighttime. Comparing with conventional 32-inch tall PCBs, this new low-profile PCB significantly improves the site distance situation for the drivers attempting to enter or exit a work zone which is delineated with concrete barriers. The improved visibility provided by the use of this new low-profile PCB allows drivers to see oncoming vehicles in the day time and at night, so that potential hazardous can be avoided. In addition, high speed work zone area can be protected by preventing intrusion of errant vehicles.

Finite element simulation analysis was conducted to determine the shape of the new barrier. Two different cases were considered for each profile concept—with and without impact tire disengagement—to represent the extreme tire behaviors during the impact event. Results showed that the T-shaped low-profile barrier had acceptable and consistent results. Detailed FE models were built based on the design of the 26-inch and 24-inch tall T-shaped PCB, with

segments and connections. The crashworthiness of the T-shaped barrier was predicted to be acceptable by successfully containing and redirecting the vehicle during the simulated impact events. The detailed FE simulation result was compared with the full-scale crash test, discrepancy was found in vehicle's maximum roll angle and barrier deflection. Modifications were then made to the barrier and vehicle models. After removing the impact tire when it disengaged from the suspension assembly during the simulation and increasing the friction factors between the barrier segments and ground, the modified simulation showed an identical vehicle and barrier behavior compared with the real full-scale crash test. The multi-channel option evaluation through the validation program RSVVP suggests that the barrier FE model realistically replicate the results observed through full-scale crash test.

Efforts still remain to conduct research on this low-profile PCB. When this new low-profile PCB is deployed, related roadside safety systems such as end treatment and transition with other barrier systems need to be developed. Since the computer simulation showed an acceptable result of the 24-inch tall T shaped PCB, the author suggests to evaluate the crashworthiness of the barrier system with height of 24 inches (or shorter) through full-scale crash tests according to MASH TL-3.

REFERENCES

1. Ross, H. E., D. L. Sicking, R. A. Zimmer, and J. D. Michie. *NCHRP Report 350: Recommended Procedures for the Safety Performance Evaluation of Highway Features*. Transportation Research Board, Washington, D.C., 1993.
2. AASHTO. *Manual for assessing safety hardware*. American Association of State Highway Transportation Officials, Washington, D.C., 2009.
3. Guidry, T. R. and W. L. Beason. *Development of a low-profile portable concrete barrier*. Report No.990-4F, Texas A&M Transportation Institute, College Station, Texas, 1992.
4. Bronstad, M. E. and J. D. Michie. *NCHRP Report 153: Recommended procedures for vehicle crash testing of highway appurtenances*. Transportation Research Board, National Research Council, Washington, D.C., 1974.
5. Transportation Research Circular 191. *Recommended procedures for vehicle crash testing of highway appurtenances*. Transportation Research Board of the National Academies, Washington, D.C., 1978.
6. Michie, J. D. *NCHRP Report 230: Recommended procedures for the safety performance evaluation of highway appurtenances*. 0077-5614, Transportation Research Board, Washington, D.C., 1981.
7. AASHTO. *Manual for assessing safety hardware*. American Association of State Highway Transportation Officials, Washington, D.C., 2016.
8. *New Jersey Median Barrier History*. 2014. Available from: http://www.roadstothefuture.com/Jersey_Barrier.html.
9. Ray, M. H. and R. G. McGinnis. *Guardrail and median barrier crashworthiness*. NCHRP Project No.20-5, Transportation Research Board, Washington, D.C., 1997.
10. Wikipedia. *F-shape barrier*. Wikipedia, 2016. Available from: https://en.wikipedia.org/wiki/F-Shape_barrier.

11. Beason, W. L., H. E. Ross, H. S. Perera, and M. Marek. *Single-slope concrete median barrier*. Transportation Research Record, 1991. 1302: 11-23.
12. Beason, W. L., W. L. Menges., and D. L. Ivey. *Compliance Testing of an End Treatment for the Low-Profile Concrete Barrier*. Report No. 1403-S, Texas Transportation Institute, College Station, Texas, 1998.
13. Klam, J. and W. L. Menges. *Low-profile barrier with Tl-3 modification*. Presented at 89th Annual Meeting of the Transportation Research Board, Washington, D.C., 2010
14. Buth, C. E., W. F. Williams, R. P. Bligh, W. L. Menges, and B. G. Butler. *NCHRP Report 350 Testing of the Texas Type T202 Bridge Rail*. Report No. 0-1804, Texas Transportation Institute, College Station, Texas, 1998.
15. Bullard, D. L., W. L. Menges, and R. R. Haug. *NCHRP Report 350 Test 3-11 of the Tubular Steel-Backed Timber Bridge Rail*. Report No. 405181-21, Texas Transportation Institute, College Station, Texas, 2003.
16. Consolazio, G. R., J. H. Chung, and K. R. Gurley. *Impact simulation and full scale crash testing of a low profile concrete work zone barrier*. Computers & Structures, 2003. 81(13): 1359-1374.
17. Her, V., J. R. Jewell, and R. Meline. *Development and Testing of a Low-profile Barrier*. Report No. FHWA/CA10-0645, California Department of Transportation, Sacramento, California, 2012.
18. Polivka, K. A., R. K. Faller, D. L. Sicking, J. R. Rohde, J. D. Reid, and J. C. Holloway. *Development of a Low-Profile Bridge Rail for Test Level 2 Applications*. Report No. TRP-03-109-02, Midwest Roadside Safety Facility, University of Nebraska-Lincoln, Lincoln, Nebraska, 2002.
19. Johnson, E. A., R. K. Faller, J. D. Reid, D. L. Sicking, B. W. Bielenberg, S. K. Rosenbaugh, and K. A. Lechtenberg. *Analysis, Design, and Dynamic Evaluation of a TL-2 Rought Stone Masonry Guardwall*. Report No. TRP-03-217-09, Midwest Roadside Safety Facility, University of Nebraska-Lincoln, Lincoln, Nebraska, 2009.
20. Bullard, D. L., W. L. Menges, C. E. Buth, and R. R. Haug. *Guardrail Testing Program IV Volume I: Technical Report*. Report No. 405181-F, Texas Transportation Institute, College Station, Texas, 2004.

21. AASHTO. *Policy on Geometric Design of Highways and Streets*. American Association of State Highway and Transportation Officials, Washington, D.C., 2011.
22. Standard, Federal Motor Vehicle Safety 108. *Lamps, Reflective Devices, and Associated Equipment*. 2004.
23. *Leading cars in the U.S. 2017 | Statistic*. Available from: <https://www.statista.com/statistics/276419/best-selling-cars-in-the-united-states/>.
24. Hallquist, J. O. *LS-DYNA Keyword User's Manual, Version 971*. Livermore Software Technology Corporation, Livermore, California, 2016.
25. NCAC. *Finite Element Vehicle Models: 2007 Chevy Silverado*. George Washington University, Virginia, 2011. Available from: <http://www.ncac.gwu.edu/vml/models.html>.
26. Desorcie, F. J. *Development of a Non-pinned Low-profile End Treatment*. Master of Science Thesis, Texas A&M University, College Station, Texas, 2013.
27. TRAP. *Test Risk Assessment Program, Version 2.3.3*. CAPSHER Technology, Inc, 2011.
28. Mongiardin, M., and M. H. Ray. *Roadside Safety Verification and Validation Program, Version 1.7*. Worcester Polytechnic Institute, 2009.